Incorporation of Lipid Nanoparticles into Pullulan Based Oral Thin Films for the Delivery of Vaccines

Incorporation of Lipid Nanoparticles into Pullulan Based Oral Thin Films for the Delivery of Vaccines

By

Dayna Bennett, B.Sc.

A Thesis

Submitted to the School of Graduate Studies

In Partial Fulfillment of the Requirements

For the Degree of

Master of Science

In Chemistry

Master of Science (2022) McMaster University

Chemistry Hamilton, Ontario, Canada

Title: Incorporation of Lipid Nanoparticles into Pullulan Based Oral Thin Films for the Delivery of Vaccines

Author: Dayna Bennett

B.Sc. (Chemistry)

McMaster University, Hamilton, Canada

Supervisor: Professor Alex Adronov

Number of Pages: xx, 111

Abstract

Infectious diseases are most effectively controlled by vaccines that can elicit an immune response and create antibodies. As it stands, most vaccines are administered using subcutaneous or intramuscular injections. Injections via needle and syringe often invoke anxiety for individuals, which can result in low vaccination rates. The cost associated with administering vaccines is also high due to the requirement of trained health care professionals for administration. Additionally, administration via injection produces significant amounts of biohazardous waste. Administration of a vaccine by the swallowing of a pill or capsule also presents challenges. The active ingredient must be able to withstand passage through the gastrointestinal tract where enzymatic or acid related degradation is possible.

Two promising sites for vaccine delivery are the sublingual region which is located on the floor of the mouth and the underside of the tongue, and the buccal region located on the gums, cheeks, and inner lip. These regions, present in the oral cavity, allow for an active ingredient to be rapidly absorbed into the bloodstream without having to undergo first pass metabolism. One drug delivery method that has recently gained interest is the oral thin film. Upon placing an oral thin film on the buccal or sublingual region of the mouth, the film will rapidly dissolve and release the active ingredient to be absorbed into the bloodstream. Rapid Dose Therapeutics, a company in Burlington, Ontario, has developed the QuickStrip, an oral thin film that can deliver caffeine, vitamin B12, melatonin, and tetrahydrocannabinol (THC) through the buccal and sublingual route. Rapid Dose Therapeutics is interested in expanding the applications of the QuickStrip into vaccine delivery. Incorporating vaccines into oral thin films would allow for a pain-free, self-administrable inoculation process. This would result in a decrease in costs associated with vaccine distribution, making vaccines more accessible, while also eliminating associated biohazardous waste.

Vaccines are traditionally classified as live and non-live. Live vaccines contain a live, weakened strain of the pathogenic organism whereas non-live vaccines contain an inactivated whole pathogenic organism or a subunit of the pathogen. Over the course of the COVID-19 pandemic, a new vaccine type, messenger RNA (mRNA) -based vaccines, emerged. The mRNA within these vaccines encodes for the target antigen and employs the ribosomes within the host cell to transcribe the mRNA into the target antigen. The mRNA is encapsulated within lipid nanoparticles (LNP) which assist in delivering and protecting the RNA. mRNA based vaccines are beneficial over traditional vaccine types as they are safe and faster to manufacture.

This thesis was performed in conjunction with Rapid Dose Therapeutics and worked toward being able to use the QuickStrip as a vaccine delivery method.

In this work, lipid polymer hybrid nanoparticles were prepared using a probe sonication technique. The effect of sonication amplitude and temperature on particle size was studied. Next, ibuprofen loaded lipid polymer hybrid nanoparticles were synthesized using a nanoprecipitation technique. A fluorescent dye, fluorescein isothiocyanate, was then loaded into the hybrid nanoparticles. This allowed the acquisition of super resolution optical microscopy images of the particles, both prior to and after being incorporated into an oral thin film.

Commercially produced lipid nanoparticles were then acquired from Acuitas Therapeutics, the company that produces the lipid nanoparticles for the Pfizer-BioNTech vaccine. These lipid nanoparticles contain a model mRNA strand as well as the fluorescent dye 1,1’-dioctadecyl-3,3,3’,3’-tetramethylindocarbocyanine. Super resolution optical microscopy was employed to visualize the Acuitas Therapeutics lipid nanoparticles on a glass coverslip and in oral thin films. The images acquired suggested that the lipid nanoparticles were unharmed during the film casting process. The integrity of the mRNA within the lipid nanoparticles was then assessed and confirmed

using gel electrophoresis. To ensure the mRNA was remaining encapsulated within the particles, the Quant-iT RiboGreen RNA assay was used. Initial studies indicated that the RNA was becoming unencapsulated from the nanoparticles once the film mixture had been cast. This resulted in several modifications to the preparation and formulation of the oral thin films. Ultimately, a film formulation containing a lipid-PEG molecule was used to stabilize the lipid nanoparticles within the oral thin film.

Acknowledgements

There are many people who I would like to thank for their support and contributions to this work over the course of the last two years.

A huge thank you, to my supervisor, Professor Alex Adronov, for giving me the opportunity to work on such a cool project. No matter how busy Alex was he was always available to give great suggestions and answer any questions I had.

I am very grateful to Dr. Jim Mayo. Jim not only gave input on the different challenges of my project, but he was also the person to go see if you had any questions about any instrument.

I am thankful for the suggestions and contributions provided by Professor Jose Moran-Mirabal, Dr. Mouhanad Babi, and Christine Cerson. Their expertise on super resolution optical microscopy really aided in understanding how the lipid nanoparticles were behaving once incorporated into the oral thin films.

A special thanks to Kai Sun, Annika Yardy, Rena Chen, Kristen Entz, Mina Stefanovic, and Bram Bussin, who all worked actively on the thin films project. Kai spent many afternoons micro pipetting RiboGreen dye, which contributed to many of the findings discussed in this thesis.

The contributions and suggestions provided by Rapid Dose Therapeutics are greatly appreciated. Ben Macphail was always available to have meetings to discuss possible controls and next steps.

Thank you to Acuitas Therapeutics for supplying lipid nanoparticles for this project and for being available to answer questions we had regarding the lipid nanoparticles.

I am grateful for Professor Mark Larché, Dr. Tom Jingyu, and Iris Wang for their recommendations regarding this project. Tom and Iris were especially helpful when I was learning how to run gel electrophoresis.

The members of the Adronov Group, both past and present, are deserving of many thanks. Their support and assistance over the last two years has been greatly valued.

On a more personal note, thank you to my family for their encouragement over the last two years. I am thankful for my parents, David and Diane, who drove six hours and through Toronto traffic to come visit me (and stock up my freezer). Thank you, Freddy, the fluffiest of felines, for being at the door every day when I got home from the lab. No matter how hard of a day it had been, Freddy was there to instantly make your day better. Finally, thank you Jack for sticking with me since our first year of university. You were always available to bounce ideas off of no matter how late at night it was, which really helped. Plus, you make pretty good chicken cheese which is always a bonus.

Table of Contents

List of Abbreviations

AFM	Atomic Force Microscopy
API	Active Pharmaceutical Ingredient
DiI	1,1’-dioctadecyl-3,3,3’,3’-tetramethylindocarbocyanine
DLS	Dynamic Light Scattering
DOPE-PEG	1,2-dioleoyl-sn-glycero-3-phosphoethanolamine-N-[methoxy(polyethylene glycol)-2000] (ammonium salt)
FITC	Fluorescein Isothiocyanate
GI	Gastrointestinal
LNP	Lipid Nanoparticles
mRNA	Messenger Ribonucleic Acid
OTF	Oral Thin Film
PEG	Polyethylene Glycol
RDT	Rapid Dose Therapeutics
RNA	Ribonucleic Acid
SRRF	Super Resolution through Radical Fluctuations
STORM	Stochastic Optical Reconstruction Microscopy
TE	Tris-Ethylenediaminetetraacetic acid
TRIS	Tris(hydroxymethyl) aminomethane
UV-Vis	Ultraviolet-visible
wt.%	Weight Percent

List of Tables

List of Figures

Chapter 1: Introduction

The two most common methods for administering therapeutic drugs and vaccines are parenteral administration and oral administration. Parenteral administration involves the administration of the active pharmaceutical ingredient (API) via a subcutaneous, intramuscular, intradermal, or intravenous injection. Oral administration often involves the swallowing of a pill or capsule that contains the API. The API is then absorbed through the gastrointestinal (GI) tract. Although effective, these methods have several drawbacks.

Parenteral administration requires a needle and syringe which can cause anxiety for individuals, which may result in low patient compliance. Injections often require a trained health care professional for administration, increasing associated costs. In addition, needles and syringes produce significant amounts of biohazardous waste.

Oral administration is less invasive than injections, however, using a pill or capsule is not suitable for all API. The oral bioavailability of the drug must be considered, to ensure the API is able to reach the blood stream and be distributed to the point where a pharmacological effect takes place.[1] Oral administration requires the drug molecule to travel through the hepatic first pass metabolism, where enzymatic or acid-related degradation is possible.[2] Additionally, the API must be able to be easily absorbed through the GI tract.[1] Once all these conditions are met, absorption through the GI tract results in a slower onset of action compared to administration through the intravenous route.[1] One additional drawback of oral administration is that children, elderly people, and people with dysphagia have difficulty swallowing pills. This makes drug delivery through the oral route to people in those demographics difficult.

The buccal and sublingual regions in the oral mucosa have recently been explored as a potential vaccine and drug delivery site.[2] The sublingual region is located on the floor of the mouth and the underside of the tongue, while the buccal region is located on the gums, cheeks, and inner lip.[2] The buccal and sublingual regions contain extensive vasculature, through which the API can be directly absorbed into the bloodstream.[1] For vaccines delivered at the buccal or sublingual region, it has been described that antigens can be transported through the mucosa by Langerhans cells.[2] Following this, myeloid dendritic cells carry the antigen along the lamina propria.[2] Dendric cells then carry the antigen to lymph nodes where an immune response is induced (Figure 1).[2]

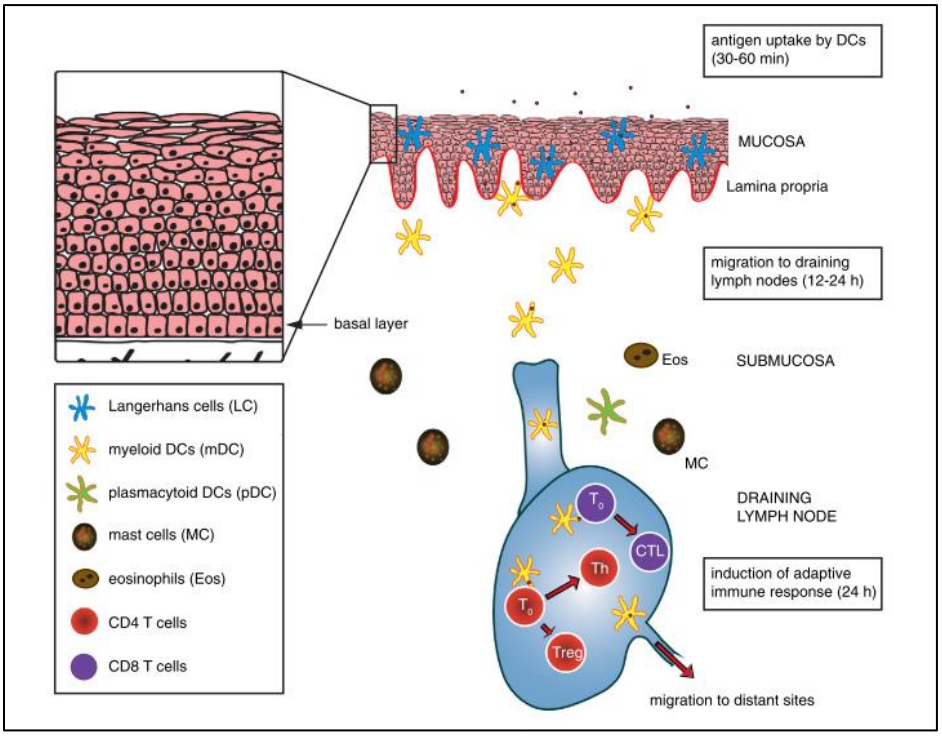

Figure 1: Schematic diagram showing how antigens delivered to the sublingual or buccal region are delivered to lymph nodes where an immune takes place. Reproduced with Permission.[2] Copyright 2014 Journal of Controlled Release.

The oral mucosa is a pain-free, non-invasive drug delivery site, in which the API can bypass first pass metabolism as well as GI enzymatic degradation, while subsequently having a fast onset of action.[3] To deliver drugs to the oral mucosa, several different drug delivery systems have been explored including oromucosal sprays, droplets, tablets, chewing gum, patches, lozenges, and oral thin films (OTFs).[4]

1.1 Oral Thin Films (OTFs)

OTFs are composed of thin layers of polymer in which an active ingredient is embedded. When an OTF is placed in the mouth, the water-soluble film dissolves to deposit the API. It is important for OTFs to easily adhere to the oral cavity and disintegrate without the use of water.[1] Depending on the desired use, the properties of an OTF can be manipulated with additives to alter the drug release and the film disintegration time.

OTFs have many advantages compared to other drug delivery platforms. They are pain free which can improve patient compliance. They do not require a needle and syringe for administration, eliminating the production of biohazardous waste. They can be self-administered without the need of a trained healthcare professional and they have the potential to be stored at ambient temperatures.[5] OTFs do not require the API to be swallowed, allowing for the active ingredient to bypass first pass metabolism and the GI tract.[6] This makes administering drugs to those that have challenges swallowing feasible. OTFs are discrete and do not require water, allowing for convenient utilization. Flavours and colouring additives can be incorporated into the film formulation, making the experience more pleasurable for the patient.

1.1.1 Preparation of Oral Thin Films

OTFs can be prepared using a variety of methods, including solvent casting,[7] semi-solid casting,[8] direct milling,[9] hot melt extrusion,[10] rolling,[11] 3D printing,[12,13] electrospinning,[14] electrospraying,[8] freeze drying,[15] and freeze thawing.[16]

Solvent casting is one of the most common techniques used and is the method that was used for preparing the OTFs in this work. Solvent casting involves first preparing the film formulation by dissolving the film excipients in an appropriate solvent such as water. The solvent content can be increased or decreased depending on the desired film formulation viscosity. Air that was entrapped within the film formulation during mixing is removed. The most effective way of removing entrapped air is by placing the film mixture under vacuum.[7] The film formulation is then transferred to a mold or cast using a doctor blade and dried. During the drying process, heat can be applied to decrease the drying time. Depending on the stability of the API the temperature at which an OTF can be dried must be considered. The film can then be cut, if necessary, to the desired drug dosage, and packaged.

The primary ingredient in an OTF is a water soluble polymer that acts as a film former.[11] Pullulan, starch, gelatin, pectin, and polyvinyl alcohol are a few examples of film formers that can be used.[11] It is important for film former polymers to be non-toxic and non-irritating. The film former polymers must be fast at disintegrating, have adequate mechanical properties, be inexpensive, and have a sufficient shelf life.[11] Plasticizers, such as glycerol, polyethylene glycol, and dibutyl phthalate can be added to the film formulation to improve the spreadability of the casting solution and the flexibility of the OTF.[11,17] Film disintegration can be aided by the incorporation of surfactants such as Tween, sodium lauryl sulfate, and benzalkonium chloride to the OTF.[11,17] Penetration enhancers can also be added to the film mixture to increase the

permeability of the buccal or sublingual region, increasing the ability of the API to be absorbed.[18] Other excipients that can be added to a film formulation are sweetening, colouring, and flavouring agents. These additives improve the overall experience for the patients receiving the OTF.[11] In some instances, additives may need to be included in the film formulation to stabilize the API. For example, trehalose has previously been found to be efficient at stabilizing proteins within OTFs.[17]

1.1.2 Examples of thin film therapeutics

Perhaps the most recognized OTF available for everyday purchase are Listerine Breath Strips. Listerine breath strips are prepared primarily from pullulan and act as an edible film that can effectively kill plaque producing germs that cause dental plaque, gingivitis, and bad breath.[19]

There are several OTFs that have been used as drug delivery platforms in the drug market. In 2009, a buccal soluble film that contained fentanyl as the API was introduced under the brand name Onsolis.[20] Buprenorphine HCl and naloxone HCl are two APIs that are combined to treat opioid addiction.[21] A sublingual film, Suboxone, was approved in 2010, prior to the approval of a buccal film, Bunavail, in 2014.[21,22] Zuplenz is an oral soluble film that was approved in 2010 that contains Ondansetron, a medication that is used to prevent nausea and vomiting following cancer chemotherapy, radiation therapy, or surgery.[23,24] In 2015, another buccal film, Belbuca, containing buprenorphine was approved. Belbuca is used to treat opioid addiction however it can also be used for acute and chronic pain.[25] Sympazan, an OTF that contains the drug Clobazam, can be used to help control seizures and was approved for use in 2018.[26] In 2019 Exservan, an OTF that can be used to treat amyotrophic lateral sclerosis (ALS) was approved.[27] A sublingual film was approved in 2020 under the brand name of Kynmobi, which contains apomorphine, an active ingredient that is used to treat episodes of difficulty moving, walking, and speaking in people with advanced Parkinson's disease.[28]

One company that is particularly interested in the development of OTFs for the use of drug delivery is Rapid Dose Therapeutics (RDT). RDT has developed the QuickStrip™, which is an OTF that currently can be used to deliver caffeine, vitamin B12, melatonin, and tetrahydrocannabinol (THC).[29] RDT has expressed interest in expanding the potential applications of the QuickStrip™ to include more pharmaceutical therapeutics as well as a vaccine delivery platform.

1.2 Vaccines

Infectious diseases are most effectively controlled by vaccine immunization programs. The World Health Organization (WHO) estimates that immunization prevents 3.5-5 million deaths each year.[30] Vaccines work by inducing an immune response that provides protection against an infection or disease.[31] Antigens, produced from the pathogen or produced synthetically to represent components of the pathogen, within the vaccine are responsible for the immune response.[31] The protection that a vaccine provides is measured using clinical trials that compare immune responses to clinical end points.[31]

Traditionally, vaccines are classified as live and non-live vaccines. Live vaccines are vaccines that contain attenuated replicating strains of the pathogenic organism.[31] The attenuated replicating strain of the pathogenic organism needs to be able to reproduce within the host to produce a strong immune response, however not enough to induce illness.[31] Live vaccines were first used in 1798 to help combat smallpox and have since been used in vaccines against diseases such as measles, mumps, rubella, influenza, and yellow fever.[31] Live vaccines produce strong immune responses and are relatively simple in their construction.[32] In immunocompromised individuals, however, live vaccines have the potential to uncontrollably replicate and as such considerations must be made during the development of live vaccines.[31] There are also high costs

associated with transporting live vaccines as they must be stored in temperature controlled environments.[32] Non-live vaccines can contain either a killed whole organism, or a subunit of the pathogen such as purified proteins, recombinant proteins, polysaccharides, or peptides from the organism.[31] The first non-live vaccine was used to combat typhoid introduced in 1896. Some additional examples of non-live vaccines include the hepatitis B virus (HBV) vaccine, the polio vaccine, and the rabies vaccine.[31] Non-live vaccines are generally considered safer for immunocompromised individuals,[31] and are more globally accessible due to existing supply chains.[32] Non-live vaccines produce weaker immune responses than live vaccines, resulting in several doses of vaccine needing to be administered.[32] The process of manufacturing both live and non-live vaccines is complex, difficult to scale, and can be dangerous due to the handling of live viruses.[32]

1.2.1 COVID-19 Vaccine

Severe acute respiratory syndrome coronavirus 2 (SARS-CoV-2) first emerged at the beginning of the year 2020, and by March 2020 the World Health Organization (WHO) had declared the coronavirus disease (COVID-19) a global pandemic.[33] There were increasing numbers of cases and deaths reported daily. Travel bans, lockdowns, and physical distancing measures were implemented. People went months without seeing family members, schools were closed, and all normal activities were suspended. The development of a COVID-19 vaccine was essential for normal life to proceed.

It was during the COVID-19 pandemic that the first nucleic acid-based vaccine was approved for human use.[32] The technology behind nucleic acid-based vaccines was inspired by the field of immune-oncology. For many years, immune-oncologists have explored using messenger RNA (mRNA) as a tool to boost the body's immune system.[32] mRNA that encodes for tumour

antigens can be delivered to cells, where the body's immune system can create antibodies against the tumor.[32] Once the antibodies have been introduced, they are able to recognize and eliminate tumors.[32] This same principle could be applied to vaccines, in which mRNA encoding for the target antigen could be delivered across cell membranes, into the cytoplasm.[32] Ribosomes present in the host cell can translate the mRNA strand into the target antigen. The antigen can then produce humoral and cellular responses by remaining localized to the cell membrane or by being exported outside of the cell.[32]

The drawback to introducing RNA in vivo for both immunotherapy and vaccines, is that RNA is highly sensitive to degradation by nucleases and immune agents.[6] As such, nanotechnology has been employed as a method to effectively deliver RNA to the cytoplasm. There are different nano-technologies that have been developed to act as delivery vehicles for nucleic acids such as: viral or bacterial vectors, nanoparticles, liposomes, and physical devices.[6] Lipid nanoparticles (LNP) have been found to be an especially effective delivery vehicle and pharmaceutical companies such as Moderna, Pfizer and BioNTech began developing mRNA therapeutics around 2010.[32] In 2020 with the emergence of the SARS-CoV2 virus, these pharmaceutical companies shifted their attention from immunotherapy to preparing an mRNA vaccine that could combat COVID-19. Pfizer and BioNTech partnered together while Moderna worked independently. Emergency use authorization was given to the vaccine formulations prepared by Pfizer-BioNTech and Moderna after they concluded their Phase 3 clinical trials in the fall and winter of 2020, resulting in the largest global vaccination campaign in human history.[32]

The mRNA-based vaccines could be developed very quickly. This was due to their production being straightforward and scalable. With the absence of live viruses and cell cultures, the safety requirements during manufacturing were much less stringent than with live and non-live

vaccines.[32] Moderna and Pfizer-BioNTech vaccines contain modified mRNA that encodes for the COVID-19 spike protein. The mRNA is produced by in vitro transcription from a plasmid DNA backbone.[34] The transcribed mRNA strand is modified to contain 5' methylguanosine triphosphate caps and 3'-poly-adenosine tails prior to being incorporated into the LNPs.[32] These modifications allow for proper ribosome binding when in the cytoplasm, and help stabilize and protect the mRNA from nuclease mediated degradation.[35]

The mRNA is encapsulated within ionizable lipid nanoparticles. The LNPs are typically comprised of an ionizable amino lipid, a phospholipid, cholesterol, and a lipid anchored PEG molecule.[32,35,36] The LNPs are prepared by a microfluidic mixing process performed at a low pH.[32] Complexation between the negatively charged mRNA strand and positively charged LNPs is encouraged by the low pH.[32] Under neutral, physiological pH the LNPs have no charge and the mRNA remains encapsulated within the LNPs. When in the endosome, the pH is approximately 6.5, causing the LNPs to become protonated.[34] Once protonated, cationic lipids interact with anionic membrane lipids, resulting in membrane disruption and endosomal escape.[34,37]

Acuitas Therapeutics, a company in British Columbia, had a huge impact on the development of the Pfizer-BioNTech COVID-19 vaccine. Specializing in the field of lipid nanotechnology, Acuitas Therapeutics have developed over 600 cationic lipids, all of which have been evaluated in LNPs.[36] They were responsible for providing the LNP delivery technology to Pfizer-BioNTech and continue to work to develop other vaccines and immunotherapies.[36]

The COVID-19 pandemic has presented many challenges over its two-year duration and has changed the way people approach everyday life. Perhaps the most optimistic thing to emerge from the pandemic was the approval for the use of mRNA-LNP based vaccines. These vaccines have paved the way for future mRNA vaccines such as influenza,[38,39] malaria,[40–42] human

immunodeficiency virus (HIV),[43,44] and herpes simplex virus (HSV).[45–47] Additionally, in the event of a new pathogen, mRNA-based vaccines can be quickly manufactured once the antigenic sequence is known.[35]

There are some possible areas of improvement for mRNA-based vaccines. As with most vaccines, the COVID-19 vaccine requires an intramuscular injection for administration. As previously discussed, injections via needle and syringe produce significant biohazardous waste, require trained health care professionals for administration, and result in lower patient compliance. Some COVID-19 vaccines also require cold chain storage. For example, the Pfizer-BioNTech vaccine requires -70°C storage temperatures. Cold chain storage requirements increase costs associated with vaccine distribution and pose challenges for areas where access to storage facilities may not be available.

One possible solution to these challenges is to incorporate the COVID-19 vaccine into an OTF. OTFs are painless, can be self-administered, produce no biohazardous waste, and have the potential to not require cold-chain storage.[5]

1.3 Objectives

This thesis was performed in conjunction with RDT and investigates the incorporation of LNPs into OTFs for the use of vaccine administration.

Chapter 2 focuses on the synthesis and characterization of lipid nanoparticles. In Chapter 2, lipid-polymer hybrid nanoparticles (h-LNP) were prepared using a probe sonication technique that was modified from a literature procedure.[48] The effect of probe sonication and sonication temperature on particle size was measured using dynamic light scattering (DLS) and atomic force microscopy (AFM). Ibuprofen loaded h-LNPs (Ibu-LNP) were then prepared using a

nanoprecipitation technique modified from a literature procedure.[49] Following this, fluorescein isothiocyanate (FITC) was loaded into the h-LNPs (FITC-LNP) and subsequently imaged using super resolution optical microscopy. Once it was confirmed that FITC-LNPs were able to be imaged, 1,1'-dioctadecyl-3,3,3',3'-tetramethylindocarbocyanine (DiI) labelled LNPs containing model mRNA were obtained from Acuitas Therapeutics (Acuitas-LNP). These particles were characterized using DLS and super resolution optical microscopy.

In Chapter 3, the LNPs characterized in Chapter 2 were incorporated into OTFs. FITC-LNPs and Acuitas-LNPs were embedded into OTFs and imaged using super resolution optical microscopy. The super resolution images acquired indicated that the LNPs remained intact after the film casting process. Following this, the Quant-iT RiboGreen RNA assay, was employed to determine if RNA remained encapsulated within the Acuitas-LNPs after being integrated into OTFs. The assay indicated that there were stability problems with the LNPs once they were embedded in OTFs. This resulted in changes to film formulation as well as studies regarding the different variables of the film casting process. By adding 1,2-dioleoyl-sn-glycero-3-phosphoethanolamine-N-[methoxy(polyethylene glycol)-2000](ammonia salt) the RNA remained encapsulated within the Acuitas-LNPs and the particles were stabilized, even after the film casting process. Gel electrophoresis was performed on Acuitas-LNP that had been embedded into an OTF and showed that the RNA was not degraded during the film casting process.

Chapter 2 - Synthesis and Characterization of Lipid Nanoparticles

2.1 Overview

In this chapter, lipid-polymer hybrid nanoparticles (h-LNP) were prepared using a probe sonication technique, modified from a literature procedure.[48] The effect of sonication power and temperature was compared to the h-LNP size. h-LNPs were characterized using dynamic light scattering (DLS) and atomic force microscopy (AFM).

Attempts to load ibuprofen into the h-LNPs were made, however, no ibuprofen was able to be loaded. As a result, the method for preparing ibuprofen loaded h-LNPs (Ibu-LNP) was altered to a nanoprecipitation technique that had previously been described in the literature.[49] This allowed for the successful loading of ibuprofen into the h-LNPs, as determined by UV-Vis spectroscopy. DLS was used to characterize blank-LNPs and Ibu-LNPs prepared using the nanoprecipitation technique.

Fluorescently labelled LNPs were prepared by loading the dye fluorescein isothiocyanate (FITC) into the LNPs using the probe sonication technique. The FITC loaded LNPs (FITC-LNP) were characterized using AFM and high-resolution optical microscopy.

Finally, fluorescently labelled LNPs containing model mRNA were obtained from Acuitas Therapeutics. The Acuitas Therapeutics LNPs (Acuitas-LNP) were characterized using DLS in addition to high resolution stochastic optical reconstruction microscopy (STORM).

2.2 Preparation of Blank LNPs Using Probe Sonication Technique

Fang et al. previously described a fast, single step, method for producing lipid-polymer hybrid nanoparticles using a bath sonicator.[48] This method allowed for particle size to be below 100 nm and contain a polydispersity index of less than 0.10.[48] These particles were made of three

components: a hydrophobic polymeric core which allowed for efficient loading of poorly water-soluble drugs[48], a lipid layer surrounding the polymeric core which promoted biocompatibility and drug retention, and a hydrophilic polymer layer surrounding the lipid layer to increase h-LNP stability.[48] In this work, h-LNPs were prepared with a probe sonicator at various sonication amplitudes and temperatures. The effect of sonication amplitude, power, and temperature on observed particle size were measured using DLS and AFM.

To prepare the h-LNPs, first, all components were added to a glass vial (Figure 2). The temperature of the sample was controlled by submerging the vial in either an ice bath, a water bath, or no bath. Following this, the sample was sonicated at an amplitude of 40, 60, or 80, for 5 minutes. After sonication, the temperature of the solution was recorded, and the particles were isolated and washed. It was predicted that as the sonication amplitude and power increased, smaller particles would be observed. Keum et al, previously reported that docetaxel loaded PLGA nanoparticles, prepared with sonication powers ranging from 70-130 watts (W), decreased in size as sonication power was increased.[50] It was also predicted that as sonication temperature increased, larger particles would form. Yang et al, previously showed that PLGA nanoparticles begin to increase in diameter once sonication temperature surpassed 25˚C.[51]

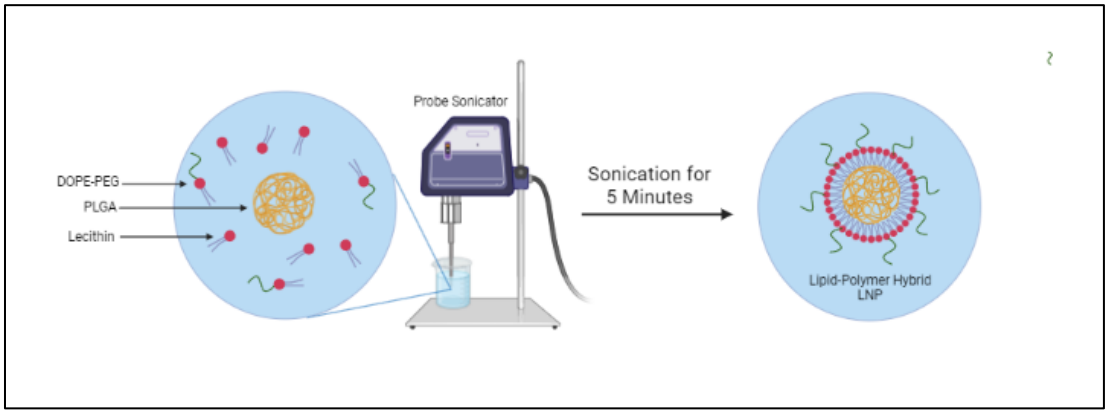

Figure 2: Illustration representing the self assembly of lipid-polymer hybrid nanoparticles using a probe sonication technique. Created using BioRender.

DLS performed on the h-LNP samples indicated that increasing sample temperature, while keeping sonication amplitude constant, resulted in an increase in particle diameter. For example, samples sonicated at an amplitude of 60 at temperatures of 31˚C, 36˚C, and 64˚C, had effective diameters of 201 ± 3 nm, 205 ± 3 nm, and 212 ± 4 nm, respectively (Table 2). Samples sonicated at varying amplitudes but under constant temperature conditions, showed no trend in diameter. Samples sonicated in an ice bath at amplitudes of 40, 60, and 80, had effective diameters of 185 ± 2 nm, 201 ± 3 nm, 195 ± 2 nm, respectively (Table 2). After comparing the sonication power that corresponded to the sonication amplitudes of 40, 60, and 80 (Table 2), it was conceivable that there was no definitive trend. The sonication power only varied from 20 to 30 W, which was a much smaller range that was used with the docetaxel loaded PLGA particles.[50] Further increasing the sonication power would likely result in smaller particles.

Table 1: Summary of the conditions at which h-LNPs prepared via probe sonication technique were made, including sonication amplitude, sonication temperature, sonication power, and sonication energy.

Sonication Amplitude	**Sample Type**	**Temperature after Sonication (˚C)**	**Calculated Power (W)**	**Energy (J)**
40	Ice Bath	28	20	6197
40	Water Bath	31	21	6303
40	No Bath	57	17	5143
60	Ice Bath	31	27	8107
60	Water Bath	36	27	8364
60	No Bath	64	22	6818
80	Ice Bath	24	35	10 725

80	Water Bath	36	33	10 136
80	No Bath	70	27	8299

Table 2: DLS size measurements of the h-LNPs prepared using the probe sonication technique. DLS measurements gave the effective diameter, mean diameter by intensity, mean intensity by number, and PDI of all samples.

Amplitude	Temperature after Sonication (˚C)	Calculated Power (W)	Effective Diameter (nm)	Mean Diameter by Intensity (nm)	Mean Diameter by Number (nm)	PDI
40	28	20	184 ± 2	206 ± 7	109 ± 15	0.13 ± 0.02
40	31	21	219 ± 2	233 ± 13	180 ± 9	0.08 ± 0.02
40	57	17	235 ± 2	236 ± 5	224 ± 13	0.05 ± 0.03
60	31	27	201 ± 3	205 ± 47	91 ± 55	0.13 ± 0.03
60	36	27	205 ± 3	218 ± 8	170 ± 25	0.08 ± 0.03
60	64	22	212 ± 4	251 ± 6	118 ± 11	0.18 ± 0.01
80	24	35	195 ± 2	209 ± 6	113 ± 32	0.10 ± 0.01
80	36	33	210 ± 2	226 ± 15	153 ± 44	0.09 ± 0.01
80	70	27	224 ± 2	248 ± 12	145 ± 20	0.12 ± 0.02

Each of the h-LNP samples were spin coated onto a silicon wafer and imaged using AFM. There were not many differences between samples. The particles were circular in shape, had approximately similar size distributions, and tended to aggregate into clusters of particles (Figures 3-11). AFM measured the diameter of the h-LNP samples to be smaller than those measured by DLS (Table 3). One possible reason for this is that when the particles are deposited on the silicon

wafer, the particles are dried out, resulting in the volume of the h-LNPs being reduced. To confirm the size distribution given by DLS, AFM in solution could be performed.

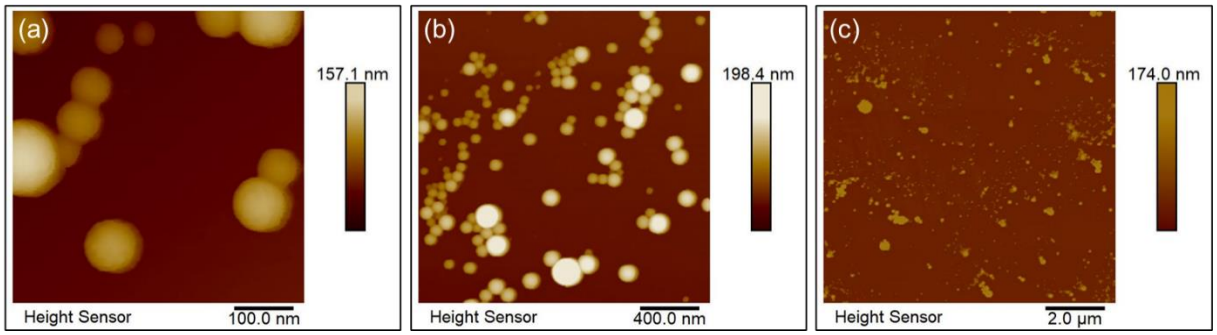

Figure 3: AFM images taken of LNPs prepared via the probe sonication technique at a sonication amplitude of 40 while in an ice bath. Area of sample imaged was (a) 500 nm x 500 nm, (b) 2 µm x 2 µm, and (c) 10 µm x 10 µm.

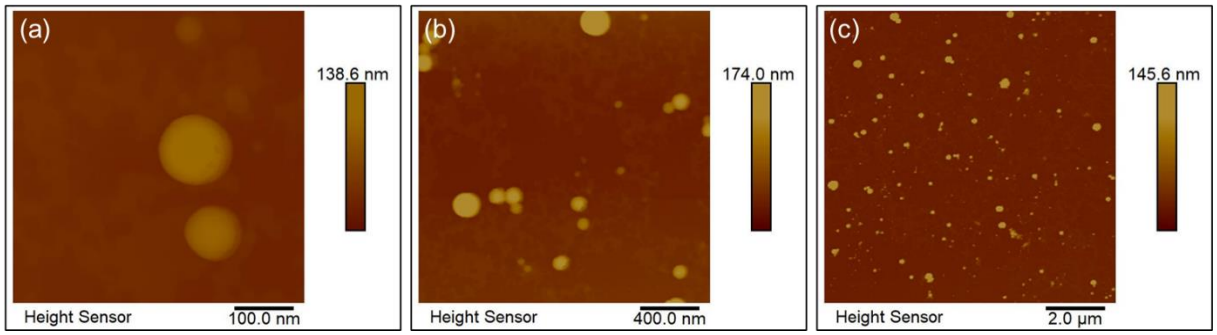

Figure 4: AFM images taken of LNPs prepared via the probe sonication technique at a sonication amplitude of 40 while in a water bath. Area of sample imaged was (a) 500 nm x 500 nm, (b) 2 µm x 2 µm, and (c) 10 µm x 10 µm.

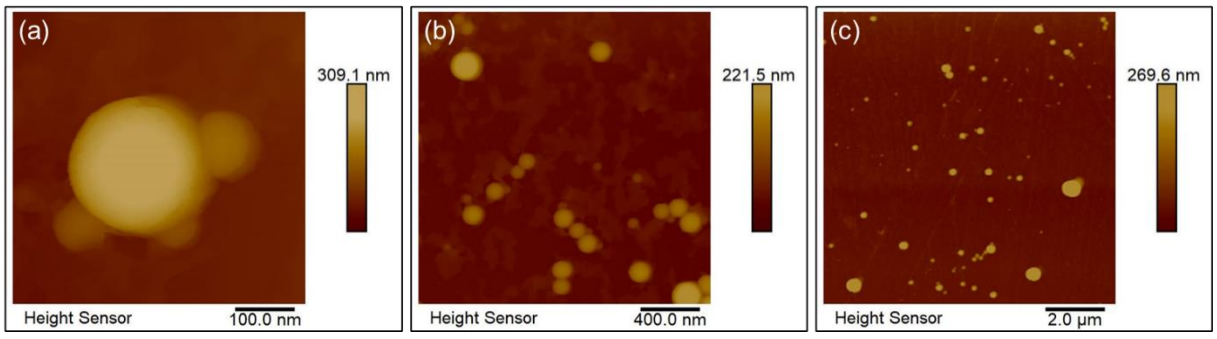

Figure 5: AFM images taken of LNPs prepared via the probe sonication technique at a sonication amplitude of 40 while in no bath. Area of sample imaged was (a) 500 nm x 500 nm, (b) 2 µm x 2 µm, and (c) 10 µm x 10 µm.

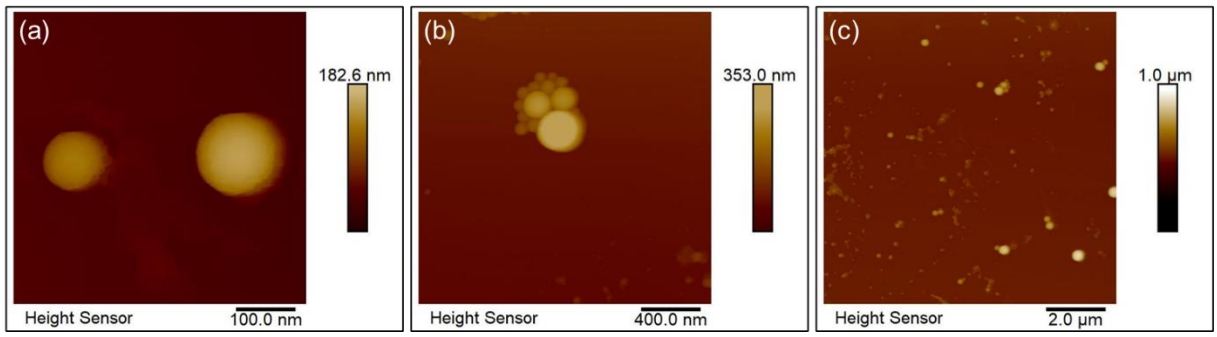

Figure 6: AFM images taken of LNPs prepared via the probe sonication technique at a sonication amplitude of 60 while in an ice bath. Area of sample imaged was (a) 500 nm x 500 nm, (b) 2 µm x 2 µm, and (c) 10 µm x 10 µm.

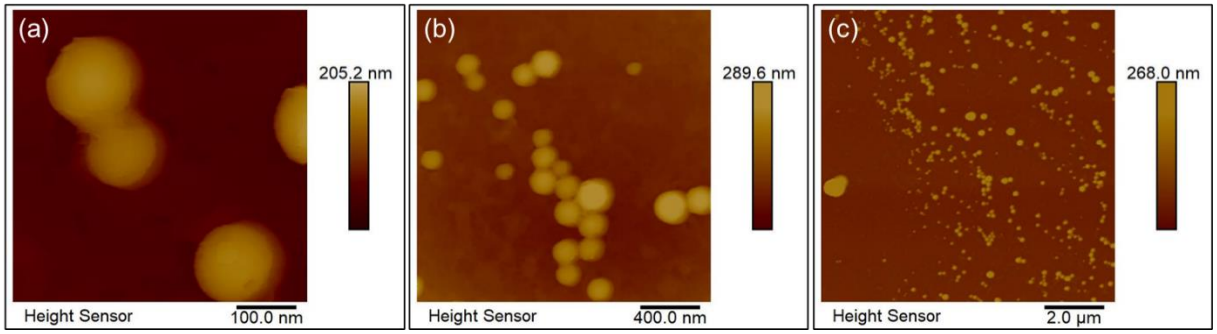

Figure 7: AFM images taken of LNPs prepared via the probe sonication technique at a sonication amplitude of 60 while in a water bath. Area of sample imaged was (a) 500 nm x 500 nm, (b) 2 µm x 2 µm, and (c) 10 µm x 10 µm.

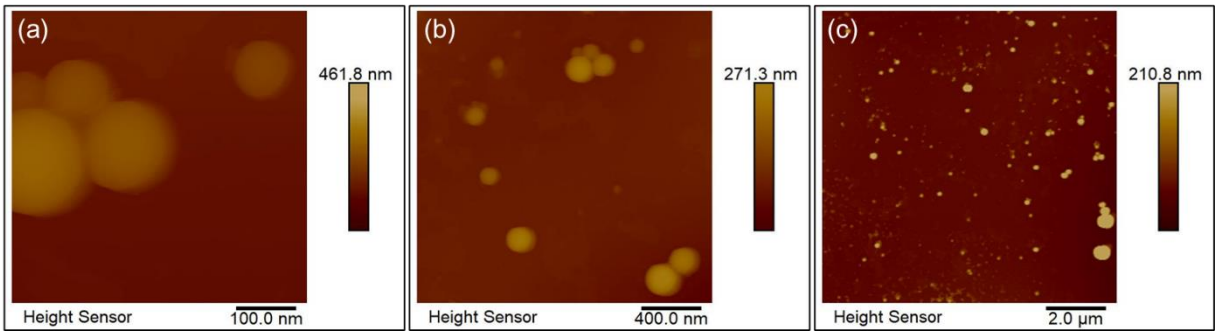

Figure 8: AFM images taken of LNPs prepared via the probe sonication technique at a sonication amplitude of 60 while in no bath. Area of sample imaged was (a) 500 nm x 500 nm, (b) 2 µm x 2 µm, and (c) 10 µm x 10 µm.

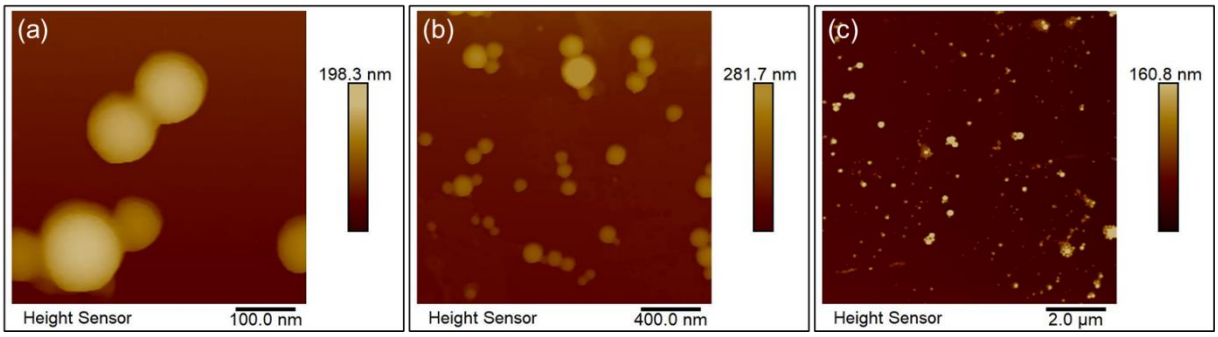

Figure 9: AFM images taken of LNPs prepared via the probe sonication technique at a sonication amplitude of 80 while in an ice bath. Area of sample imaged was (a) 500 nm x 500 nm, (b) 2 µm x 2 µm, and (c) 10 µm x 10 µm.

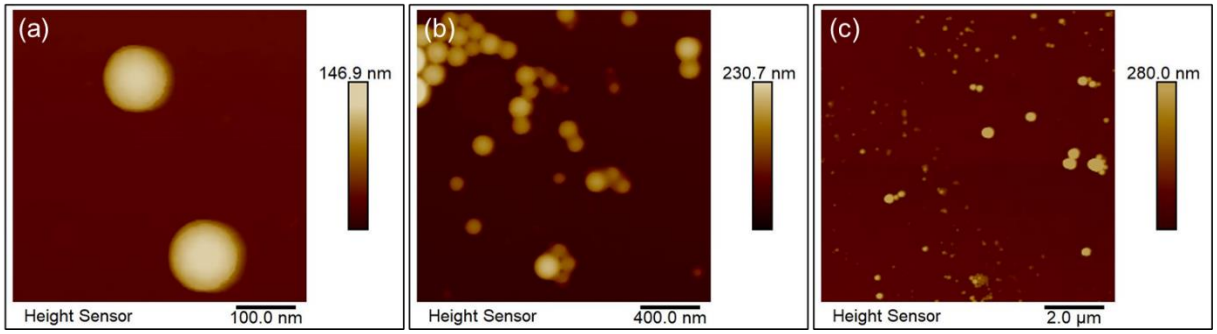

Figure 10: AFM images taken of LNPs prepared via the probe sonication technique at a sonication amplitude of 80 while in a water bath. Area of sample imaged was (a) 500 nm x 500 nm, (b) 2 µm x 2 µm, and (c) 10 µm x 10 µm.

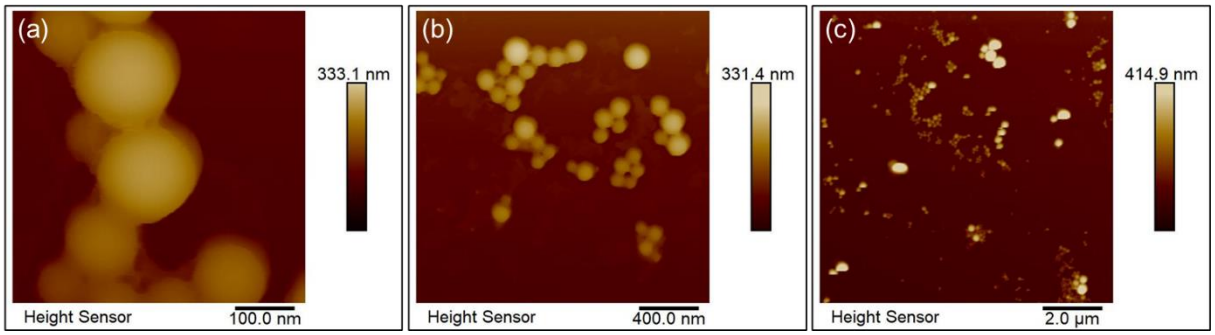

Figure 11: AFM images taken of LNPs prepared via the probe sonication technique at a sonication amplitude of 80 while in no bath. Area of sample imaged was (a) 500 nm x 500 nm, (b) 2 µm x 2 µm, and (c) 10 µm x 10 µm.

Table 3: Average diameter of h-LNPs determined by AFM.

Amplitude	Temperature after Sonication (˚C)	Calculated Power (W)	Average Diameter (nm)
40	28	20	60 ± 20
40	31	21	106 ± 25
40	57	17	102 ± 35
60	31	27	90 ± 60
60	36	27	144 ± 34
60	64	22	122 ± 50
80	24	35	98 ± 35
80	36	33	115 ± 28
80	70	27	94 ± 33

2.3 Ibuprofen Loaded LNPs

Once blank LNPs were successfully prepared using the probe sonicator technique, attempts to prepare Ibu-LNPs were made. Ibuprofen, in solution, was added to the sample prior to sonication. After sonication, the LNPs were isolated, and all unencapsulated ibuprofen was washed away using Amicon centrifugal filter units. This wash containing the unencapsulated ibuprofen was collected and assessed using ultraviolet-visible (UV-Vis) spectroscopy. By comparing UV-Vis spectra of the wash of the Ibu-LNPs to that of the blank-LNPs, the amount of unencapsulated ibuprofen could be calculated. The amount of unencapsulated ibuprofen was equal to the initial amount of ibuprofen that was added to the solution, indicating that the encapsulation of ibuprofen was not successful. As such, a different method for preparing Ibu-LNPs was attempted.

Zhang et al. had previously reported a single step nanoprecipitation technique in which h-LNPs self assembled to encapsulate docetaxel, a hydrophobic anticancer drug.[49] This nanoprecipitation technique was modified to include ibuprofen as the active ingredient. For this technique, polymer, and ibuprofen, in solution, were added dropwise to rapidly stirring, hot lipids (Figure 12). Once all the polymer-ibuprofen solution had been added to the lipids, the sample was vortexed, and then returned to a gradual stirring as the sample cooled to room temperature (Figure 12). The LNPs were isolated and washed in the same manner as the probe sonicator technique. A blank LNP sample was also prepared using this technique.

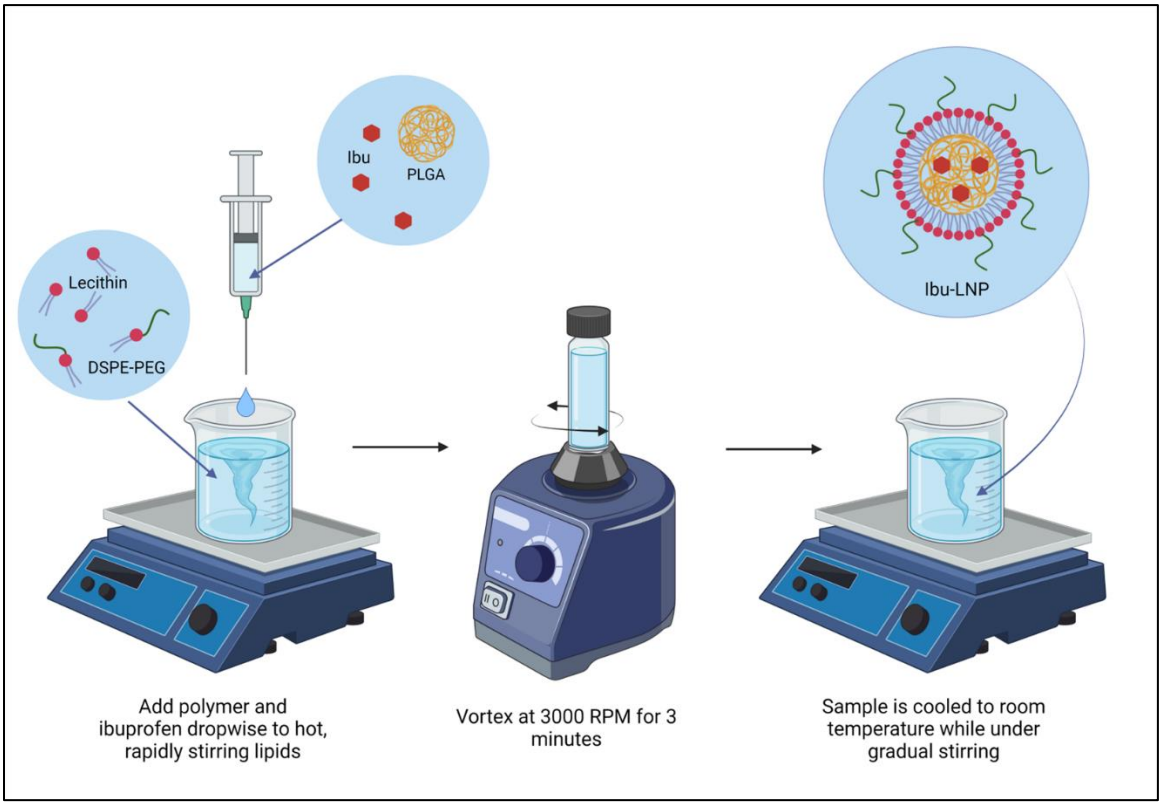

Figure 12: Illustration representing the self assembly of Ibu-LNPs using a nanoprecipitation technique. Created using BioRender.

UV-Vis spectroscopy was performed on blank LNP and Ibu-LNP samples (Figure 14). Subtracting the UV-Vis spectrum of the blank LNPs from the UV-Vis spectrum of the Ibu-LNPs, gave the absorbance spectrum from ibuprofen in the Ibu-LNP sample (Figure 15). The peak present

at 222 nm corresponded to 1.44 ± 0.02 mg of ibuprofen in the sample, as determined by an ibuprofen calibration curve prepared in hexane. 3 mg of ibuprofen was initially added to the sample, meaning that an encapsulation efficiency of 48% was achieved.

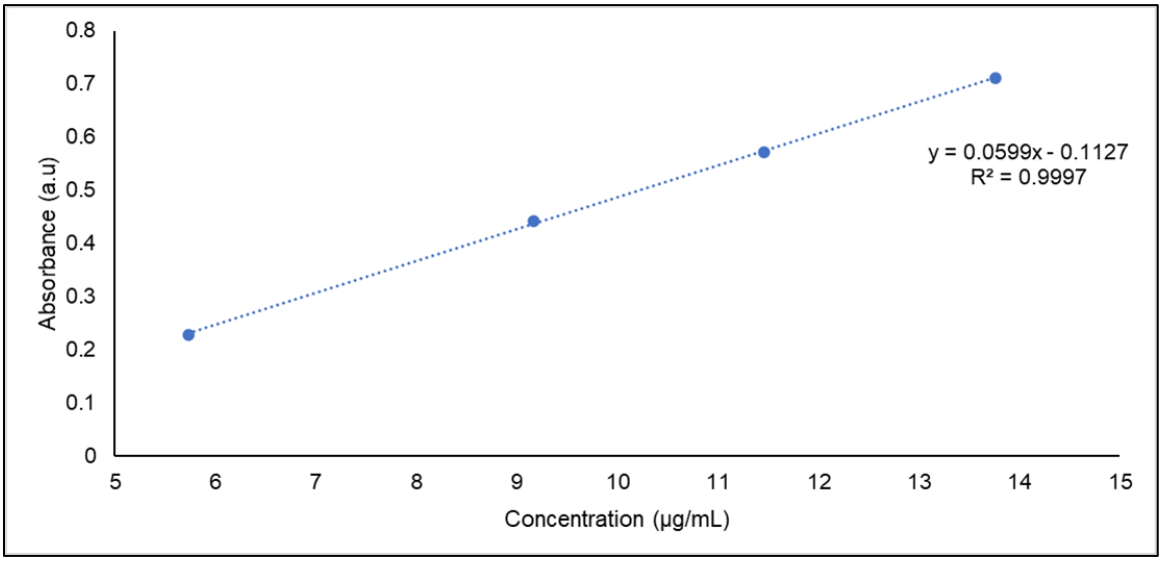

Figure 13: Ibuprofen calibration curve with concentrations ranging from 5-15 µg/mL.

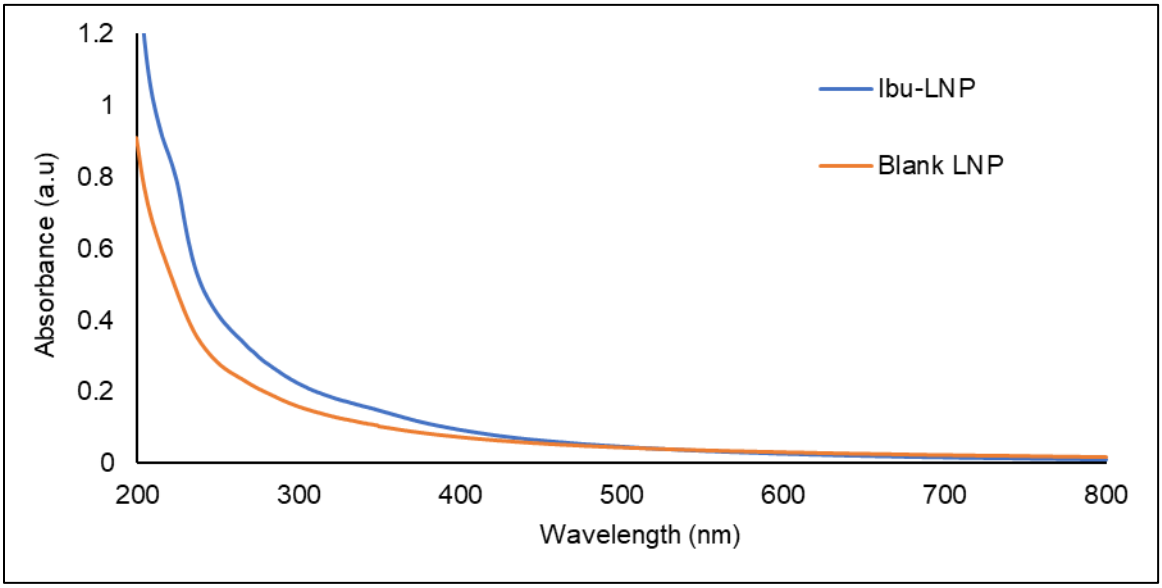

Figure 14: UV-Vis spectra of Ibu-LNPs and blank-LNPs, dispersed in H_2O.

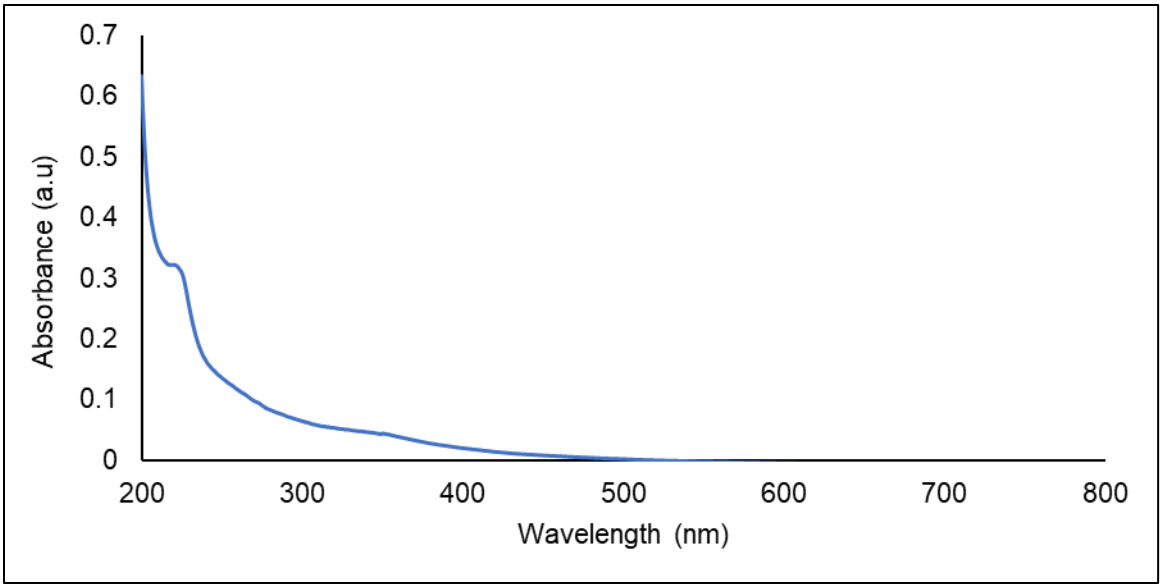

Figure 15: UV-Vis spectrum of ibuprofen present in the Ibu-LNPs, prepared by subtracting the UV-Vis spectrum of blank-LNPs from that of Ibu-LNPs.

2.4 FITC Labelled LNPs

FITC loaded LNPs (FITC-LNP) were prepared via the probe sonication technique. FITC was added to the sample solution prior to sonication, and excess FITC was removed via washing with Amicon centrifugal filter units, followed by dialysis. Under ambient light conditions, the FITC-LNPs were bright yellow in colour. Upon excitation with a long wave UV-lamp ($\lambda = 365$nm) the LNPs fluoresced a bright yellow-green colour (Figure 16).

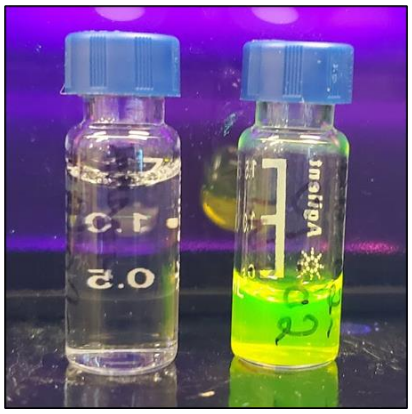

Figure 16: Blank LNPs (left) and FITC-LNPs (right) illuminated under long wave UV-light (365nm).

The FITC loaded LNPs were imaged using AFM. There were large LNP aggregates present with a mean diameter of 250 ± 30 nm in addition to small individual particles with a mean diameter of 60 ± 10 nm (Figure 17).

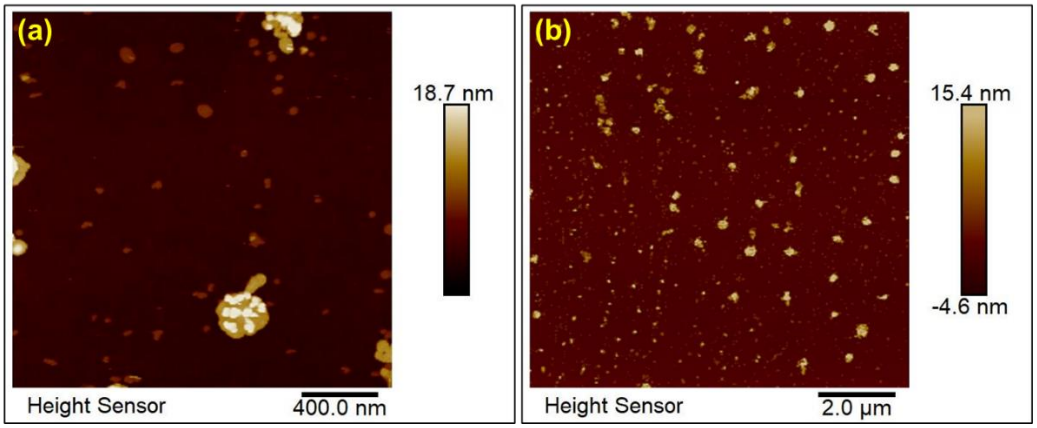

Figure 17: AFM images taken of FITC-LNPs prepared via the probe sonication technique at an amplitude of 60, spin coated on a silicon wafer. Area of sample imaged was (a) 2 µm x 2 µm (b) 10 µm x 10 µm.

FITC-LNPs were then drop cast on a glass coverslip and imaged using epifluorescence microscopy followed by super resolution imaging through radical fluctuations (SRRF) and stochastic optical reconstruction microscopy (STORM) (Figure 18). Individual particles were observed using epifluorescence microscopy, however, SRRF and STORM provided higher resolution images with low background levels. These super resolution images allowed for the morphology of the particles to be visualized and diameter of the particles to be measured in the range of 50-70 nm. Through these experiments, it was determined that FITC was a poor dye choice for this type of microscopy. FITC is prone to photobleaching which resulted in a reduced number of raw images that could be acquired for the reconstruction of SRRF and STORM images. For future super resolution microscopy experiments, a dye that exhibited better fluorescence properties would need to be used.

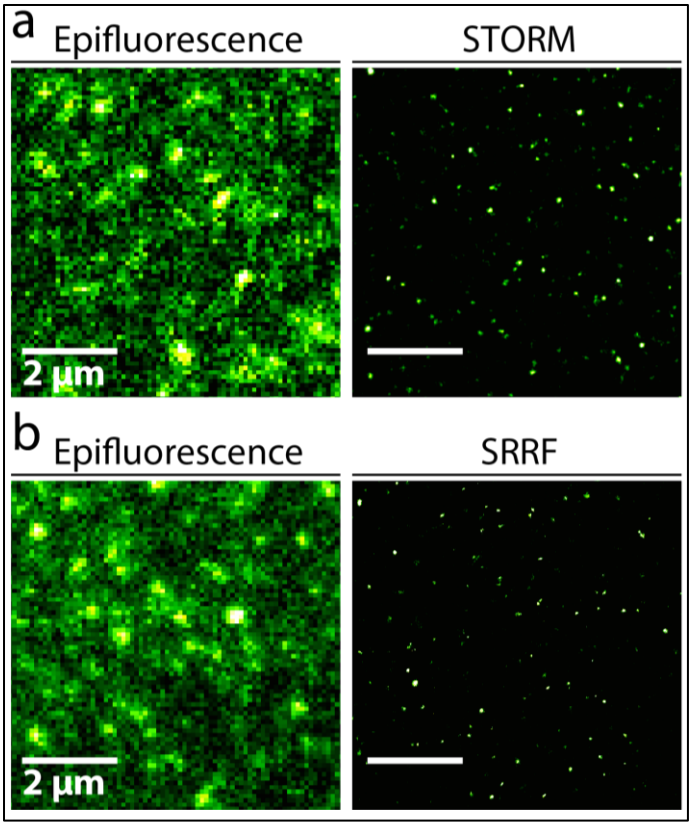

Figure 18:(a) STORM and (b) SRRF images taken of FITC-LNPs drop cast onto a clean glass coverslip.

2.5 LNPs from Acuitas Therapeutics

Commercially produced LNPs containing 1 milligram of model RNA per 1 milliliter of LNP sample were acquired from Acuitas Therapeutics. Embedded within the lipid layer of the LNPs was the fluorescent lipophilic cationic dye, 1,1'-dioctadecyl-3,3,3',3'-tetramethylindocarbocyanine (DiI). Compared to FITC, DiI is brighter, and has higher photostability and photo blinking properties.[52] When incorporated into lipid membranes, DiI is highly fluorescent, however in aqueous solutions is weakly fluorescent. DiI has an excitation wavelength of 549 nm, an emission wavelength of 565 nm, and gives the LNP sample a bright pink colour (Figure 19). The exact composition of these LNPs is proprietary. The diameter of the particles was disclosed to be approximately 86 nm.

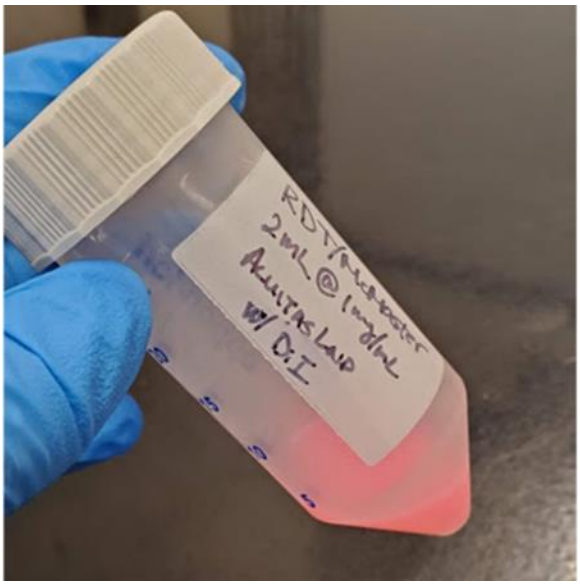

Figure 19: DiI labelled Acuitas-LNP sample containing 1 mg/mL model mRNA.

2.5.1 Dynamic Light Scattering on Acuitas Lipid Nanoparticles

Incorporating these particles into OTFs requires the LNPs to be able to withstand casting temperatures. To determine what temperatures the Acuitas-LNPs can withstand, they were subjected to a DLS temperature program. The DLS temperature program involved monitoring the effective diameter and polydispersity of the LNPs as the temperature was increased in 5˚C intervals from 25 to 90˚C. It was observed that the effective diameter of the particles remained constant at approximately 100 nm until the sample reached a temperature of 65˚C, at which point the effective diameter and polydispersity of the sample began to increase, indicating that aggregates were beginning to form (Figure 20). The observed effective diameter of the LNPs, at room temperature, was slightly higher 100 ± 1 nm than that of the theoretical mean diameter (86 nm). One possible explanation for the increase in the effective diameter is that the LNPs were dispersed in sterile-filtered water, suitable for cell culture. DLS measurements should not be performed in pure de-ionized water, as the size measured in deionized water will be 2-10 nm too large, due to

electrostatic interactions between particles. For more accurate size measurements, a salt, such as potassium nitrate should be added to the water.[53]

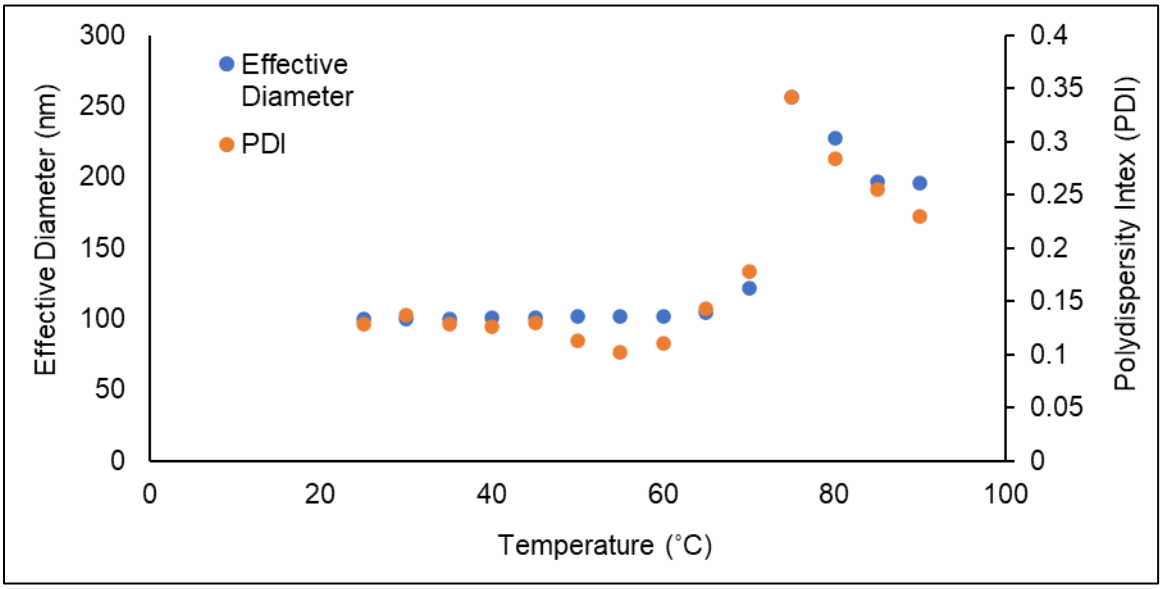

Figure 20: Plotted results from a DLS temperature program performed on Acuitas-LNPs showing the effective diameter and polydispersity index of the particles measured at temperatures ranging from 25-90˚C.

Table 4: Effective diameter and polydispersity index measured from a DLS temperature program performed on Acuitas-LNPs measured at temperatures ranging from 25-90˚C.

Temperature (˚C)	Effective Diameter (nm)	PDI
25	100 ± 1	0.13 ± 0.01
30	100 ± 1	0.14 ± 0.02
35	100 ± 1	0.13 ± 0.01
40	101 ± 1	0.13 ± 0.01
45	101 ± 1	0.13 ± 0.01
50	102 ± 1	0.11 ± 0.01
55	101 ± 1	0.10 ± 0.021
60	102 ± 1	0.11 ± 0.02

65	105 ± 1	0.14 ± 0.01
70	122 ± 4	0.18 ± 0.03
75	257 ± 31	0.34 ± 0.05
80	227 ± 24	0.28 ± 0.04
85	196 ± 14	0.25 ± 0.05
90	196 ± 14	0.23 ± 0.06

2.5.2 High Resolution Optical Microscopy on Acuitas-LNPs

Epifluorescence and high resolution stochastic optical reconstruction microscopy (STORM) was used to visualize Acuitas LNPs on a clean glass coverslip (Figure 21(a,b)). The LNPs were observed to be circular in shape (Figure 21(c)) with an average diameter of 85 ± 7 nm (Figure 21(e)). This average diameter corresponds very well with the theoretical average diameter of 86 nm.

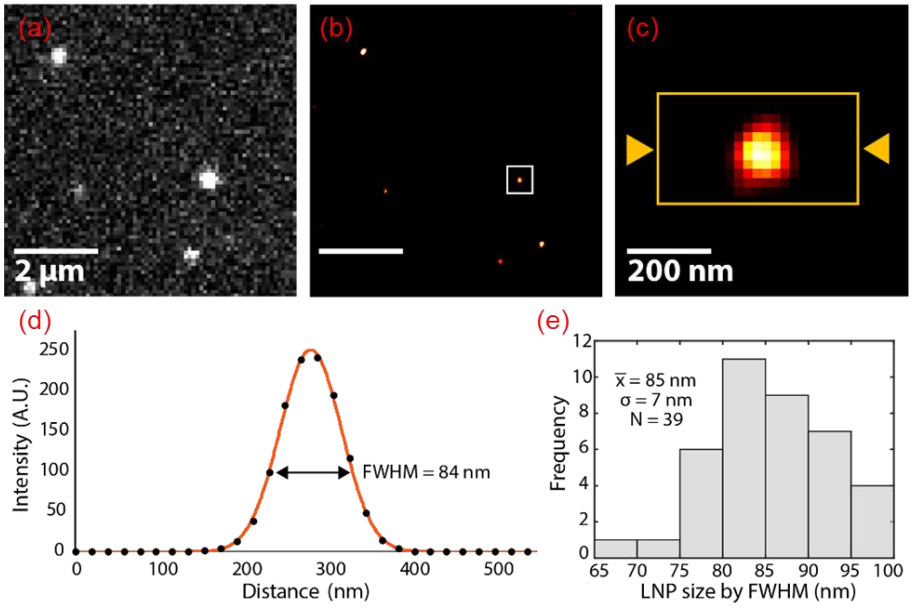

Figure 21: Epifluorescence (a) and STORM images (b,c) of Acuitas LNPs on a glass coverslip. Size of particles determined using full-width half max of single-particle line intensity profiles (d) to give an average particle diameter of 85 ± 7 nm (e).

2.6 Conclusion

Hybrid polymer-lipid nanoparticles were prepared via a probe sonication technique. Samples were prepared at various sonication amplitudes and temperatures. DLS measurements indicated that at a constant sonication amplitude but increasing sonication temperature, particle size increased. There was no size related trend observed for samples prepared under the same temperature conditions but at different sonication amplitudes. Next, blank and Ibu-LNPs were prepared using a nanoprecipitation technique. This method of preparation allowed for an ibuprofen encapsulation efficiency of 48%. FITC-LNPs were then prepared using the probe sonication technique. This resulted in the LNPs fluorescing a bright yellow-green colour when exposed to long wave UV light. The morphology and size of the FITC-LNPs were visualized using AFM and high-resolution optical microscopy. It was determined that using FITC as a fluorophore for this type of optical microscopy was not ideal due to its poor photostability properties. As such, LNPs produced by Acuitas Therapeutics were labelled with DiI, a fluorophore that exhibited higher photostability, brightness, and photo blinking properties than FITC. STORM was used to image Acuitas LNPs on a glass coverslip. A size distribution of the particles that matched the theoretical particle size was measured from the STORM images. Finally, a DLS temperature program was performed on the Acuitas LNPs in which the size distribution of the sample was measured while the sample was heated from 25-90˚C. After characterizing all the different LNPs discussed in this chapter, the LNPs were ready to be incorporated into OTFs.

2.7 Experimental

General

All optical microscopy images in this section were acquired by Dr. Mouhanad Babi and Christine Cerson. Acuitas-LNPs were obtained from Acuitas Therapeutics. All other reagents and

solvents were acquired from commercial sources. DLS measurements were acquired using a NanoBrook 90Plus PALS from Brookhaven. AFM images were acquired on a Bruker Dimesion iCon AFM in ScanAsyst mode with a ScanAsyst-Air tip. UV-Vis measurements were performed on a Cary 5000 UV-Vis NIR Spectrometer in double beam mode, using 3.5 mL quartz cuvettes with a 1 cm pathlength. Epifluorescence microscopy, SRRF, and STORM images were acquired on a custom-built Leica DMI6000B inverted microscope, equipped with a 100x/1.47NA oil-immersion objective. Samples were sonicated with a QSonica Q700 sonicator equipped with a microtip. Samples were centrifuged using a Thermo Scientific Sorvall Legend X1R Centrifuge.

Preparation of Blank LNPs Using Probe Sonicator – *modified from literature procedures.*[48]

Table 5: Concentration and volumes of stock solutions used for preparing h-LNPs via the probe sonicator technique.

Ingredient	Stock Solution Concentration	Volume of Stock Solution Added to Vial (mL)	Mass Added to Vial (mg)
DOPE-PEG	1 mg/mL in 4% EtOH Aqueous Solution	1	1
Lecithin	1 mg/mL in 4% EtOH Aqueous Solution	0.062	0.062
PLGA	2.5 mg/mL in ACN	2	2.5
H_2O	N/A	18.935	18 935

Stock solutions of DOPE-PEG, lecithin, and PLGA, were prepared as described in Table 5. The volume of each stock solution, as outlined in Table 5, were then added to a 40 mL glass vial. The tip of the probe sonicator was then placed halfway into the sample solution, and the glass vial was submerged in an ice bath, water bath, or no bath. The sample was sonicated at an amplitude of 40, 60, or 80 for 5 minutes. Immediately following sonication, the temperature of the sample was recorded. The samples were cooled to room temperature and washed 3 times with DI water using a Millipore Amicon Ultra centrifuge filter with a molecular weight cutoff of 100 kDa.

The LNPs were concentrated using the same centrifuge filter and dispersed in 2 mL DI water. The samples were stored in the fridge until needed.

h-LNPs Prepared via Nanoprecipitation – *modified from literature procedures.*[49]

Table 6: Concentration and volumes of stock solutions used for preparing h-LNPs via the nanoprecipitation technique.

Ingredient	Stock Solution Concentration	Volume of Stock Solution Added to Vial (mL)	Mass of Ingredient Used (mg)
DOPE-PEG	1 mg/mL in 4% EtOH Aqueous Solution	5	5
Lecithin	1 mg/mL in 4% EtOH Aqueous Solution	1	1
PLGA	5 mg/mL in ACN	4	20

Stock solutions of DOPE-PEG, lecithin, and PLGA were prepared as described in Table 6. 5 mL of the DOPE-PEG stock solution and 1 mL of the lecithin stock solution were added to a 20 mL glass vial. The lipids were heated in an oil bath at 92˚C, while stirring at 500 RPM. 3 mg of ibuprofen was dissolved in 4 mL of the PLGA stock solution and loaded into a 10 mL syringe. The ibuprofen-PLGA solution was added dropwise using a syringe pump into the 92˚C stirring lipids at a speed of 0.2 mL/min. The glass vial was then capped, removed from the oil bath, and vortexed at 3000 RPM for 3 minutes. The cap was removed from the vial and returned to the oil bath, stirring at a speed of 500 RPM. The heating for the oil bath was turned off, and the sample was allowed to gradually cool to room temperature. To prepare blank-LNPs the procedure was repeated except no active ingredient was dissolved in the PLGA stock solution. The sample was washed 3 times with DI water, using a Millipore Amicon Ultra centrifuge filter with a molecular weight cutoff of 100kDa. The LNPs were concentrated using the same centrifuge filter and dispersed in 2 mL DI water. The samples were stored in the fridge until needed.

Preparation of FITC-LNPs via the Probe Sonicator Technique

Table 7: Concentration and volumes of stock solutions used for preparing FITC-LNPs via the probe sonicator technique.

Ingredient	Stock Solution Concentration	Volume of Stock Solution Added to Vial (mL)	Mass Added to Vial (mg)
DOPE-PEG	1 mg/mL in 4% EtOH Aqueous Solution	0.127	0.127
Lecithin	1 mg/mL in 4% EtOH Aqueous Solution	0.029	0.029
PLGA	2.5 mg/mL in ACN	0.400	1
FITC	1 mg/mL in EtOH	0.100	0.1
H_2O	N/A	3.785	3785

Stock solutions of DOPE-PEG, lecithin, PLGA, and FITC were prepared as described in Table 7. The volume of each stock solution, as outlined in Table 7, were then added to a 20 mL glass vial. The tip of the probe sonicator was then placed halfway into the sample solution. The sample was sonicated at an amplitude of 60 for 5 minutes. The sample was washed with 4% EtOH aqueous solution 6 times, then 2 times with DI water, using a Millipore Amicon Ultra centrifuge filter with a molecular weight cutoff of 10kDa. The LNPs were concentrated using the same centrifuge filter and dispersed in 0.5 mL DI water. The FITC-LNPs were then dialyzed with 12 kDa cutoff tubing against water, until the dialysis water was no longer fluorescent under a long wave UV-lamp (365 nm). This required the LNPs to be dialyzed for 48 hours, with a water change at 24 hours. The samples were stored in the fridge until needed.

AFM Sample Preparation

30 µL of LNP sample was spin coated onto a silicon wafer, at 10 µL increments, at a speed of 1000 RPM for 30 seconds.

Optical Microscopy Sample Preparation

FITC-LNPs were diluted 1:100 in DI water. 5µL of the 1:100 FITC-LNP solution was dried onto a plasma cleaned glass coverslip.

Acuitas-LNPs were diluted 1:100 and 1:1000 in DI water. The samples were spin coated onto plasma cleaned glass coverslips at 3000 RPM for 30 seconds.

DLS Sample Preparation

h-LNPs, prepared via the probe sonication technique, were diluted 1:200 with DI water and 2mL of sample was added to a polystyrene cuvette.

Acuitas-LNPs were diluted by adding 25 µL of Acuitas-LNPs to 2 mL sterile water. The Acuitas-LNPs were then further diluted by adding 50 µL of the dilute Acuitas-LNPs to 2 mL sterile water. 2 mL of this sample was then added to a quartz cuvette.

UV-Vis Sample Preparation

Ibu-LNPs and blank-LNPs were diluted 1: 1000 in DI water, and 2 mL of sample was added to a quartz cuvette.

Chapter 3 – Incorporation of Lipid Nanoparticles into Oral Thin Films

3.1 Overview

In this chapter, FITC-LNPs that were prepared and discussed in Chapter 2 were embedded in an OTF (FITC-LNP-OTF). The FITC-LNP-OTF was then imaged using STORM. STORM allowed imaging of individual particles within the film and indicated that the particles remained intact after the film casting process.

Acuitas-LNPs were then loaded into an OTF (Acuitas-LNP-OTF) and imaged using STORM. STORM was again able to image the individual particles within the film and indicated that the particles remained intact after the film casting process.

The Quant-iT RiboGreen RNA assay was then employed to determine the encapsulation of RNA within the Acuitas-LNPs both prior to and after being incorporated into an OTF. The RiboGreen assay indicated that there were stability issues with the LNPs when incorporated into an OTF. This resulted in changes to film formulation, and several studies surrounding how the LNPs could be handled during the incorporation into the film mixture and during film casting process.

Confocal microscopy was used to visualize what was occurring during the RiboGreen assay. Once the films were dissolved there were large aggregates of lipids that contained fluorescence for both RiboGreen dye and DiI. These aggregates were not observed prior to the film dissolution. Different film additives were incorporated into the Acuitas-LNP-OTF in attempts to stabilize the LNPs. DOPE-PEG being one of those additives. DOPE-PEG was found to stabilize the LNPs in a manner that resulted in the RNA remaining encapsulated within the LNPs after the film casting process.

3.2 Super Resolution Optical Microscopy on LNPs Embedded in OTFs

Super resolution microscopy was performed on OTFs that contained both FITC-LNPs and Acuitas-LNPs. The goal of acquiring these images was to compare the images of the LNPs on a glass coverslip to the images of the LNPs in the OTF. If the particle size and distribution of the LNPs within the OTF was unchanged compared to that on the glass slide, this would indicate that the LNPs remained intact after the film casting process. If there were large aggregates of particles, or streaks of fluorescence throughout the OTF, this would indicate that the LNPs were compromised during the film casting process.

3.2.1 Incorporating FITC Labelled LNPs in OTFs

FITC-LNPs produced as described in Chapter 2 were incorporated into an OTF (FITC-LNP-OTF). When under ambient light conditions, the films were clear and colourless (Figure 22(a)). However, when exposed to long wave ultraviolet (UV) light (365nm) the films became fluorescent and were a bright green-yellow colour (Figure 22(b)). When irradiated with UV-light, bubbles within the film became apparent. The bubbles are produced during the paddle mixing that is used to incorporate the LNPs into the film mixture. One way to reduce the number of bubbles present in the OTF is to let the film mixture settle for longer time periods after paddle mixing.

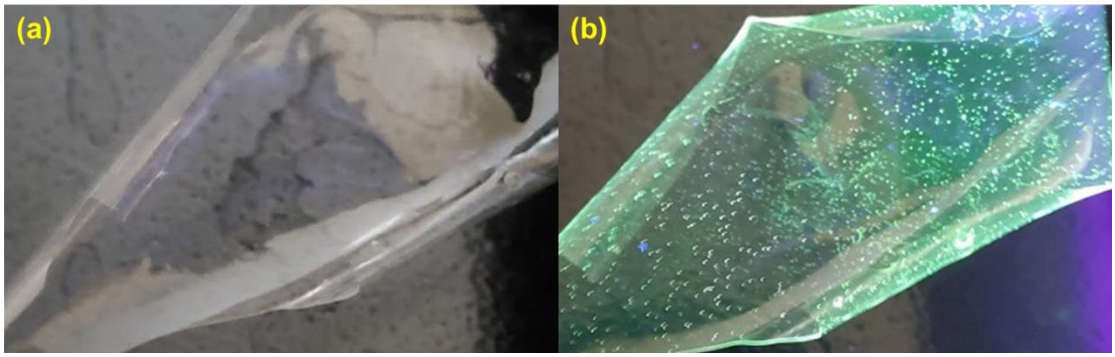

Figure 22: OTF containing FITC-LNPs under (a) No UV-light (b) Long wave UV-Light (365nm).

To determine if the FITC-LNPs were damaged during the film casting process, the FITC-LNP-OTF was imaged using epifluorescence microscopy followed by SRRF (Figure 23). Individual, circular, particles with an average size of 100 ± 24 nm were observed in the images.

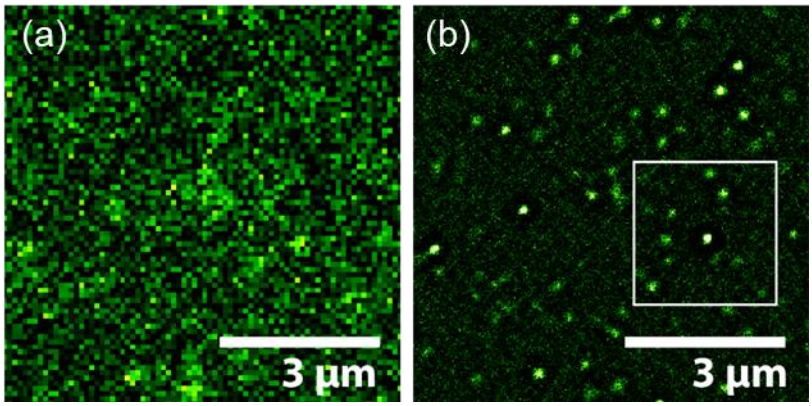

Figure 23: Images of FITC loaded LNPs incorporated into an oral thin film obtained using (a) Epifluorescence microscopy and (b) SRRF.

The ability to image the FITC-LNPs embedded within the OTF showed promise for being able to image Acuitas-LNPs in an OTF. Particularly because DiI, the dye in the Acuitas LNPs, is brighter and less prone to photobleaching than FITC, which allows for more acquisitions.[52]

3.2.2 Incorporating Acuitas LNPs into OTFs

Acuitas-LNPs were embedded in an OTF (Acuitas-LNP-OTF) in the same manner as the FITC-LNPs. The films were cast at 35˚C to limit any effects temperature had on the stability of the LNPs. To acquire super resolution microscopy images of the Acuitas-LNP films, the film mixture was cast directly onto a clean glass coverslip (Figure 24).

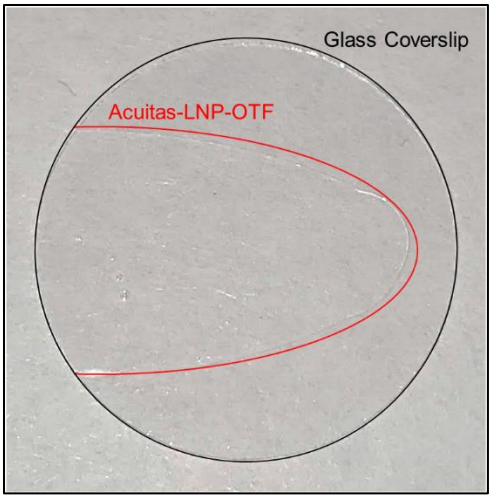

Figure 24: Acuitas-LNP-OTF (red) cast on a glass coverslip (black) for optical microscopy.

The STORM images of the Acuitas-LNP-OTF indicated that after being incoporated into the OTF, the LNPs remained circular in shape (Figure 25(e)) and had an average diameter of 75 ± 11 nm. If the LNPs were compromised during the film casting process they would likely appear larger in diameter due to particle aggregation. In addition, if the LNPs were compromised their shape might be irregular due to the particles being sheared.

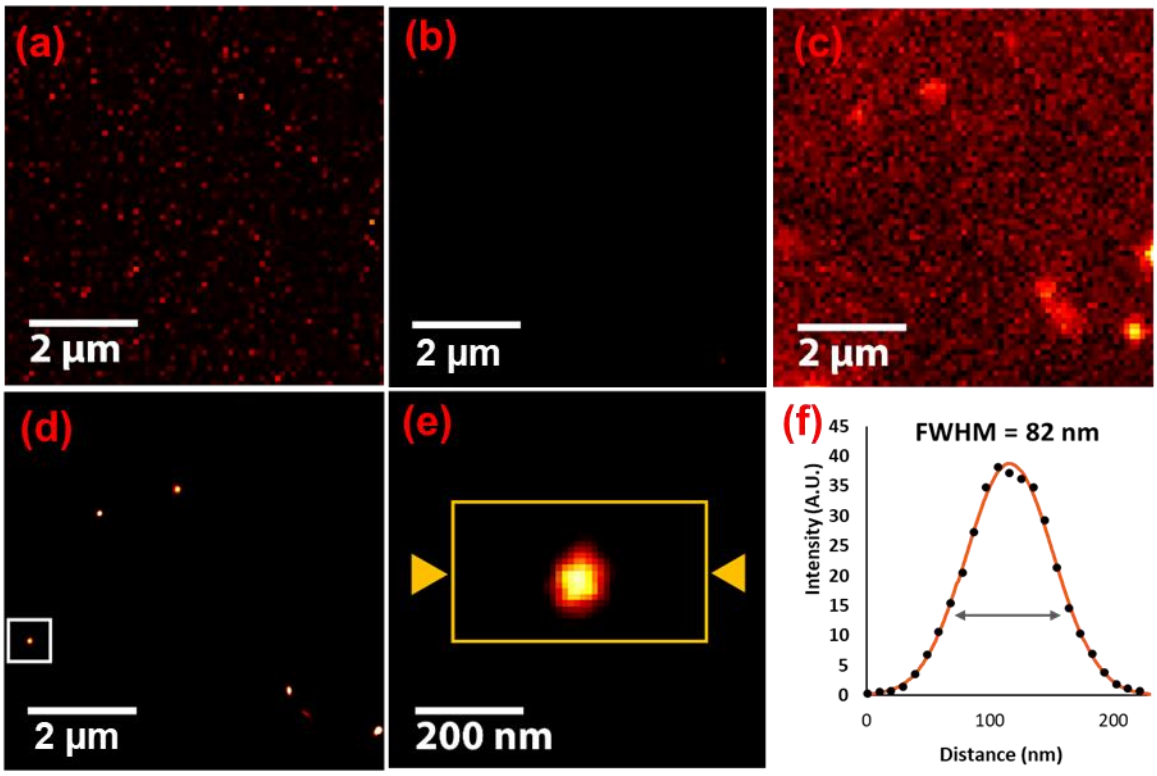

Figure 25: (a) Epifluorescence image of blank film. (b) STORM image of blank film. (c) Epifluorescence image of 1:1000 diluted Acuitas film. (d) STORM image of 1:1000 diluted Acuitas film. (e) Image of Acuitas-LNP in OTF shown in white box in (d). (f) Single-particle line-intensity profile of Acuitas-LNP shown in (e).

3.3 Determining LNP RNA Encapsulation Using the Quant-it RiboGreen RNA Assay

Once the Acuitas-LNPs had been imaged within the OTF and appeared to be structurally intact, it was necessary to ensure that the RNA remained encapsulated within the LNPs after the film casting process. The Quant-iT RiboGreen RNA assay kit was used to determine RNA encapsulation. RiboGreen dye is a monomethine dye and is used in the assay to detect RNA. In its unbound form, RiboGreen dye is non fluorescent; however, when it binds to nucleic acids it fluoresces a bright green colour. The fluorescence of the sample can then be used to quantify the amount of RNA present, using a calibration curve prepared with known amounts of RNA standard (Figure 26).

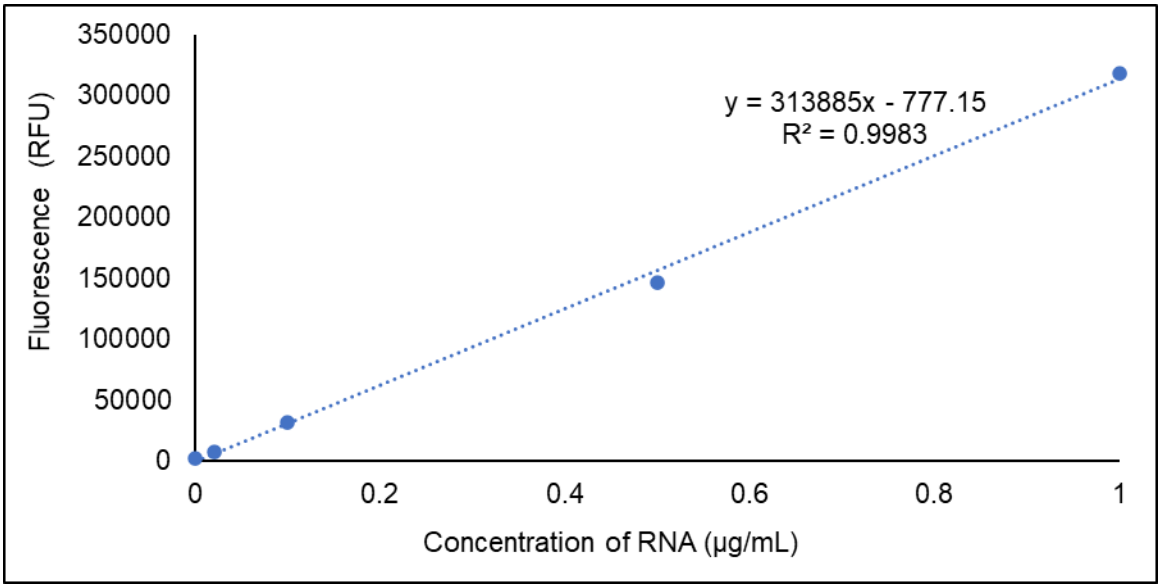

Figure 26: Calibration curve prepared for the Quanti-iT RiboGreen RNA assay showing the concentration of RNA and its respective amount of fluorescence.

To determine RNA encapsulation within the LNP samples, the samples were diluted using TE buffer. If the RNA remained encapsulated within the LNPs, the RiboGreen dye was not able to access the RNA. This resulted in no fluorescence from the sample (Figure 27). If the LNPs were compromised, the RiboGreen dye could access the RNA, which resulted in fluorescence from the sample. The Acuitas-LNP samples were then added to a 2% Triton solution. Triton is a surfactant, that breaks open the Acuitas-LNPs. Treating the LNP sample with 2% Triton, allowed for the RiboGreen dye to access the RNA and quantify how much RNA was present in the sample (Figure 27).

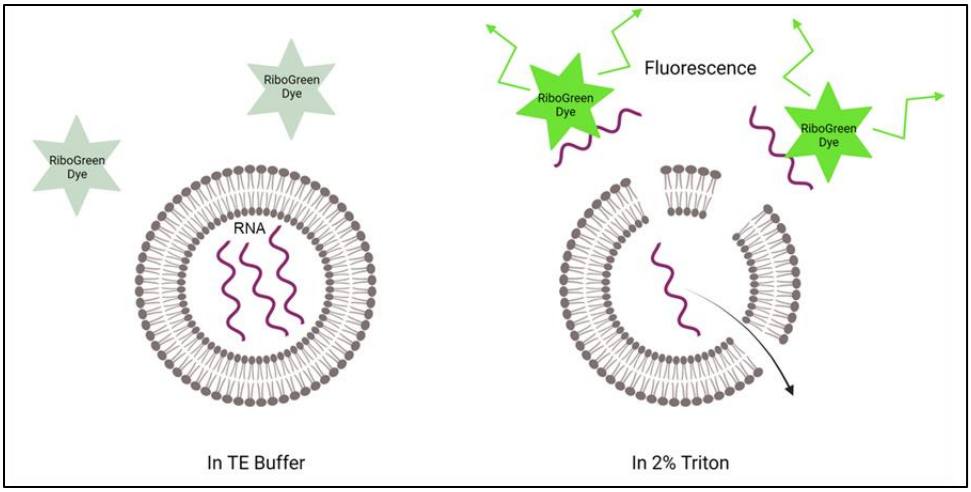

Figure 27: Illustration representing how the RiboGreen dye interacted with the RNA present in the Acuitas-LNPs in TE buffer vs 2% Triton solution. Created using BioRender.

3.3.1 Quant-iT RiboGreen Assay on Acuitas-LNPs

The RiboGreen assay was first performed on Acuitas-LNPs, as received, in the absence of any film components. Over the course of this project, two shipments of Acuitas-LNP samples were received. The theoretical RNA concentration of both shipments was 1 mg of RNA per mL of LNP solution. Both samples had similar RiboGreen assay results. There were low amounts of RNA detected when the sample was in TE buffer, and high amounts of RNA detected after being treated with Triton.

The RiboGreen assay was performed on the first shipment of Acuitas-LNPs (Acuitas-LNP-1) at theoretical concentrations of 1.25 µg/mL, 0.75 µg/mL, and 0.5 µg/mL (Figure 28). In TE buffer, these samples gave RNA concentrations of 0.055 ± 0.004 µg/mL, 0.04 ± 0.01 µg/mL, and 0.025 ± 0.001 µg/mL, respectively. After being treated with Triton, these samples gave RNA concentrations of 0.92 ± 0.06 µg/mL, 0.62 ± 0.01 µg/mL, and 0.31 ± 0.05 µg/mL, respectively. All three concentrations of Acuitas-LNP-1 had lower values of RNA detected, in the 2% Triton, than the theoretical value indicated.

The second shipment of Acuitas-LNPs (Acuitas-LNP-2) had higher amounts of RNA present in the 2% Triton than the theoretical value. The RiboGreen assay performed on Acuitas-LNP-2 at a theoretical concentration of 0.625 µg/mL, gave 0.099 ± 0.001 µg/mL of RNA in TE buffer, and an RNA concentration of 0.774 ± 0.004 µg/mL after treatment with Triton (Figure 28).

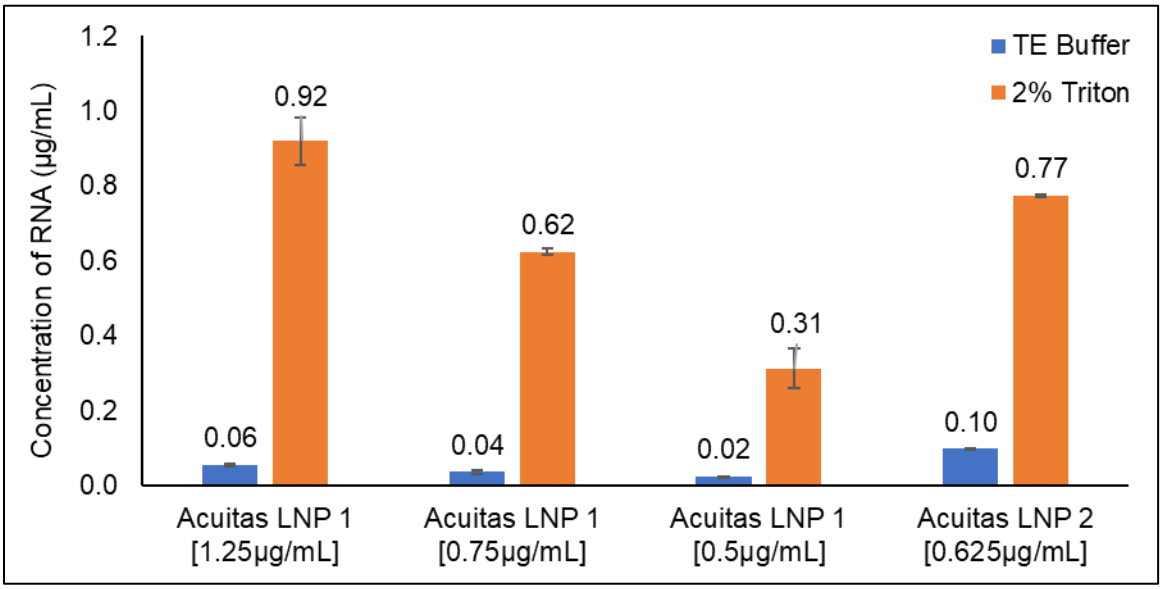

Figure 28: RiboGreen assay performed on Acuitas-LNP-1 and Acuitas-LNP-2. Theoretical RNA concentrations varied from 0.5 µg/mL to 1.25 µg/mL and are denoted by the square brackets.

3.3.2 Isolating Acuitas-LNPs from an OTF

Once the RNA encapsulated within the Acuitas-LNPs had been successfully quantified using the RiboGreen assay, the next step was to incorporate the Acuitas-LNPs into an OTF (Acuitas-LNP-OTF-1). Once the film was prepared, attempts to isolate the LNPs from the film components were made. The main reason for isolating the Acuitas-LNPs from the film components was to be able to perform DLS on the particles and verify that the particle size distribution had not changed. In addition, the RiboGreen assay could be performed directly on the particles without possible interference from the film components.

Initially, to isolate the Acuitas-LNPs from the film components, Acuitas-LNP-OTF-1 was dissolved in buffer. The dissolved film was then placed in a Millipore Amicon centrifugal filter with a molecular weight cutoff of 100 kDa and centrifuged for 30-minute time intervals. After every 30 minutes, additional buffer was added to try re-dispersing the film mixture that had become concentrated. Despite several hours of centrifuging, the entire film mixture could not be fully removed from the LNPs. Pullulan was remaining in the filter with the LNPs, due to its molecular weight being 200 kDa.

To remove the entire film solution, pullulanase, an enzyme that degrades pullulan by the hydrolysis of α-1,6 and α-1,4 linkages within the pullulan, was added to the dissolved film solution prior to centrifugation. This allowed the Acuitas-LNPs to be isolated from the other film components with significantly less centrifuging. The LNPs were then re-dispersed with buffer and characterized using the RiboGreen assay. When the RiboGreen assay was performed on the isolated LNPs, there was essentially no RNA detected for the sample in TE buffer or 2% Triton (Figure 29). The sample had a theoretical concentration of 1.25 µg/mL RNA. In TE buffer the sample had an RNA concentration of 0.0204 ± 0.0003 µg/mL and in 2% Triton the sample had an RNA concentration of 0.072 ± 0.002 µg/mL.

There were two immediate possible explanations for these results. The first being that the centrifugation during the isolation process had damaged the LNPs and the RNA had been removed from the particles. The second possibility was that the pullulanase was interfering with the assay or damaging the particles in some way. To determine the cause, Acuitas-LNPs were centrifuged for 2 hours under the same conditions as during the isolation process, and then had the RiboGreen assay performed on them (Figure 29). The theoretical RNA concentration of the sample was 1.25 µg/mL RNA. The RiboGreen assay showed that the sample had 0.090 ± 0.001 µg/mL RNA in TE

buffer and 0.880 ± 0.009 µg/mL RNA in 2% Triton, indicating that the centrifugation was not the cause of the issue.

Next, one drop of pullulanase was added to Acuitas-LNPs in TE buffer. The sample was prepared to have a theoretical concentration of 1.25 µg/mL RNA. The RiboGreen assay performed on that sample indicated very low amounts of RNA present (Figure 29). In TE buffer the sample had an RNA concentration of 0.0239 ± 0.0004 µg/mL and in 2% Triton the sample had an RNA concentration of 0.17 ± 0.02 µg/mL. These results indicated that pullulanase could not be used to isolate the LNPs from the OTF.

To remove most of the film components from the Acuitas-LNP-OTF, an Acuitas-LNP-OTF-1 was dissolved, without the addition of pullulanase, and filtered with a Millipore Amicon centrifugal filter with a molecular weight cutoff of 100kDa, as previously described. The RiboGreen assay performed on this sample indicated that there was 0.21 ± 0.03 µg/mL of RNA present in the Triton treated sample (Figure 29). This was significantly lower than the 1.25 µg/mL theoretical concentration. In addition, there was 0.274 ± 0.002 µg/mL of RNA present in the sample prior to treatment with Triton. Given that there was such a low concentration of RNA present in the 2% Triton solution and that there was an equivalent amount of RNA present in the TE buffer, it was concluded that the RNA was not encapsulated within the Acuitas-LNPs after being incorporated into the OTF.

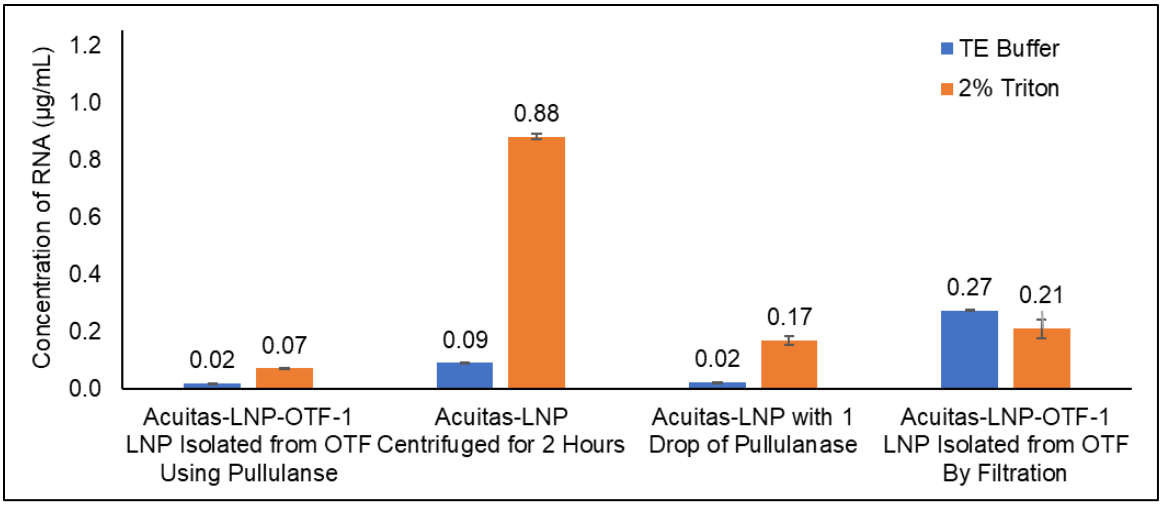

Figure 29: Results from the RiboGreen assay performed on isolated Acuitas-LNPs, centrifuged Acuitas-LNPs, and Acuitas-LNPs with Pullulanase. The theoretical concentration of all samples was 1.25 ug/mL.

The results from these experiments brought up two questions. The first being whether it was necessary to isolate the Acuitas-LNPs from the other film components when performing the RiboGreen assay. The second being whether the RNA within the Acuitas-LNPs remained encapsulated when the Acuitas-LNPs were in a wet film mixture.

3.3.3 Determining if LNP Isolation from Film Components is Necessary

There were two main concerns related to the film components interfering with the RiboGreen assay. The first concern was that the RiboGreen dye would bind to one of the film components resulting in fluorescence not caused by RNA. A blank-OTF, containing no Acuitas-LNPs was prepared. The RiboGreen assay was performed on the blank-OTF and showed 0.0037 ± 0.0004 µg/mL of RNA in TE buffer and 0.0054 ± 0.0001 µg/mL of RNA after being treated with Triton (Figure 30). This indicated that the film components did not contribute to fluorescence values observed during the RiboGreen assay.

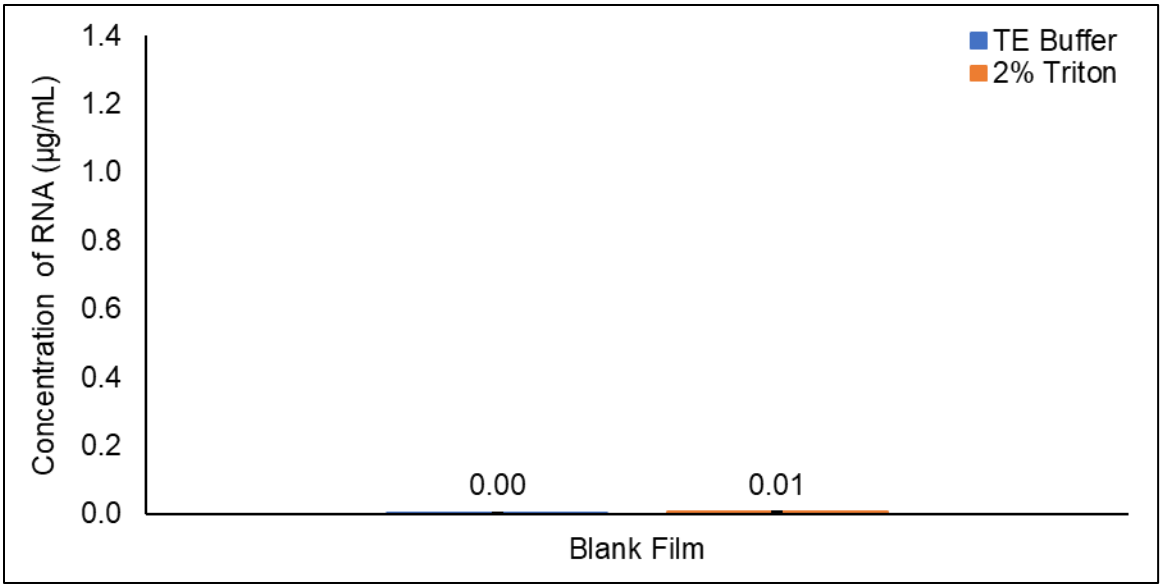

Figure 30: Results from the RiboGreen Assay performed on a blank-OTF containing no RNA.

The second concern regarding the film components interfering with the RiboGreen assay, was that the film components would inhibit RiboGreen's ability to access the RNA. To test this, the RNA standard from the RiboGreen assay kit was incorporated into a film mixture (RNA-FM) and an OTF (RNA-OTF) was prepared. Since the RNA standard was not incorporated into LNPs, the sample was expected to have equal amounts of fluorescence both prior to and after being treated with Triton. The RNA samples were prepared to give a theoretical concentration of 0.625µg/mL RNA. The RNA-FM gave an RNA concentration of 0.426 ± 0.006 µg/mL in TE buffer, and a concentration of 0.41 ± 0.04 µg/mL when treated with Triton (Figure 31). The RNA-OTF had an RNA concentration of 0.394 ± 0.002 µg/mL in TE buffer, and a value of 0.405 ± 0.009 µg/mL when treated with Triton (Figure 31). This means that approximately 62 - 66% of the RNA that was added to film mixtures could be detected. This is also not accounting for any loss of RNA during the paddle mixing of the film mixture or the casting of the film mixture. In addition, since the amount of RNA measured in the RNA-OTF was approximately the same as that measured in

the RNA-FM, it could be concluded that the drying of the RNA in the film mixture does not prevent the RiboGreen dye from binding to the RNA.

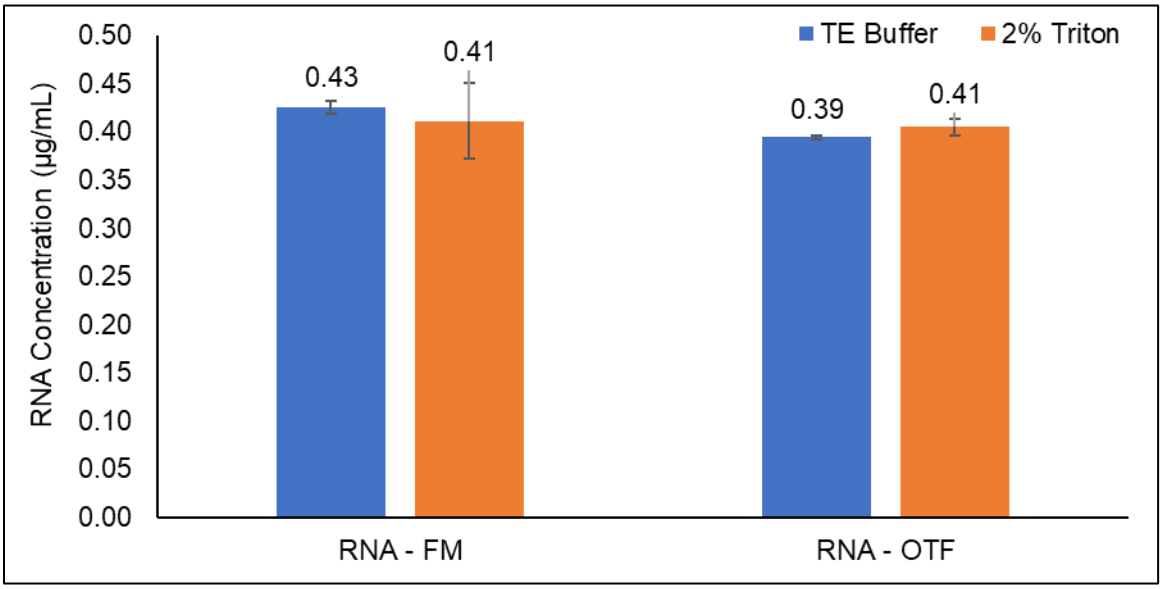

Figure 31: Results from the RiboGreen assay performed on an RNA-FM and an RNA-OTF. The theoretical RNA concentration of both samples was 0.625 µg/mL.

The results obtained from performing the RiboGreen assay on the blank OTF, the RNA-FM, and the RNA-OTF, indicated that the film components did not interfere with the assay, and that future Acuitas-LNP-OTF samples would not need to have the LNPs isolated.

3.3.4 The Effects of Tween on the Stability of the LNPs

The next experiment that was performed involved running the RiboGreen assay on a dissolved Acuitas-LNP film mixture (Acuitas-LNP-FM-1) that had previously been used to prepare Acuitas-LNP-OTF-1. It had previously been observed that the LNPs were unstable in Acuitas-LNP-OTF-1, as indicated by RNA being detected in the sample prior to being treated with Triton (Figure 29). By running the assay on the Acuitas-LNP-FM-1 the cause of the instability could be determined. The instability of the LNPs could have been caused by the casting of the film, or by a component in the film mixture compromising the LNP stability. The Acuitas-LNP-

FM-1 was prepared to have a theoretical RNA concentration of 1.25 µg/mL. The RiboGreen assay performed on the Acuitas-LNP-FM-1 showed an RNA concentration of 0.89 ± 0.07 µg/mL in TE buffer and an RNA concentration of 0.68 ± 0.09 µg/mL after treatment with Triton (Figure 32). The large amount of RNA present in the TE buffer, indicated that there was something in the film mixture that was degrading the LNPs.

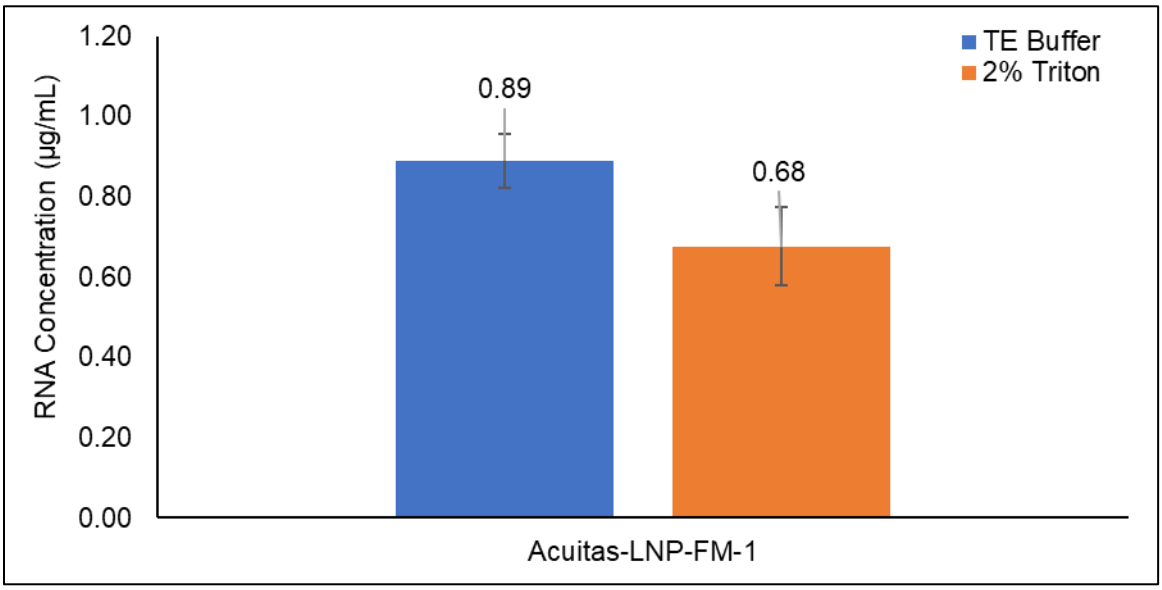

Figure 32: Results from the RiboGreen assay performed on Acuitas-LNP-FM-1. The theoretical RNA concentration of the sample was 1.25 µg/mL.

The composition of the film was then considered. One of the ingredients that was in the film mixture was Tween, a surfactant similar to Triton. To determine if Tween can break open the LNPs, the RiboGreen assay was repeated on Acuitas-LNPs, with an RNA concentration of 1.25 µg/mL. Instead of the treating the particles with Triton, however, Tween was used. The assay indicated that Tween is equally effective at breaking open Acuitas-LNPs, with the assay giving an RNA concentration of 0.0529 ± 0.0005 µg/mL in TE buffer, and an RNA concentration of 0.90 ± 0.02 µg/mL when treated with Tween (Figure 33).

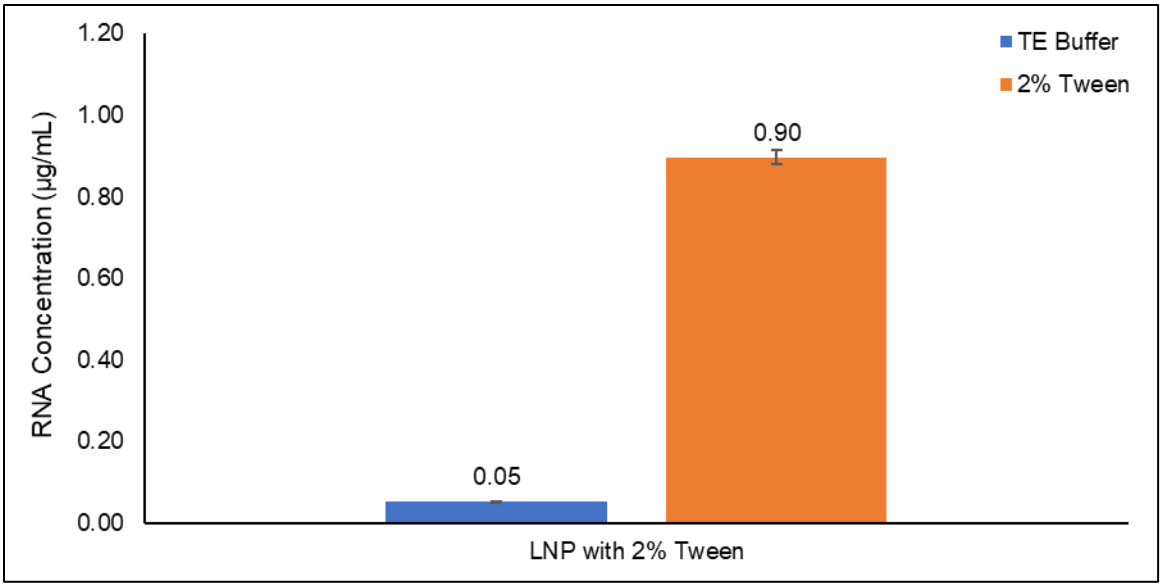

Figure 33: Results from the RiboGreen assay performed on Acuitas-LNPs where 2% Triton has been substituted for 2% Tween. The theoretical RNA concentration of the sample was 1.25 ug/mL.

As a result, an Acuitas-LNP-FM was prepared without Tween (Acuitas-LNP-FM-2), at a theoretical RNA concentration of 1.25 µg/mL. The RiboGreen assay performed on Acuitas-LNP-FM-2 showed 0.45 ± 0.01 µg/mL of RNA present in the TE Buffer and 0.603 ± 0.005 µg/mL of RNA present when treated with Triton. This was an improvement as there was roughly half the amount of RNA present in the TE buffer than there was in Acuitas-LNP-FM-1, however removing the Tween from the film mixture did not fully stabilize the LNPs. As such, further experiments were required to determine the cause of the instability of the Acuitas-LNPs.

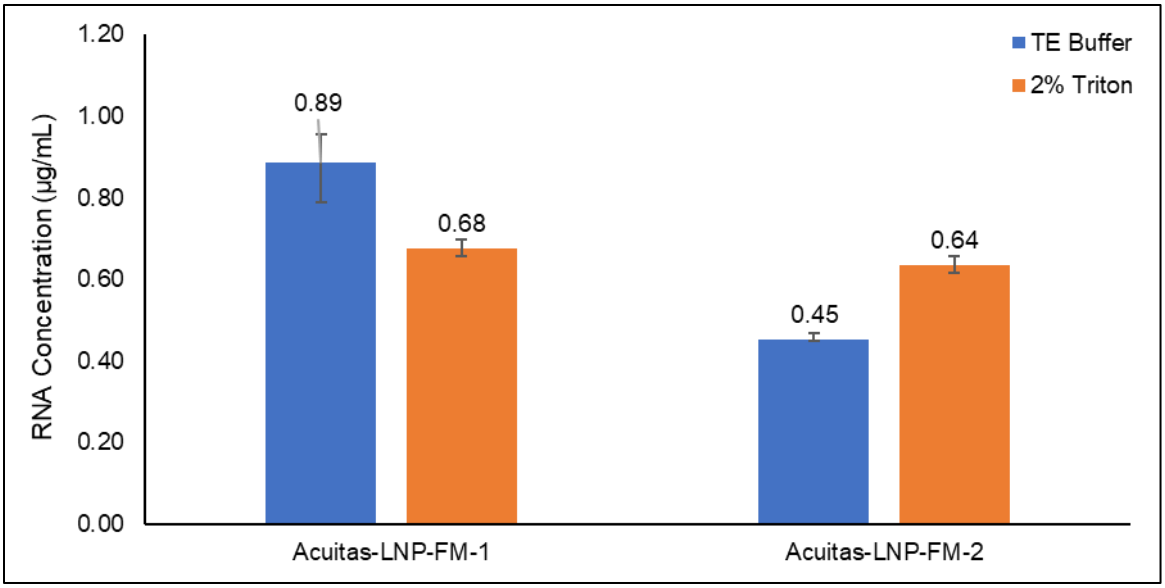

Figure 34: Results from the RiboGreen assay performed on Acuitas-LNP-FM-1 and Acuitas-LNP-FM-2. The theoretical RNA concentration of both samples was 1.25 µg/mL.

3.3.5 The Effect of Film Mixture pH on LNP Stability

The next variable that was considered was the pH of the film mixture. Acuitas-LNPs are designed to be stable under physiological pH conditions, and allow the release of RNA at a pH of 6.5, the pH conditions of the endosome.[34,37] The pH of the film mixture used to prepare Acuitas-LNP-FM-2 was measured to be 6.4. To increase the pH, a new film mixture was prepared in which some of the water within the film mixture was replaced with tris(hydroxymethyl) aminomethane (tris) buffer (0.1 M, pH = 8). This resulted in the film mixture pH increasing to 7.8.

Acuitas-LNPs were incorporated into this film mixture (Acuitas-LNP-FM-3), and the RiboGreen assay was performed, with a theoretical RNA concentration of 1.25 µg/mL. The amount of RNA present in the TE buffer was decreased to 0.227 ± 0.005 µg/mL, with 0.65 ± 0.02 µg/mL being detected after treatment with Triton (Figure 35).

Unfortunately, when the Acuitas-LNP-FM-3 was cast into a film (Acuitas-LNP-OTF-2), an RNA concentration of 0.75 ± 0.09 µg/mL was detected in the TE buffer (Figure 35). This

indicated that even if the particles were stable in the film mixture, the drying of the film compromises the LNPs ability to encapsulate RNA.

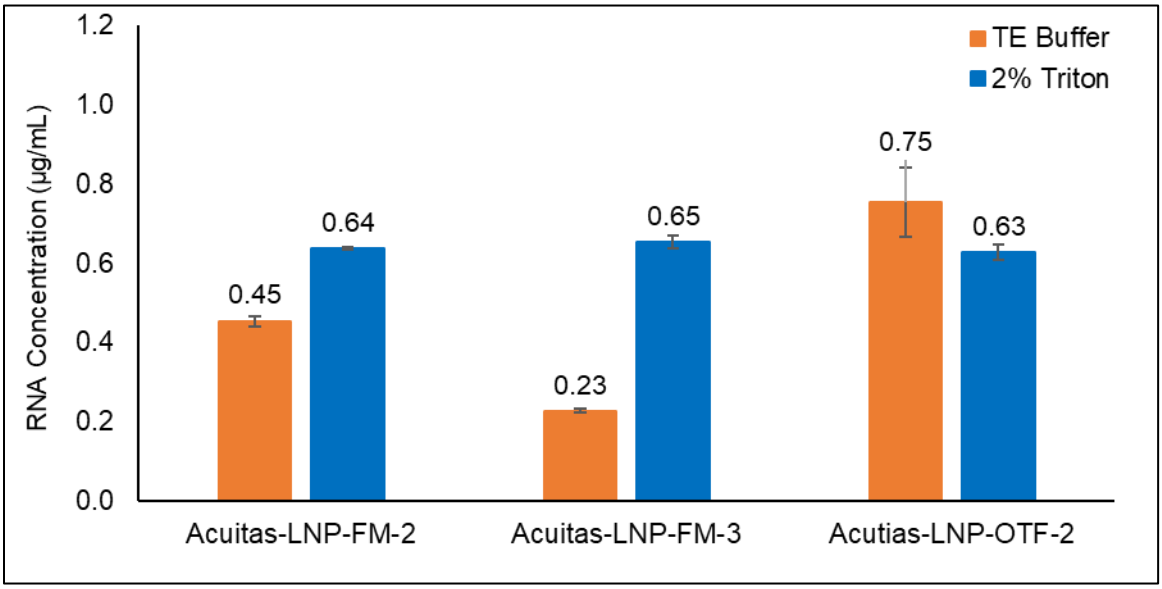

Figure 35: Results from the RiboGreen assay performed on Acuitas-LNP-FM-2, Acuitas-LNP-FM-3, and Acuitas-LNP-OTF-2. The theoretical RNA concentration of all samples was 1.25 ug/mL.

Additionally, a film mixture in which all the water component was replaced with tris buffer (0.1 M, pH=8) was prepared. This increased the pH of the film mixture to 8.2. Acuitas-LNPs were added to this film mixture (Acuitas-LNP-FM-4) and the RiboGreen assay was performed. There were very few differences between Acuitas-LNP-FM-3 and Acuitas-LNP-FM-4. Acuitas-LNP-FM-4 had an RNA concentration of 0.26 ± 0.01 µg/mL when the sample was in TE buffer, and a concentration of 0.63 ± 0.04 µg/mL when the sample was treated with Triton (Figure 36).

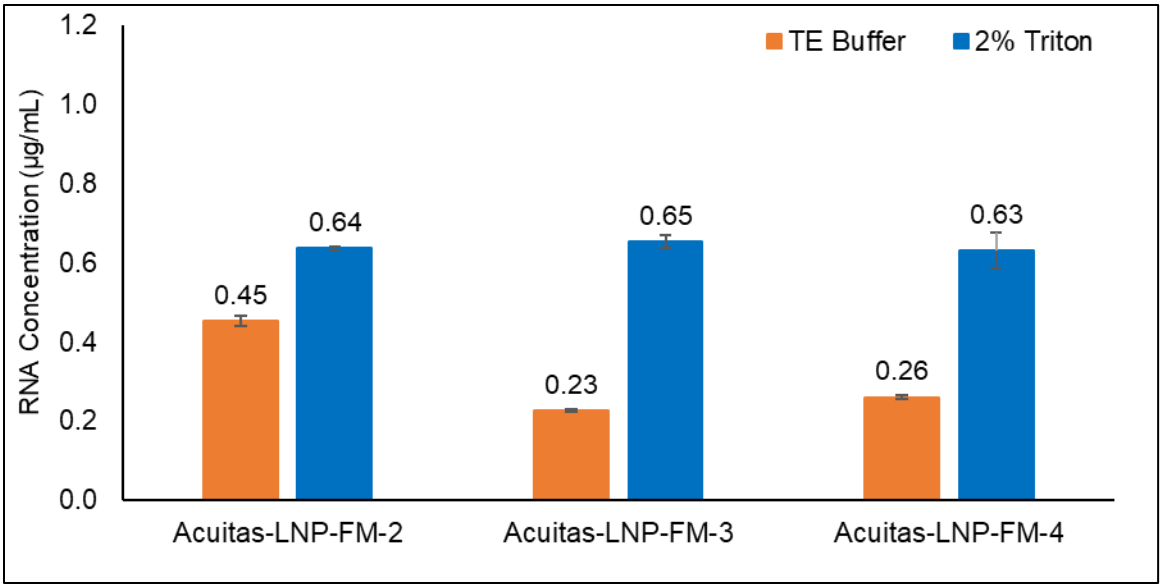

Figure 36: Results from the RiboGreen assay performed on Acuitas-LNP-FM-2, Acuitas-LNP-FM-3, and Acuitas-LNP-FM-4. The theoretical RNA concentration of all samples was 1.25 µg/mL.

3.3.6 Effects of Other Film Components on LNP Stability

To ensure that no other film components were interfering with stability of the Acuitas-LNPs, each individual component was mixed with Acuitas-LNPs. The amount of each component found in 1-gram of film mixture was dissolved in the amount of tris buffer found in a 1-gram film mixture. Acuitas-LNPs were then paddle mixed into each sample, and the RiboGreen assay was performed. Each sample had a theoretical RNA concentration of 1.25 µg/mL, Dimethyl sulfone, glycerol, and trehalose all showed limited influence on LNP stability. The dimethyl sulfone sample had an RNA concentration of 0.102 ± 0.005 µg/mL when dissolved in TE buffer, and an RNA concentration of 0.852 ± 0.002 µg/mL when treated with Triton. The glycerol sample had an RNA concentration of 0.079 ± 0.003 µg/mL in TE buffer, and an RNA concentration of 0.82 ± 0.02 µg/mL in 2% Triton. The trehalose sample had an RNA concentration of 0.08 ± 0.01 µg/mL when in TE buffer, and an RNA concentration of 0.73 ± 0.06 µg/mL in 2% Triton. The Pullulan had a slightly higher concentration of RNA measured in TE buffer, in addition to a lower concentration of RNA measured after treatment with Triton. The pullulan sample had an RNA concentration of

0.18 ± 0.01 µg/mL in buffer and an RNA concentration of 0.62 ± 0.02 µg/mL after treatment with Triton. It is not surprising that pullulan would be the film component with the largest effect on LNP stability, since pullulan makes up 33 wt.% of the film mixture.

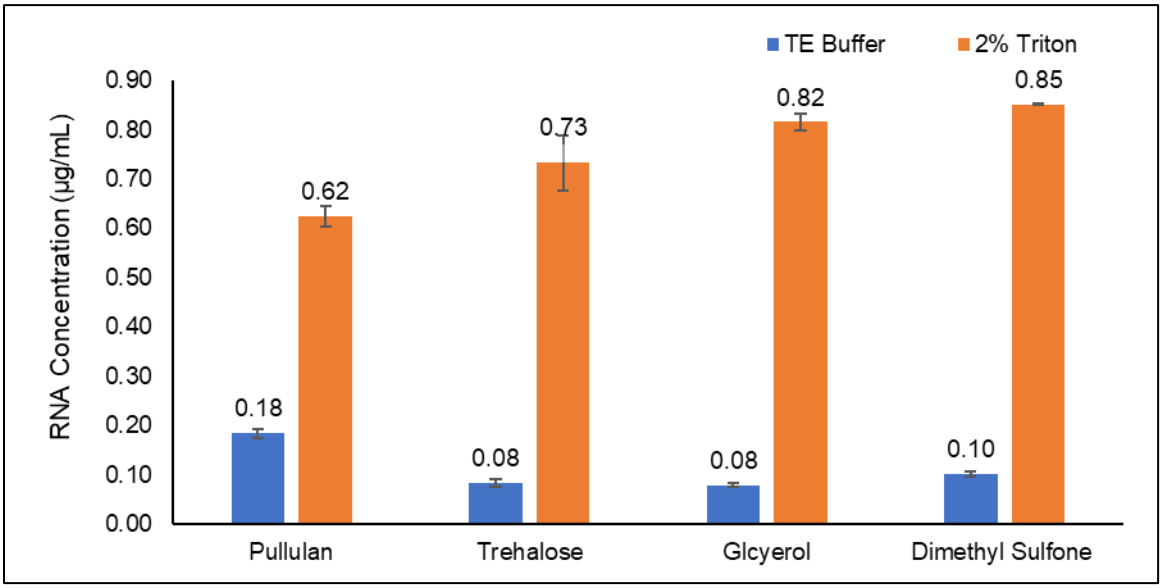

Figure 37: Results from the RiboGreen assay performed on Acuitas-LNPs paddle mixed with different components of the film formulation. The theoretical RNA concentration for all samples was 1.25 ug/mL.

To determine how much of an effect pullulan has on the stability of the Acuitas-LNPs, the ratio of pullulan to LNPs was increased and decreased. In Acuitas-LNP-FM-3 and Acuitas-LNP-FM-4, 33 wt.% of the film mixture was pullulan. Pullulan equal to the amounts of 12 wt.% and 42 wt.% in a film mixture were dissolved in tris buffer. Acuitas-LNPs were paddle mixed into these pullulan solutions and the RiboGreen assay was performed. The sample that contained a 12 wt.% of pullulan had an RNA concentration of 0.123 ± 0.008 µg/mL in buffer, and an RNA concentration of 0.650 ± 0.001 µg/mL when treated with Triton. The sample that contained a 42 wt.% had an RNA concentration of 0.16 ± 0.01 µg/mL in buffer, and an RNA concentration of 0.51 ± 0.04 µg/mL when treated with Triton.

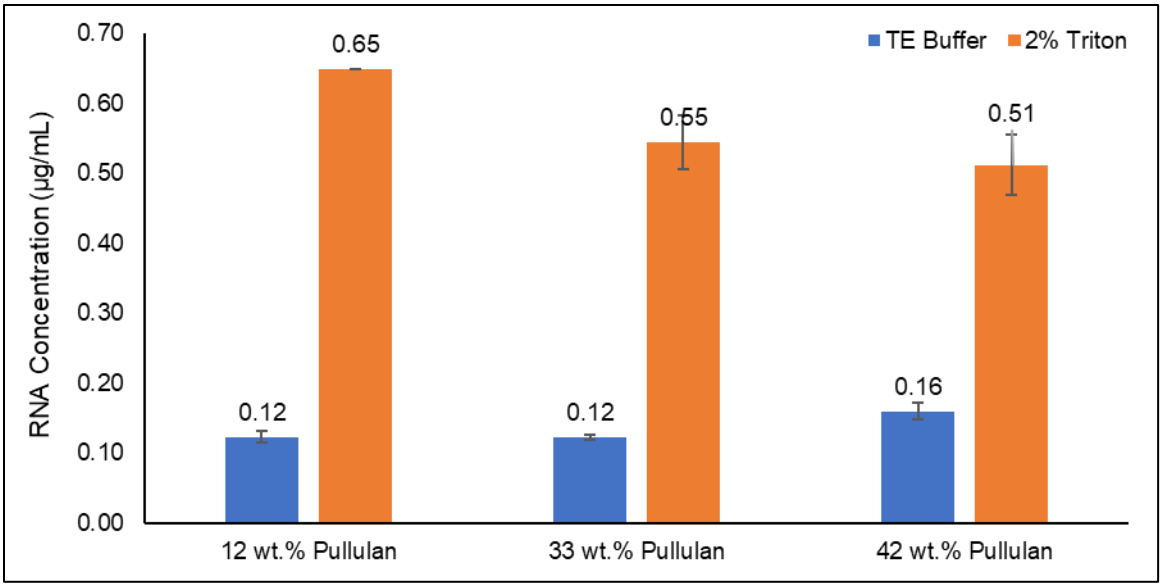

Figure 38: Results from the RiboGreen assay performed on Acuitas-LNPs paddle mixed into different ratios of pullulan. The theoretical RNA concentration for all samples was 0.625 ug/mL.

Overall, these experiments demonstrated that the film components within the film mixture were not greatly impacting the stability of the Acuitas-LNPs in a wet film mixture.

3.3.7 Drying Acuitas-LNPs

Throughout all the experiments there was always one constant. The Acuitas-LNPs were compromised after the film dried, even when they were stable in the wet film mixture. As such, the stability of the particles when dried in the absence of film mixture was investigated. Acuitas-LNPs were dried in a vial, re-dispersed in buffer, and then underwent the RiboGreen assay at a theoretical RNA concentration of 1.25 µg/mL. The dried Acuitas-LNPs had an RNA concentration of 1.07 ± 0.06 µg/mL in TE buffer, and an RNA concentration of 1.1 ± 0.9 µg/mL in 2% Triton, indicating that the LNPs were generally unstable when dried (Figure 39).

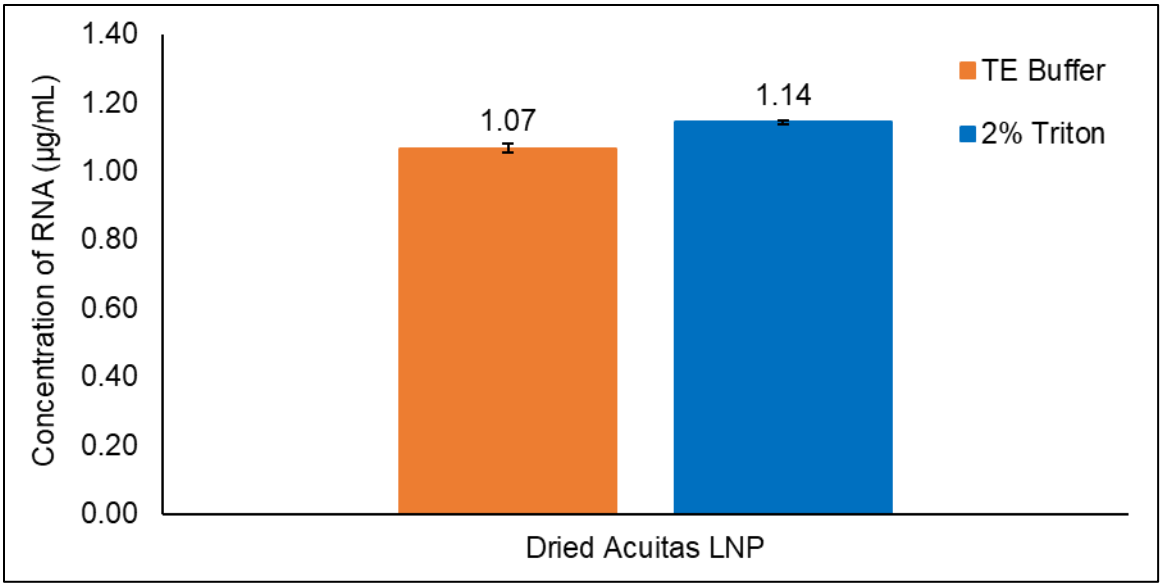

Figure 39: Results from the RiboGreen assay performed on Acuitas-LNPs dried out and re-dispersed. The theoretical RNA concentration for all samples was 0.625 ug/mL.

These results were predictable, as LNPs are not typically able to withstand being dried out and re-dispersed without an additive for stabliziation.[54] There have been reports of LNPs being stabilized during freeze drying if the process is performed in the presence of sugars such as trehalose, glucose and fructose.[54] It was initially hypothesized, that incorporating the Acuitas-LNPs into a polysaccharide OTF would help stabilize the particles, as the sugars had with freeze drying.

3.3.8 Electrophoresis Performed on Acuitas-LNPs, Acuitas LNP Film Mixtures, and Acuitas LNP OTFs

Before continuing to try to stabilize the LNPs within an OTF, it was imperative to ensure that the RNA, regardless of encapsulation, was stable after the film casting process. To do this, agarose gel electrophoresis was used. An RNA ladder, Acuitas-LNPs in buffer, a blank film, an Acuitas-LNP film (Acuitas-LNP-OTF-3), and an Acuitas-LNP film mixture (Acuitas-LNP-FM-5) all underwent electrophoresis. As expected, the RNA ladder reference showed eight distinct

molecular weights (6000, 4000, 3000, 2000, 1500, 1000, 500, and 200 bases) (Figure 40). The blank film showed no RNA present (Figure 40). The Acuitas-LNPs in buffer, the Acuitas-LNP-OTF, and the Acuitas-LNP-FM all had bands in the same location which corresponded to a molecular weight of 3000 bases (Figure 40). Since the bands for the RNA present in the Acuitas-LNP-OTF corresponded to the band of the Acuitas-LNPs in buffer, it was concluded that the RNA remained in-tact after the film casting process. If the RNA had been degraded when incorporated into the film mixture or OTF, the band would be shifted to a lower molecular weight and there may be multiple bands representing multiple molecular weights.

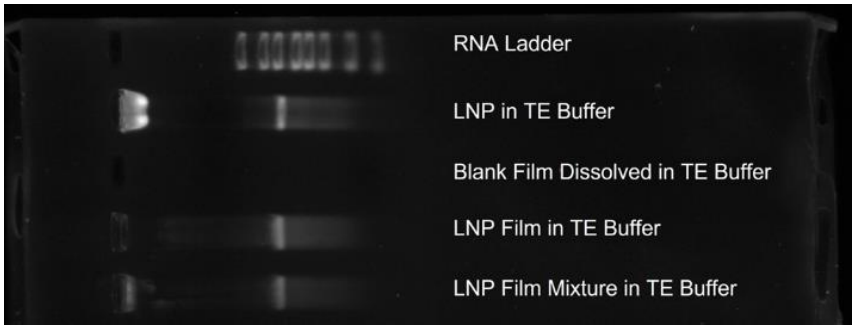

Figure 40: Agarose gel electrophoresis performed on Acuitas-LNPs in buffer, in a film mixture, and in an OTF.

3.3.9 Acuitas-LNP Stability Controls

At this point, it was known that the LNPs were not stable when dried but that the RNA remained in-tact even when not encapsulated within the LNPs. The extent to which these particles could be handled needed to be further explored through a series of controls.

The first set of Acuitas-LNP controls involved agitating the Acuitas-LNPs, using different methods. Typically, when dissolving the Acuitas-LNP-OTFs in buffer, they require some amount of agitation. Prior to these controls, agitation was done by gently shaking the sample by hand. This agitation method, however, had the possibility to introduce inconsistency between samples. Also, if the sample was shaken too vigorously, this could result in damage to the LNPs. It was therefore

imperative to determine an agitation method that allowed for consistent agitation without damaging the Acuitas-LNPs. Controls 1-6 were all performed at theoretical concentrations of 1.25 µg/mL.

Control 1 involved paddle mixing the Acuitas-LNPs, while dispersed in buffer, at a speed of 20 RPM for 30 minutes and storing the sample overnight in a fridge. Control 1 was performed to mimic the agitation that the LNPs undergo while the LNPs are being paddle mixed into the film mixture. The RiboGreen assay results for control 1 were similar to those seen for Acuitas-LNPs by themselves. There was 0.19 ± 0.007 µg/mL RNA present in the TE buffer and 1.23 ± 0.02 µg/mL RNA present in the 2% Triton (Figure 41).

Control 2 was the same as control 1, except that the sample was stored on the benchtop overnight. The reason for Control 2 was to determine if the Acuitas-LNPs are stable at room temperature over long time periods. Control 2 demonstrated high LNP stability as there was only 0.210 ± 0.001 µg/mL RNA present in the TE buffer and 1.23 ± 0.02 µg/mL RNA present in the 2% Triton (Figure 41).

Control 3 was paddle mixed in the same manner as control 1 and 2, however, afterwards it was shaken vigorously by hand for 20 minutes. This control was shaken much more vigorously than normal, to see if it was possible to damage the LNPs by hand. The Ribogreen assay performed on Control 3 indicated that if shaken vigorously for 20 minutes the particles could be compromised. Control 3 had an RNA concentration of 1.02 ± 0.01 µg/mL in TE buffer and an RNA concentration of 1.25 ± 0.02 µg/mL after to treatment with Triton (Figure 41). It was imperative to find a method that would provide consistent agitation while the films were being dissolved, without impacting the stability of the LNPs.

Control 4 involved stirring the Acuitas-LNPs on a stir plate at 100 RPM for 30 minutes. A speed of 100 RPM was chosen as it was the lowest speed setting allowed on the stir plate. Control 5 involved adding the LNPs in buffer to an orbital mixer and stirring at a setting of 5 for 30 minutes. Both Control 4 and 5 showed high LNP stability, with RNA concentrations in TE buffer of 0.190 ± 0.001 µg/mL and 0.220 ± 0.007 µg/mL, respectively (Figure 41). The RNA concentrations of control 4 and 5 in 2% Triton were 1.373 ± 0.008 µg/mL and 1.39 ± 0.01 µg/mL, respectively (Figure 41). Moving forward, during dissolution, the Acuitas-LNP-OTFs were agitated using the orbital mixer as it did not require the addition of a stir bar to the sample, reducing the possibility for contamination.

Finally, to ensure that the LNPs could withstand the casting temperature, Control 6 involved heating the LNPs in buffer at 35˚C for 30 minutes while stirring at 100 RPM. Again, a speed of 100 RPM was used as it was the lowest speed available on the stir plate. Control 6 showed high LNP stability with 0.175 ± 0.004 µg/mL RNA in TE buffer and 1.28 ± 0.01 µg/mL RNA in 2% Triton (Figure 41).

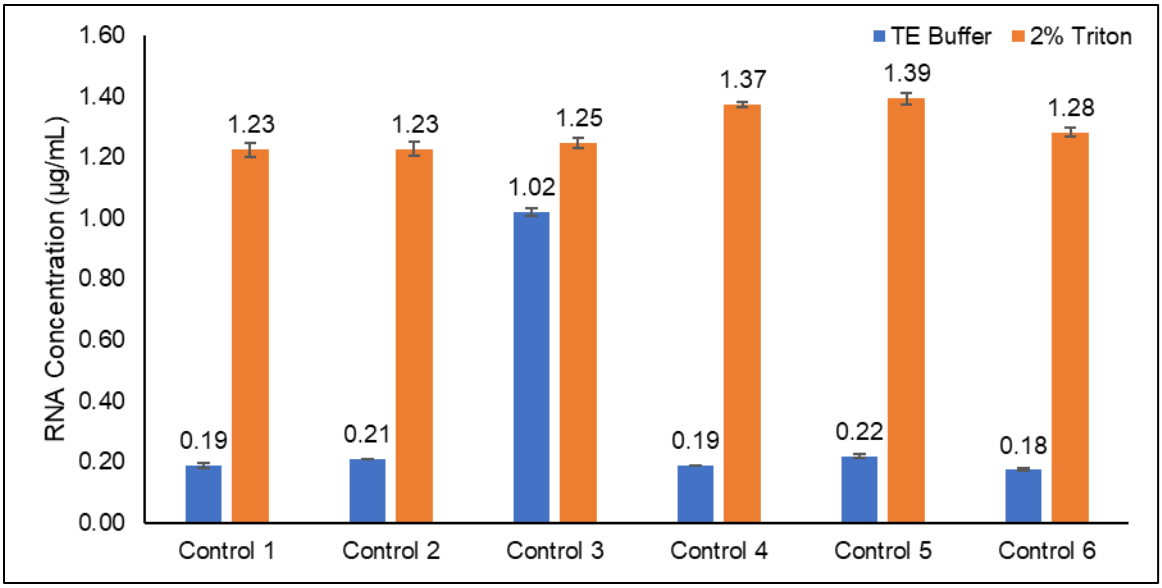

Figure 41: Results from the RiboGreen assay performed on Acuitas-LNPs in TE buffer agitated under various conditions. Acuitas-LNPs in TE buffer were paddle mixed at 20 RPM for 30 minutes, following which they were stored in a fridge for 24 hours (control 1), stored at room temperature for 24 hours (control 2), and shaken vigorously by hand for 20 minutes (control 3). Acuitas-LNPs in TE buffer were stirred at 100 RPM for 30 minutes at room temperature (control 4) and 35˚C (control 6). Acuitas-LNPs were agitated on an orbital mixer for 30 minutes at a speed of 2 (control 5). The theoretical RNA concentration of all samples was 1.25 µg/mL.

Next, it was important to determine what conditions the LNPs could withstand while being incorporated in a film mixture. The first study involved looking at how the length of paddle mixing time affected the stability of the LNPs. The LNP film mixture was paddle mixed at 20 RPM for 30- (control 7), 45- (control 8), and 60- minutes (control 9). The RiboGreen assay was performed on each of these samples at a theoretical concentration of 0.625 µg/mL. In TE buffer, control 7, control 8, and control 9 had RNA concentrations of 0.222 ± 0.002 µg/mL, 0.195 ± 0.003 µg/mL, and 0.326 ± 0.004 µg/mL, respectively (Figure 42). In 2% Triton, these controls had concentrations of 0.54 ± 0.02 µg/mL, 0.55 ± 0.04 µg/mL, and 0.46 ± 0.07 µg/mL, respectively (Figure 42). These results indicate that paddle mixing for too long can compromise the Acuitas-LNPs. The Acuitas-LNP-FM could not be paddle mixed for less than 30 minutes, as this resulted in a non-homogenous film.

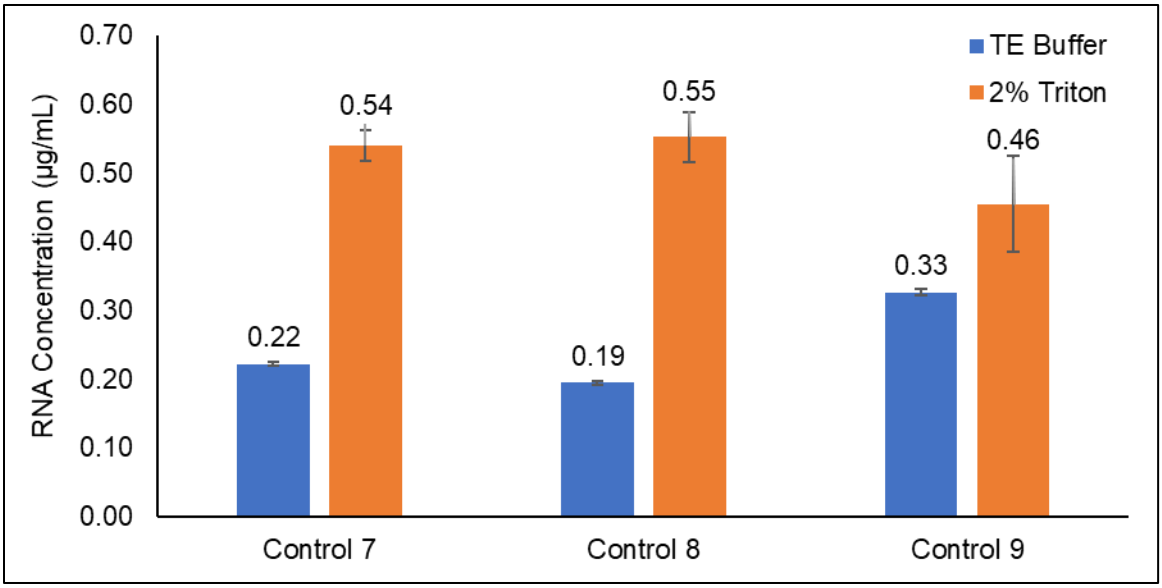

Figure 42: Results from the RiboGreen assay performed on Acuitas-LNP-FMs paddle mixed at 20 RPM for 30 minutes (control 7), 45 minutes (control 8), and 60 minutes (control 9). The theoretical RNA concentration of all samples was 0.625 µg/mL

The next series of controls involved paddle mixing the film mixture with the LNPs at different speeds. The mixtures were paddle mixed for 30 minutes at speeds of 20 (control 7), 35 (control 10), and 50 RPM (control 11). These three controls were all diluted to a concentration of 0.625 µg/mL. The RiboGreen assay showed similar results between these three samples with no pattern of increasing or decreasing amounts of RNA present in the TE buffer and Triton. In TE buffer, control 7, control 10, and control 11 had RNA concentrations of 0.222 ± 0.002 µg/mL, 0.128 ± 0.002 µg/mL, and 0.162 ± 0.003 µg/mL, respectively (Figure 43). In 2% Triton, these controls had concentrations of 0.54 ± 0.02 µg/mL, 0.50 ± 0.02 µg/mL, and 0.46 ± 0.03 µg/mL, respectively (Figure 43).

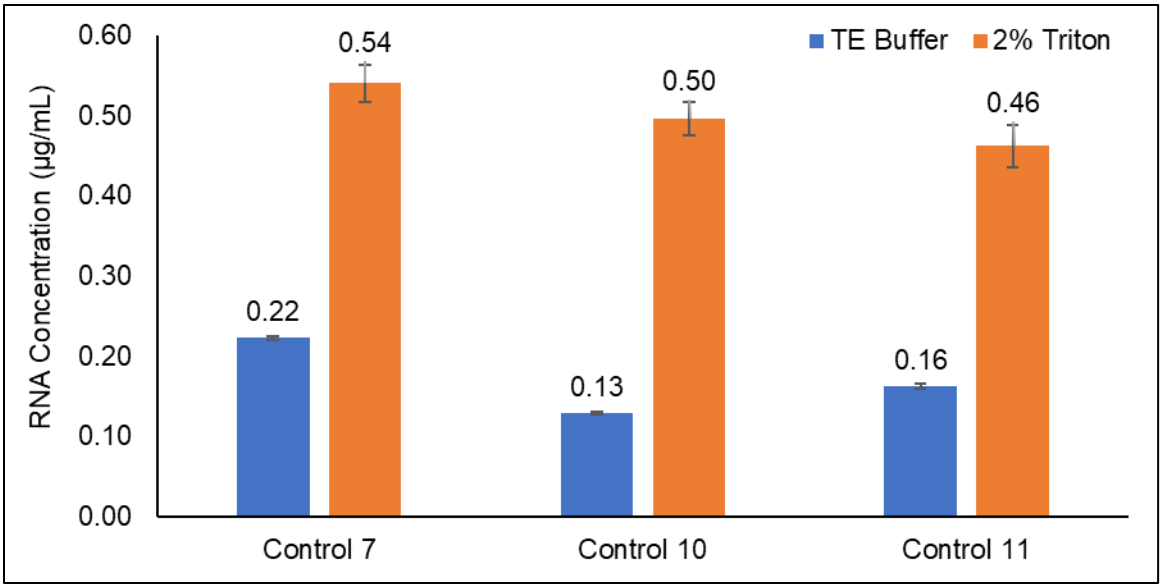

Figure 43: Results from the RiboGreen assay performed on Acuitas-LNP-FMs paddle mixed for 30 minutes at speeds of 20 RPM (control 7), 35 RPM (control 11), and 55 RPM (control 12). The theoretical RNA concentration of all samples was 0.625 µg/mL

The final set of controls performed were used to determine if increasing the casting temperature affects the LNP stability. Acuitas-LNP-OTFs were cast at 35˚C (Control 12), 45˚C (Control 13), and 55˚C (Control 14). These three films had theoretical RNA concentrations of 0.625 µg/mL and showed no difference between the amount of RNA present in the TE buffer. In TE buffer, control 12, control 13, and control 14 had RNA concentrations of 0.447 ± 0.005 µg/mL, 0.45 ± 0.03 µg/mL, and 0.439 ± 0.003 µg/mL, respectively (Figure 44). In 2% Triton, these controls had concentrations of 0.45 ± 0.02 µg/mL, 0.44 ± 0.02 µg/mL, and 0.45 ± 0.03 µg/mL, respectively (Figure 44).

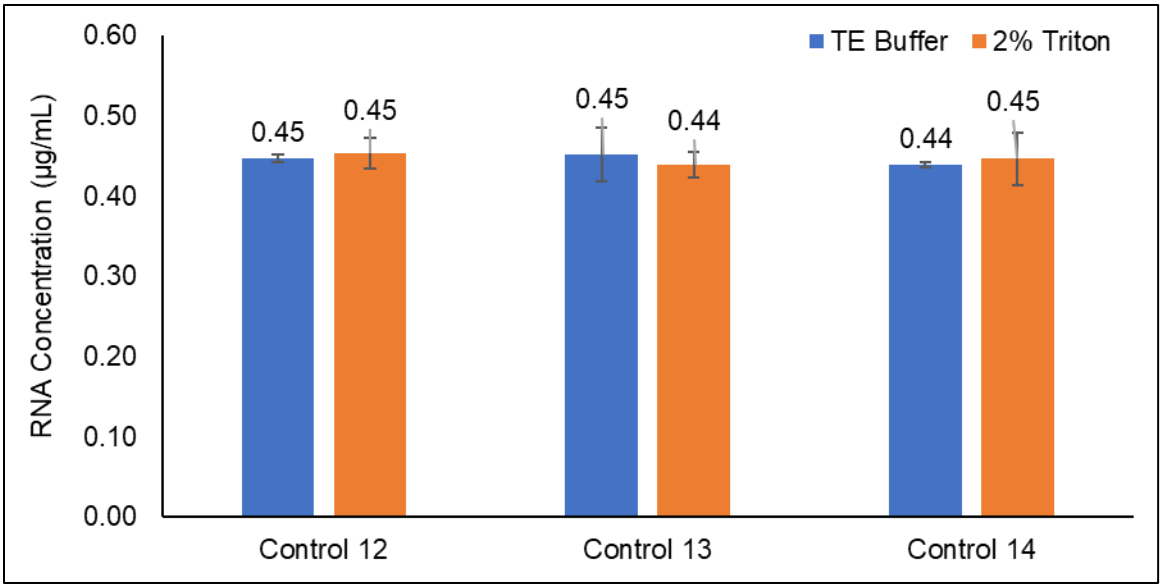

Figure 44: Results from the RiboGreen assay performed on Acuitas-LNP-OTFs cast at 35˚C (controls 13), 45˚C (control 14), and 55 ˚C (control 15). The theoretical RNA concentration of all samples was 0.625 µg/mL.

3.3.10 Using Optical Microscopy to Understand the RiboGreen Assays

There were conflicting results regarding whether the LNPs were remaining intact after the film casting process. As discussed in Chapter 3.2.2, STORM images performed on the Acuitas LNP-OTF indicated that the structure of the LNPs remained intact. The particle size distribution was approximately the same as the size distribution of the particles prior to film incorporation. In addition, the particle shape did not change after film incorporation. The RiboGreen assay, however, indicated that there was essentially no RNA retained within the LNPs after film casting. These results indicated that either RNA was exiting the LNPs, but the LNP structure remained intact or that the RiboGreen dye was able to enter the LNPs without causing damage to the LNP structure. To gain a better understanding of how the RiboGreen dye was accessing the RNA, the assay was performed while imaging with confocal microscopy. Imaging was performed with two different light channels, one that would be able to visualize the fluorescence from the RiboGreen dye, and one that would be able to visualize the fluorescence from the DiI.

First, as a control, RiboGreen dye was added to TE buffer and imaged. Considering there was no RNA or LNPs present in this control, no fluorescence in either channel was expected. As expected, there was no fluorescence in either the DiI or the RiboGreen channel (Figure 45).

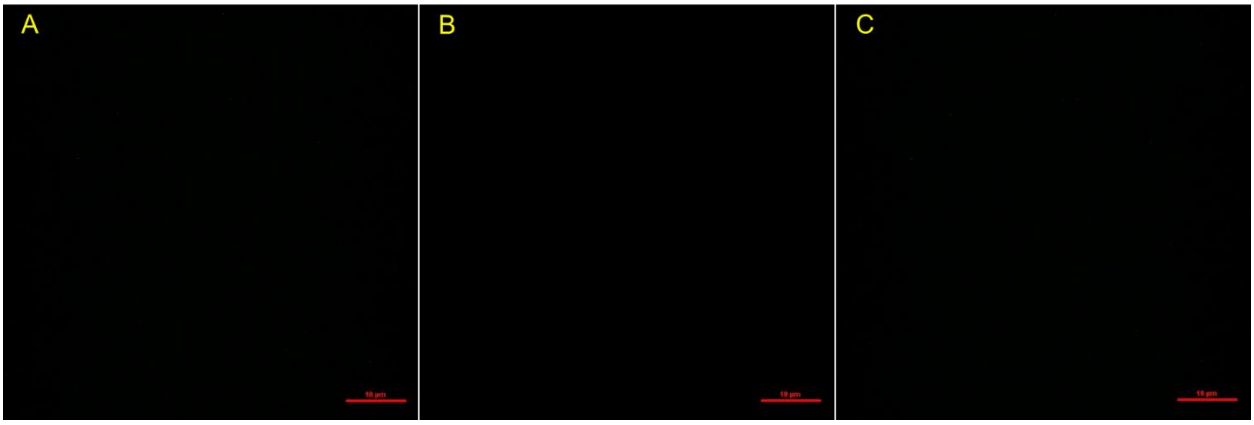

Figure 45: Optical microscopy images of RiboGreen dye added to TE buffer. Imaged with A) RiboGreen and DiI Channel, B) DiI channel, C) RiboGreen channel. Scale bar represents 10 µm.

The second control that was performed involved adding RiboGreen dye to a sample of free RNA, in TE buffer. Given that the RiboGreen dye could access the free RNA, there was visible fluorescence in the RiboGreen channel (Figure 46(C)). There remained no fluorescence in the DiI channel (Figure 46(B)).

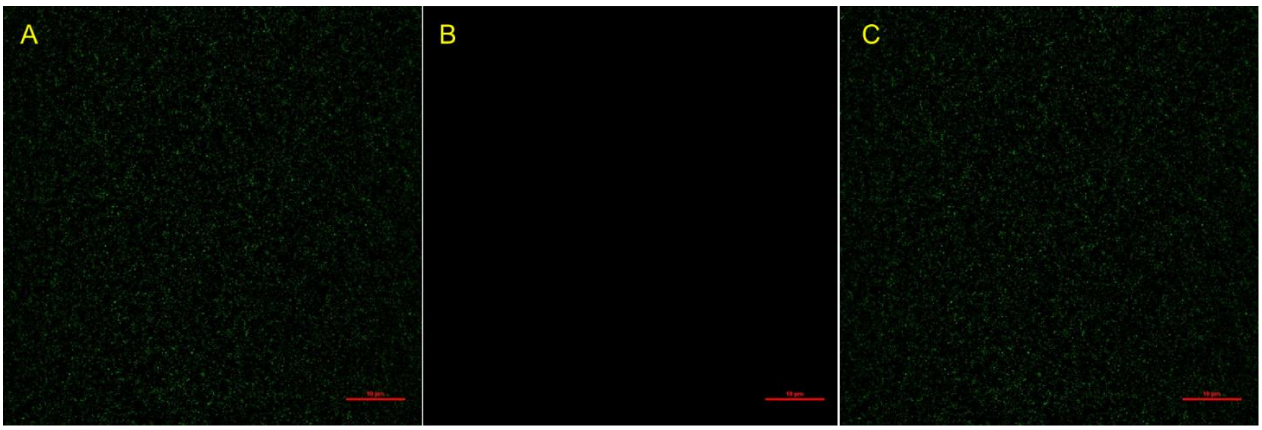

Figure 46: Optical microscopy images of RiboGreen dye added to free RNA in TE buffer. Imaged with A) RiboGreen and DiI Channel, B) DiI channel, C) RiboGreen channel. Scale bar represents 10 µm.

Acuitas-LNPs in TE buffer were then imaged without the addition of RiboGreen dye. Fluorescence in the DiI channel allowed for the visualization of the LNPs which appeared as small circles (Figure 47(B)). The resolution of the microscope being used to image these particles was 300 nm. Given that the Acuitas-LNPs are approximately 85 nm, accurate size measurements of the particles could not be made. As such, the images were used only for qualitative analysis.

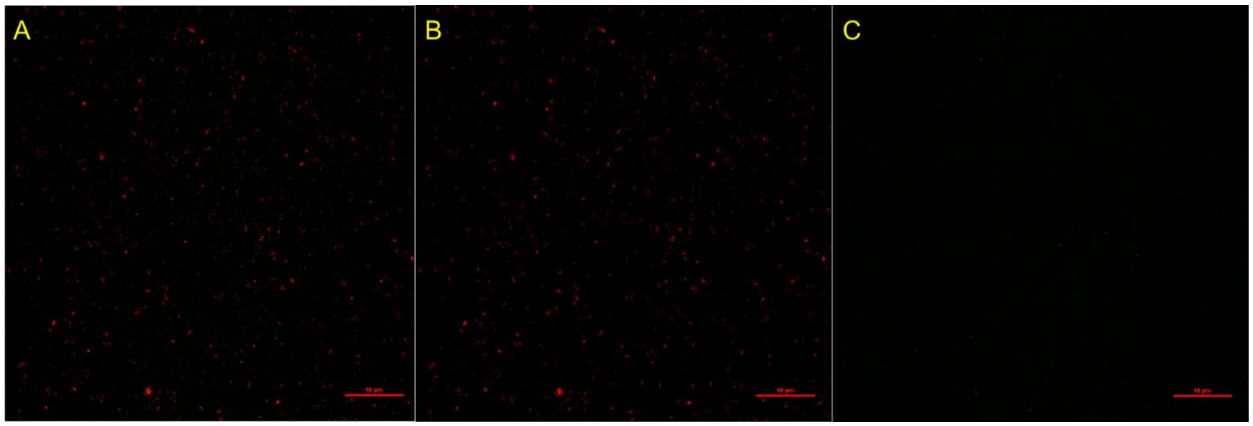

Figure 47: Optical microscopy images of Acuitas LNPs in TE buffer. Imaged with A) RiboGreen and DiI Channel, B) DiI channel, C) RiboGreen channel. Scale bar represents 10 µm.

Next, RiboGreen dye was added to the Acuitas-LNPs in TE buffer. As previously visualized, there was fluorescence in the DiI channel that was representative of the LNPs (Figure 48(B)). There was also some fluorescence in the RiboGreen channel that did not correspond to fluorescence from the LNPs (Figure 48(C)). The fluorescence in the RiboGreen channel was likely caused by unencapsulated RNA that was expelled from the LNPs or free RNA that remained in the sample after the LNPs were synthesized.

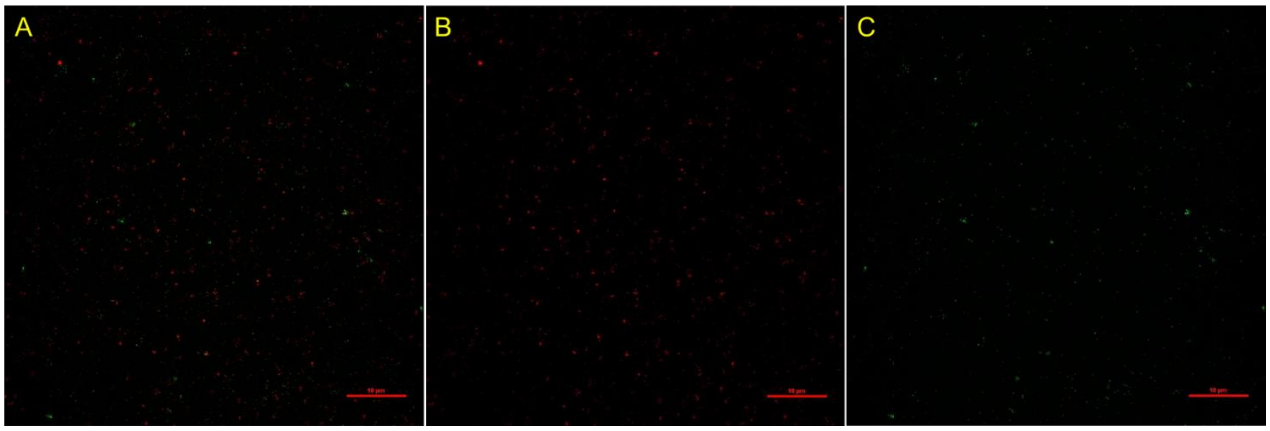

Figure 48: Optical microscopy images of RiboGreen dye added to Acuitas LNPs in TE buffer. Imaged with A) RiboGreen and DiI Channel, B) DiI channel, C) RiboGreen channel. Scale bar represents 10 µm.

The Acuitas-LNPs were then treated with Triton, in the same manner as when the RiboGreen assay is performed. Following this, RiboGreen dye was added to the sample and the sample was imaged. There was a high amount of fluorescence in the RiboGreen channel (Figure 49(C), and essentially no fluorescence in the DiI channel (Figure 49(B)). The lack of fluorescence in the DiI channel is likely due to the lipid layer of the LNPs being disrupted. The addition of Triton disrupted the lipid layer causing DiI to become unbound from the lipids. DiI exhibits minimal fluorescence when in aqueous conditions and fluoresces brightly when in a hydrophobic environment.

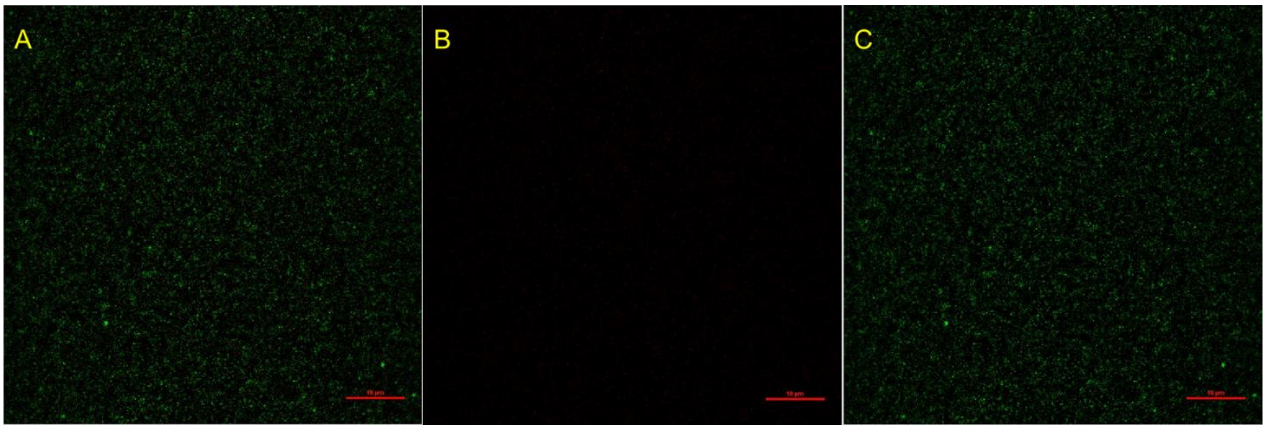

Figure 49:Optical microscopy images of RiboGreen dye added to Triton treated Acuitas LNPs in TE buffer. Imaged with A) RiboGreen and DiI Channel, B) DiI channel, C) RiboGreen channel. Scale bar represents 10µm.

Next, LNP-OTFs were prepared by casting at 35˚C (Control 12), 45˚C (Control 13), and 55˚C (Control 14), as well as being drop cast at room temperature. These films were all dissolved in TE buffer as they are when the RiboGreen assay is performed. RiboGreen dye was added to each of these samples and the samples were imaged.

In each of these samples, large aggregates were visualized in the DiI channel (Figure 50-53(B)). Acuitas Therapeutics had previously indicated that if the LNPs are unstable they will form large aggregates. These aggregates were not previously observed when the Acuitas-LNP-OTF was imaged using STORM, as described in Chapter 3.2.2. When the Acuitas-LNP-OTF was previously imaged, the film was un-dissolved. This suggests that the LNPs remain in-tact when in the cast film matrix, however film dissolution is what disrupts the LNP structure.

Additionally, when looking at the large aggregates present in these samples, there was a significant amount of colocalization between the DiI and RiboGreen channels (Figures 50-53). This explained why there were high amounts of fluorescence observed in the TE buffer for the RiboGreen assays performed on the cast films. Interestingly, the samples that were prepared by drop casting at room temperature and cast at 35˚C appeared to have more colocalization between the RiboGreen and DiI channels than the samples cast at 45˚C and 55˚C.

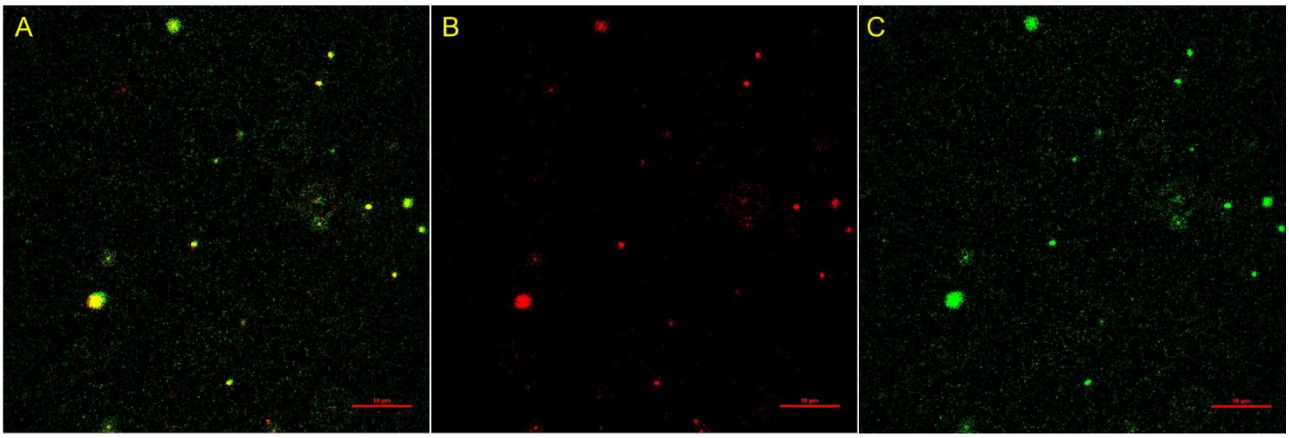

Figure 50: Optical microscopy images of RiboGreen dye added to dissolved Acuitas-LNP-OTF drop cast at room temperature. Imaged with A) RiboGreen and DiI Channel, B) DiI channel, C) RiboGreen channel. Scale bar represents 10 µm.

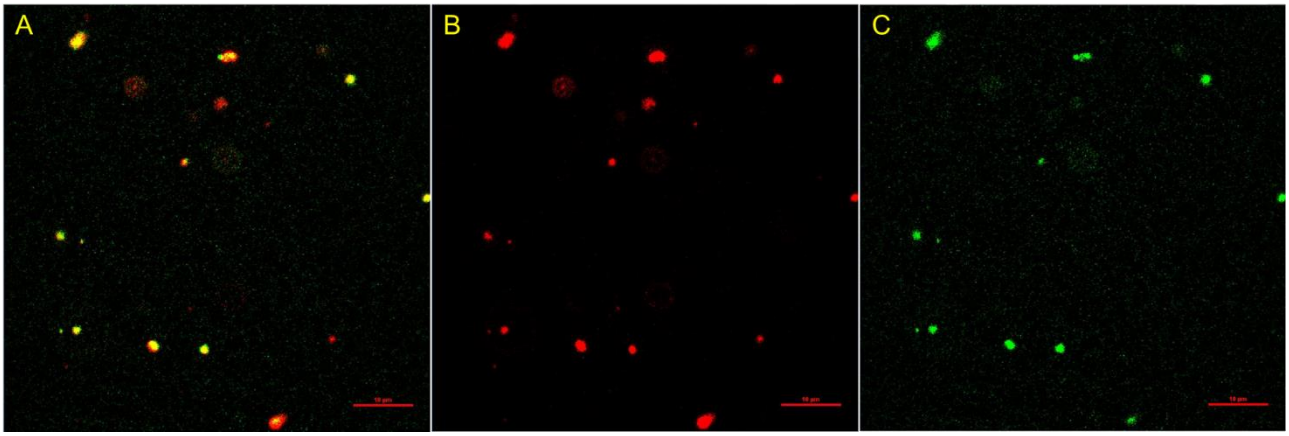

Figure 51: Optical microscopy images of RiboGreen dye added to dissolved Acuitas-LNP-OTF prepared at 35˚C (control 12). Imaged with A) RiboGreen and DiI Channel, B) DiI channel, C) RiboGreen channel. Scale bar represents 10 µm.

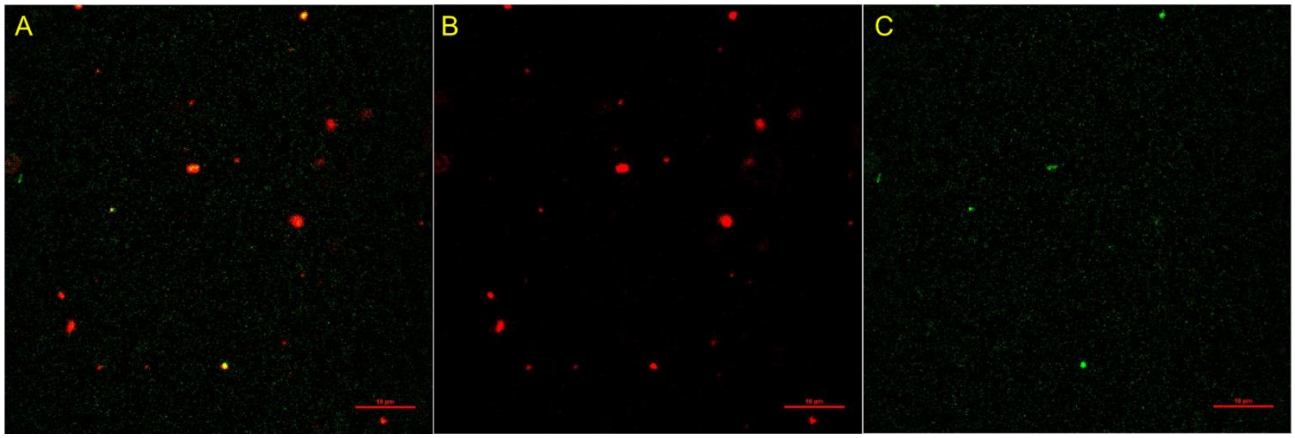

Figure 52: Optical microscopy images of RiboGreen dye added to dissolved Acuitas-LNP-OTF prepared at 45˚C (control 13). Imaged with A) RiboGreen and DiI Channel, B) DiI channel, C) RiboGreen channel. Scale bar represents 10 µm.

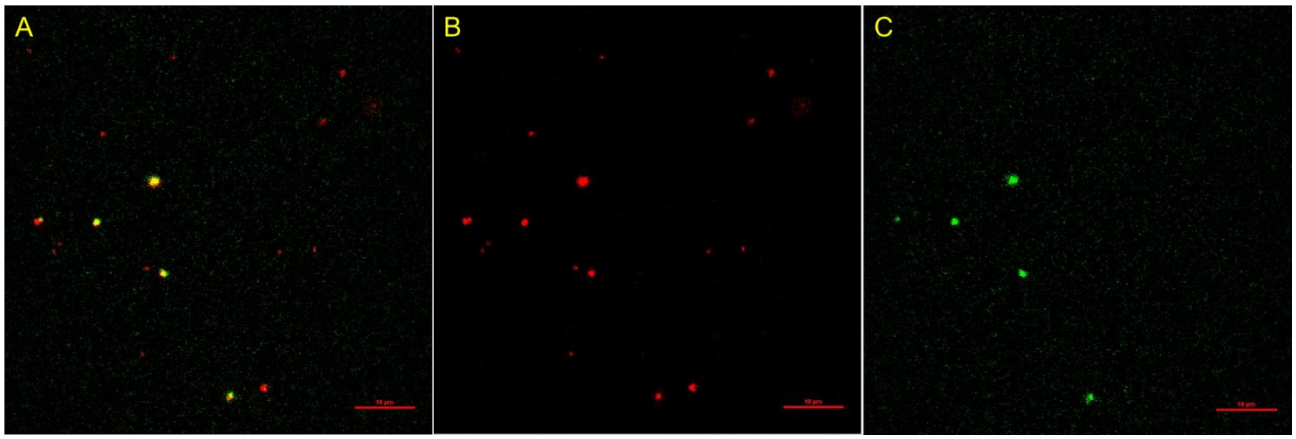

Figure 53:Optical microscopy images of RiboGreen dye added to dissolved Acuitas-LNP-OTF prepared at 55˚C (control 14). Imaged with A) RiboGreen and DiI Channel, B) DiI channel, C) RiboGreen channel. Scale bar represents 10 µm.

From the RiboGreen assay, it was known that the Acuitas-LNPs were more stable when in a wet film mixture than in an OTF. Optical microscopy was performed on a dissolved LNP film mixture (Acuitas-LNP-FM-4) (Figure 54). The fluorescence in the RiboGreen channel for Acuitas-LNP-FM-4 was significantly lower than that of the Acuitas-LNP-OTFs (Figure 54(C)). The large aggregates that were visible in the Acuitas-LNP-OTFs were also not as prevalent in the Acuitas-LNP-FM. These results corresponded well with the previous RiboGreen assay findings.

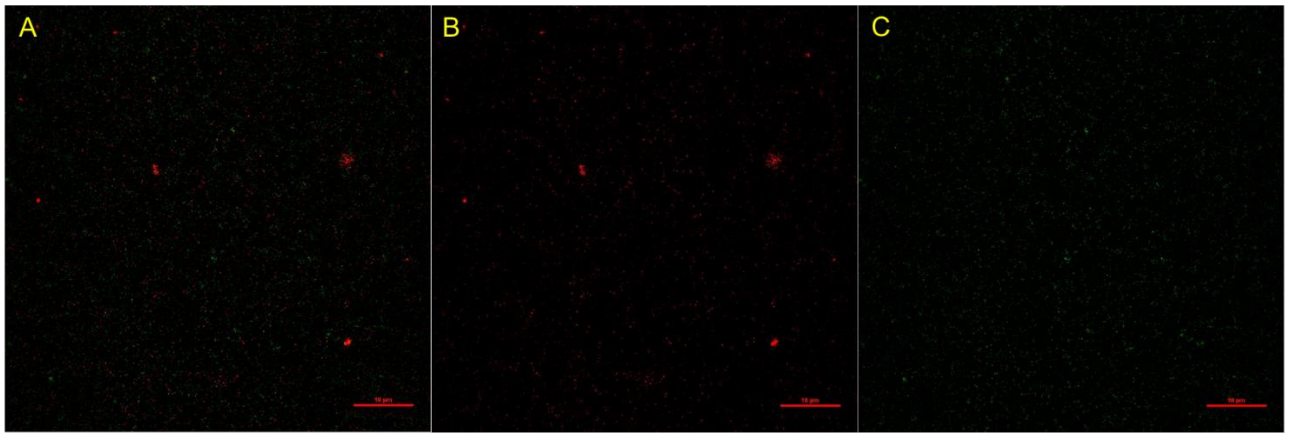

Figure 54: Optical microscopy images of RiboGreen dye added to dissolved Acuitas-LNP-FM-4. Imaged with A) RiboGreen and DiI Channel, B) DiI channel, C) RiboGreen channel. Scale bar represents 10 µm.

Optical microscopy was used to better understand the RiboGreen assay and the behavior of the Acuitas-LNPs in film mixtures vs OTFs. When imaging the LNPs in an OTF, the Acuitas-

LNPs were of the proper size and shape. However, upon dissolving the Acuitas-LNP-OTFs for the RiboGreen assay, the particles form large LNP aggregates which results in the RiboGreen dye being able to access the RNA. These aggregates are very concerning with regards to possible applications because the RNA is no longer being protected by the LNPs.

3.3.11 Increasing the Trehalose Content of the Films

A possible solution to LNP aggregates forming when the OTF is dissolved is to introduce an additive to the film mixture that would help protect or stabilize the LNPs.

The first additive that was introduced in the film was trehalose. Trehalose has previously been shown to stabilize proteins in OTFs,[17,55] as well as nifedipine loaded LNPs during freeze-drying.[54] All film mixtures up until this point had previously contained a 5-weight percentage (wt.%) of trehalose. A film mixture containing 10 wt.% trehalose was prepared and used to prepare an Acuitas-LNP-FM (Acuitas-LNP-FM-6) and an Acuitas-LNP-OTF (Acuitas-LNP-OTF-4). The RiboGreen assay performed on the Acuitas-LNP-FM-6 and Acuitas LNP-OTF-4 showed no increase in LNP stability. Both samples had a theoretical RNA concentration of 0.625µg/mL. Acuitas-LNP-FM-6 had 0.264 ± 0.007 µg/mL RNA in TE buffer and 0.58 ± 0.03 µg/mL RNA in 2% Triton (Figure 55). Acuitas-LNP-OTF-4 had 0.47 ± 0.03 µg/mL RNA present in TE buffer, and 0.49 ± 0.04 µg/mL of RNA after being treated with Triton (Figure 55). Since there was no increase in Acuitas-LNP stability with the extra addition of trehalose, different additives were investigated.

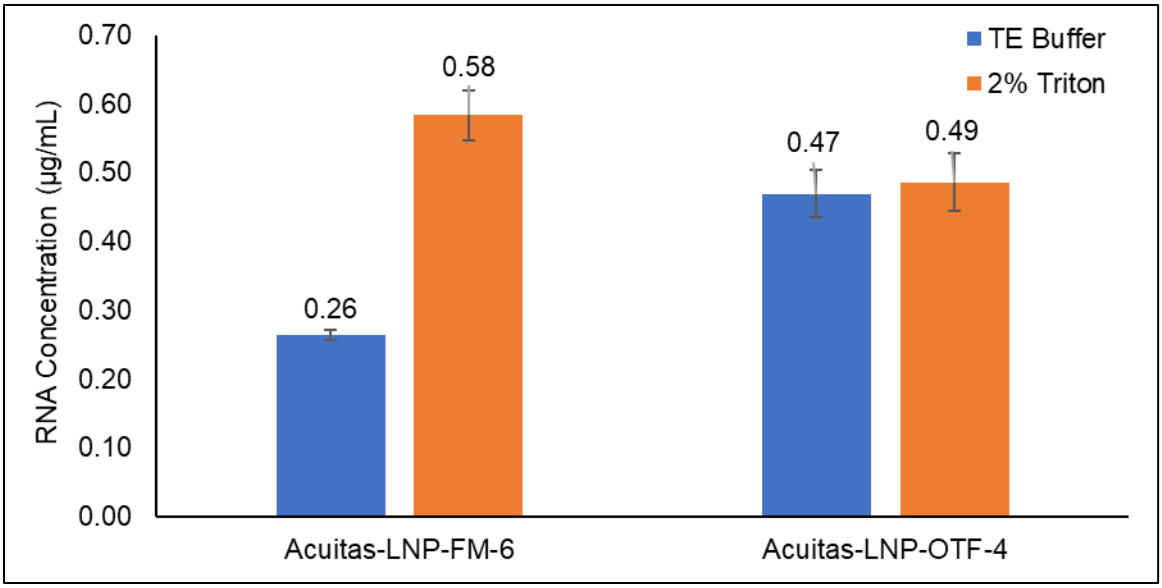

Figure 55: Results from the RiboGreen assay performed on Acuitas-LNP-FM-6 and Acuitas-LNP-OTF-4. The theoretical concentration of both samples was 0.625 µg/mL.

3.3.12 Incorporating Lipid-PEG into the Acuitas-LNP-OTFs

The next additive that was incorporated into the film mixture was 1,2-dioleoyl-sn-glycero-3-phosphoethanolamine-N-[methoxy(polyethylene glycol)-2000] (ammonium salt) (DOPE-PEG). The goal of incorporating DOPE-PEG into the film mixture was to add a protective shell around the LNPs. When the film is dissolved, the film components are pulling on the lipids of the shell of the LNPs. This could cause defects in the LNP shell which allows the RiboGreen dye to enter. These defects in the LNP shell could also be the points in which two LNPs aggregate together. By forming a protective shell of DOPE-PEG around the LNPs, the film components pull on the DOPE-PEG during dissolution rather than the lipids of the LNPs, leaving behind the undamaged LNPs.

Acuitas-LNP-DOPE-PEG-OTFs were prepared with 0.3 wt.% (Acuitas-LNP-DOPE-PEG-OTF-1), 0.7 wt.% (Acuitas-LNP-DOPE-PEG-OTF-2), 1.4 wt.% (Acuitas-LNP-DOPE-PEG-OTF-3), and 6.3 wt.% of DOPE-PEG (Acuitas-LNP-DOPE-PEG-OTF-4). The Acuitas-LNP-DOPE-

PEG-OTF samples underwent the RiboGreen assay at a theoretical RNA concentration of 0.625 µg/mL. The results of the assay indicated that the addition of DOPE-PEG was successful at stabilizing the LNPs in the cast film in a concentration-dependent manner.

The two films prepared with 0.3 wt.% DOPE-PEG had 0.30 ± 0.01 µg/mL and 0.226 ± 0.004 µg/mL RNA in TE buffer and 0.45 ± 0.02 µg/mL and 0.32 ± 0.03 µg/mL RNA in 2% Triton (Figure 56). The two films prepared with 0.7 wt.% DOPE-PEG had 0.233 ± 0.004 µg/mL and 0.196 ± 0.004 µg/mL RNA in TE buffer and 0.481 ± 0.001 µg/mL and 0.479 ± 0.008 µg/mL RNA in 2% Triton (Figure 56). The film prepared with 1.4 wt.% DOPE-PEG had 0.150 ± 0.003 µg/mL RNA in TE buffer and 0.41 ± 0.03 µg/mL RNA in 2% Triton (Figure 56). The two films prepared with 6.3 wt.% DOPE-PEG had 0.08 ± 0.01 µg/mL and 0.071 ± 0.002 µg/mL RNA in TE buffer and 0.42 ± 0.01 µg/mL and 0.349 ± 0.007 µg/mL RNA in 2% Triton (Figure 56).

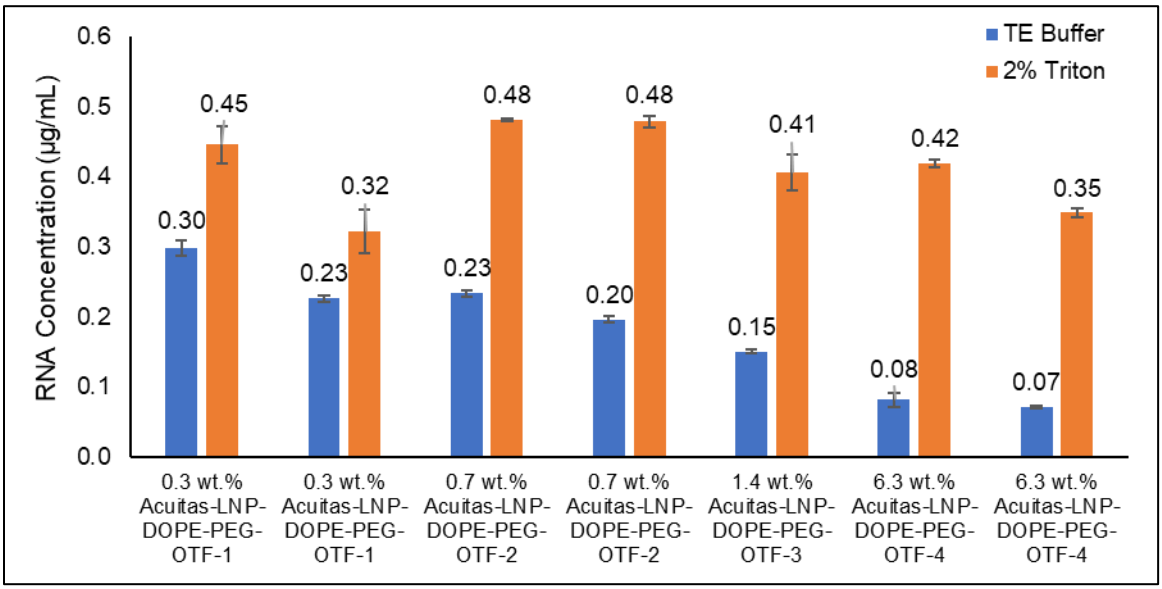

Figure 56: Results from the RiboGreen assay performed on Acuitas-LNP-DOPE-PEG-OTFs with 0.3, 0.7, 1.4, and 6.3 wt.% DOPE-PEG incorporated into film mixture.

A T-test was performed on the 0.3 wt.% Acuitas-LNP-DOPE-PEG-OTF and the 6.3 wt.% Acuitas-LNP-DOPE-PEG-OTF to determine whether the increase in DOPE-PEG resulted in a statistically significant difference in RNA present in the TE buffer as well as 2% Triton. The T-test performed for the samples in 2% Triton gave a p-value of 0.89. This indicated there was no significant difference in the amount of RNA present in 2% Triton between the 0.3 wt.% Acuitas-LNP-DOPE-PEG-OTF and the 6.3 wt.% Acuitas-LNP-DOPE-PEG-OTF. This was expected as the amount of DOPE-PEG added to the film should not be affecting the amount of RNA in the LNPs and once the 2% Triton is added to the sample, all RNA should be released. The T-test performed for the samples in TE buffer gave a p-value of 0.03. This indicated that there was a significant difference in the amount of RNA present in the TE buffer between the 0.3 wt.% Acuitas-LNP-DOPE-PEG-OTF and the 6.3 wt.% Acuitas-LNP-DOPE-PEG-OTF. This confirms that the addition of DOPE-PEG can help stabilize the Acuitas-LNPs in the OTF.

In addition to stabilizing Acuitas-LNP, DOPE-PEG appears to also improve the mechanical properties of the Acuitas-LNP-OTFs. Acuitas-LNP-OTFs that do not contain DOPE-PEG are very difficult to remove from the mylar that the OTF is cast on. OTFs that do not contain DOPE-PEG are also brittle and can easily break when folded in half (Figure 57(f)). In contrast, the DOPE-PEG film is easy to remove from the mylar and is very flexible (Figure 57(c)). One possible concern for the DOPE-PEG OTF is that the film mixture is viscous (Figure 57(a)) in comparison to a film mixture that contains no DOPE-PEG (Figure 57(d)). This is because the wt.% of water in the film decreased with the addition of DOPE-PEG. Increasing the water content would likely solve this issue. Furthermore, the addition of DOPE-PEG into the film mixture results in a significant number of bubbles in the film mixture and OTF (Figure 57(c)), to resolve this, the film mixture should be allowed to sit overnight or should be placed under vacuum.

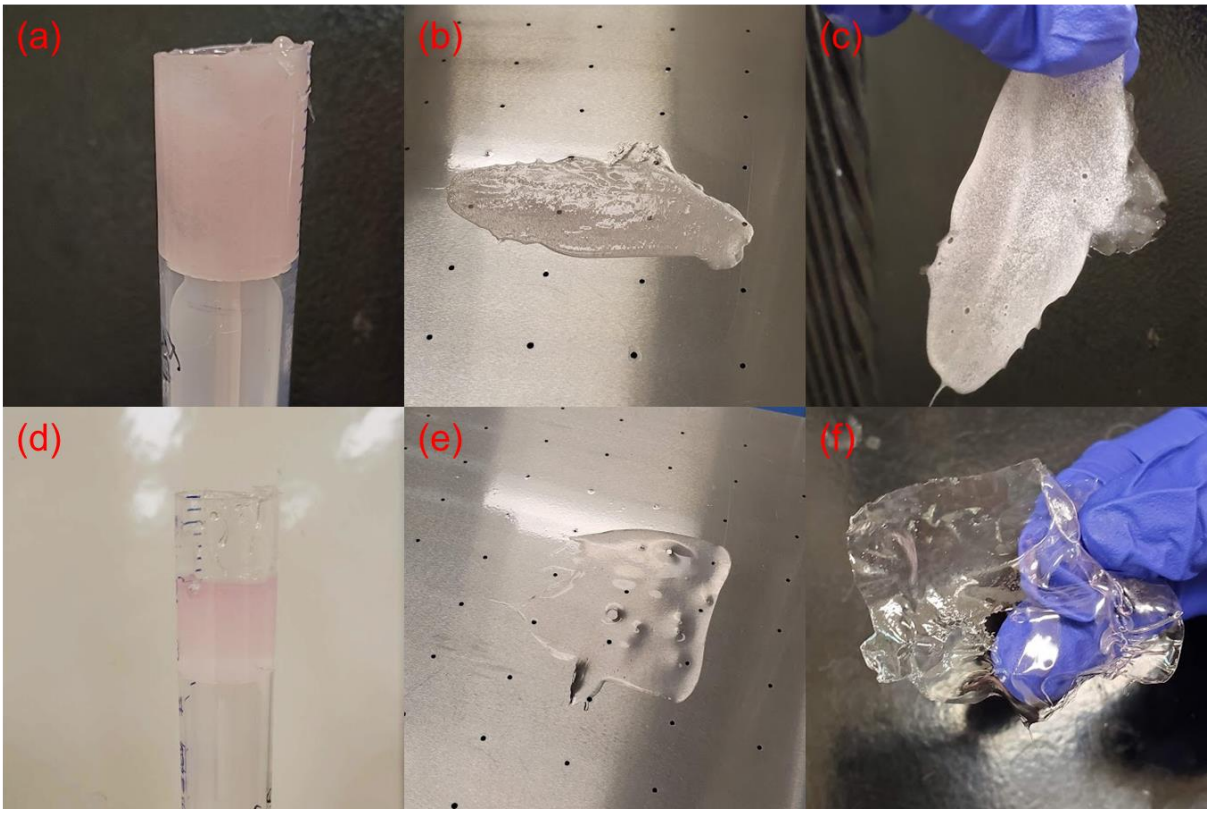

Figure 57: Images showing the (a) film mixture, (b) cast film mixture, and (c) dried OTF of Acuitas-LNP-DOPE-PEG-OTF and the (d) film mixture, (e) cast film mixture, and (f) dried OTF of Acuitas-LNP-OTF without DOPE-PEG.

3.3.13 Incorporating Lecithin and PEG into the Acuitas-LNP-OTFs

DOPE-PEG was effective at stabilizing the LNPs in the OTFs, however, DOPE-PEG contains both a lipid and a PEG chain. It was important to determine if was necessary to use DOPE-PEG or if a lipid or PEG by themselves would work. Lecithin was used as a model lipid as it has a similar structure to the lipid portion of DOPE-PEG. Films with 0.3 wt.% (Acuitas-LNP-Lecithin-OTF-1), 0.7 wt.% (Acuitas-LNP-Lecithin-OTF-2), and 1.4 wt.% (Acuitas-LNP-Lecithin-OTF-3) lecithin were prepared.

An initial addition of lecithin showed some improvement in the Acuitas-LNP stability, however, further increasing the amount of lecithin in the OTFs did not show much improvement. In addition, these films contained a significantly higher number of moles of lipid than the DOPE-

PEG films. To ensure that lipid alone cannot be used, DOPE instead of lecithin would need to be added to the OTFs.

The film prepared with a 0.3 wt.% of lecithin had an RNA concentration of (0.30 ± 0.01) µg/mL in TE buffer and a concentration of 0.48 ± 0.03 µg/mL of RNA in 2% Triton (Figure 58). The film prepared with a 0.7 wt.% of lecithin had an RNA concentration of 0.280 ± 0.006 µg/mL in TE buffer and a concentration of 0.53 ± 0.02 µg/mL of RNA in 2% Triton (Figure 58). The film prepared with a 1.4 wt.% of lecithin had an RNA concentration of 0.238 ± 0.002 µg/mL in TE buffer and a concentration of 0.50 ± 0.01 µg/mL of RNA in 2% Triton (Figure 58).

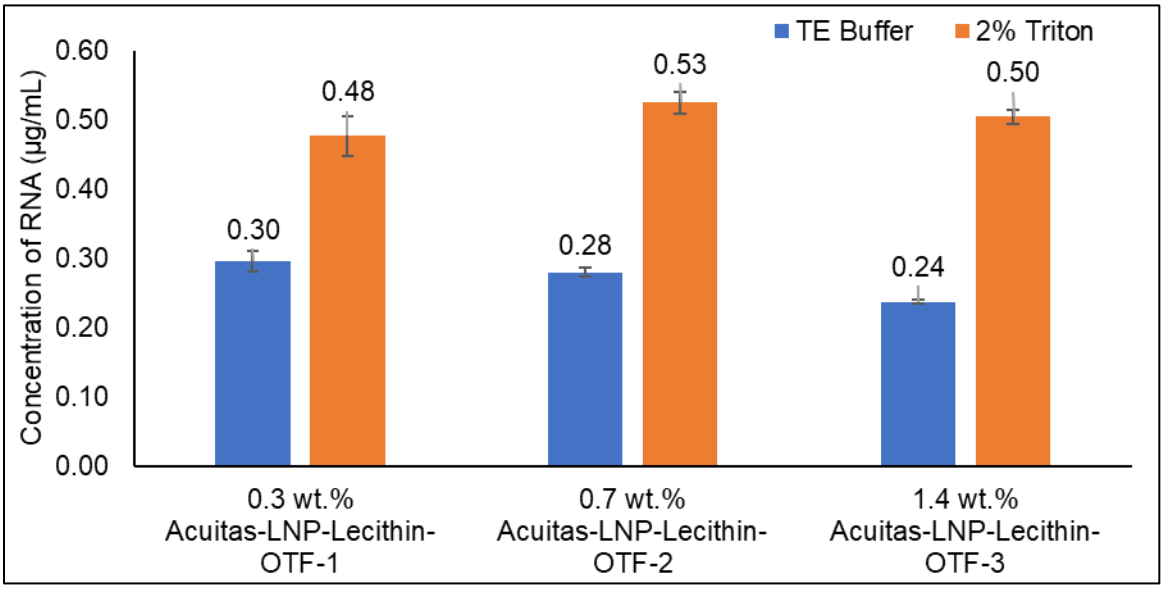

Figure 58: Results from the RiboGreen assay performed on Acuitas-LNP-Lecithin-OTFs with 0.3, 0.7, and 1.4 wt.% lecithin incorporated into film mixture.

Next, three different molecular weight PEG molecules were added to the film mixture. PEG-10 000 (Acuitas-LNP-PEG-OTF-1), PEG-2000 (Acuitas-LNP-PEG-OTF-2), and PEG-3350 (Acuitas-LNP-PEG-OTF-3) were added at 1.4 wt.% to the film mixture. The PEG-10 000 and PEG-2000, did not seem to have any stabilizing effects on the LNPs in the OTFs. Surprisingly the PEG-3350 did have a slight stabilizing effect on the LNPs.

The three films were dissolved in buffer and underwent the RiboGreen assay at a theoretical concentration of 0.625 µg/mL. The film prepared with a PEG-10 000 had an RNA concentration of 0.46 ± 0.01 µg/mL in TE buffer and a concentration of 0.48 ± 0.01 µg/mL of RNA in 2% Triton (Figure 59). The film prepared with PEG-2000 had an RNA concentration of 0.46 ± 0.006 µg/mL in TE buffer and a concentration of 0.49 ± 0.02 µg/mL of RNA in 2% Triton (Figure 59). The film prepared with PEG-3350 had an RNA concentration of 0.304 ± 0.002 µg/mL in TE buffer and a concentration of 0.44 ± 0.02 µg/mL of RNA in 2% Triton (Figure 59).

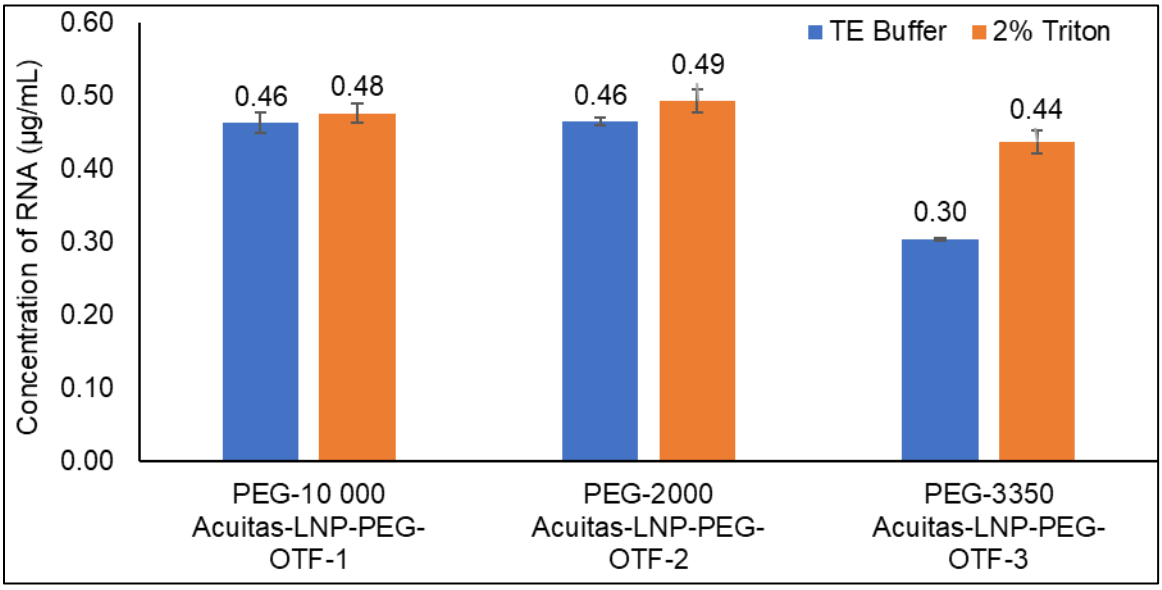

Figure 59: Results from the RiboGreen assay performed on Acuitas-LNP-PEG-OTFs with PEG-10 000, PEG-2000, and PEG-3350.

These results indicate that DOPE-PEG is far better at stabilizing the LNPs in a OTF than lecithin or PEG alone.

3.4 Conclusions

FITC-LNPs and Acuitas-LNPs were incorporated into OTFs. Both the FITC-LNP-OTF and Acuitas-LNP-OTF were imaged using epifluorescence microscopy followed by super resolution optical microscopy. The super resolution images acquired of the FITC-LNP-OTF and

Acuitas-LNP-OTF indicated the particles were not damaged during the film casting process. The particle size distribution of the LNPs in the OTF was similar to that of the LNPs on a glass coverslip. Moreover, there were no streaks of fluorescence visible in the images and the particles remained circular in shape, indicating the particles were not sheared during the film casting process.

The Quant-iT RiboGreen RNA assay was then performed on Acuitas-LNPs and Acuitas-LNP-OTFs to determine if the RNA was remaining encapsulated within the LNPs once incorporated in the OTFs. The RiboGreen assay indicated that RNA was becoming un-encapsulated from the Acuitas-LNPs sometime between being added to the film mixture and being dissolved for the assay. There were high amounts of RNA present in the Acuitas-LNP-OTF sample prior to the disruption of the lipids within the LNPs. This resulted in changes to the film formulation, and evaluations performed on how the Acuitas-LNPs could be handled. It was concluded that an additive would need to be added to the film mixture to help stabilize the Acuitas-LNPs. Varying amounts of trehalose, DOPE-PEG, lecithin, PEG -10 000, PEG-2000, and PEG-3350 were all added to the film formulation. Trehalose, PEG-10 000, PEG-2000 had no stabilizing effects on the Acuitas-LNPs. Lecithin and PEG-3350 showed some improvements in Acuitas-LNP stability, however there was still significant amounts of unencapsulated RNA present in the sample. DOPE-PEG was very effective at stabilizing the LNPs. As the DOPE-PEG content of the OTFs was increased from 0.3 wt.% to 6.3 wt.%, the stability of the LNPs was increased. Gel electrophoresis was also used to evaluate the integrity of RNA present in the Acuitas-LNPs, Acuitas-LNP-FM-5, and Acuitas-LNP-OTF-3. Gel electrophoresis showed the RNA remained intact even after the film casting process.

3.5 Experimental

General

All optical microscopy images in this section were acquired by Dr. Mouhanad Babi and Christine Cerson. Acuitas LNPs were obtained from Acuitas Therapeutics. All other reagents and solvents were acquired from commercial sources. All plastics (micropipette tips, syringes, Eppendorf tubes, centrifuge tubes, microplate, etc.) used with the Acuitas-LNPs and the RiboGreen assay were purchased as sterile DNA/ DNase/RNase/PCR inhibitor/ATP/pyrogen free certified micropipette. Epifluorescence microscopy, SRRF, and STORM images were acquired on a custom-built Leica DMI6000B inverted microscope, equipped with a 100x/1.47NA oil-immersion objective. All confocal microscopy images were obtained using an upright confocal Nikon A1R HD25 microscope, using a 60x objective. DLS measurements were acquired using a NanoBrook 90Plus PALS from Brookhaven. Fluorescence values for the RiboGreen assay were obtained using a BioTek Cytation 5 Cell Imaging Multimode Reader. Horizontal agarose gel electrophoresis was performed using a One Lambda, Inc cell with a Bio Rad PowerPac basic power supply. Samples were centrifuged using a Thermo Scientific Sorvall Legend X1R Centrifuge. Paddle mixing was performed using a Caframo BDC3030 paddle mixer, equipped with spatula as the paddle. Samples were paddle mixed in a plastic disposable syringe in which the barrel had been cut. (Figure 60). OTF samples were cast on a Minder Hightech MD-TMJ200. Samples were agitated on a VWR S-500 orbital shaker.

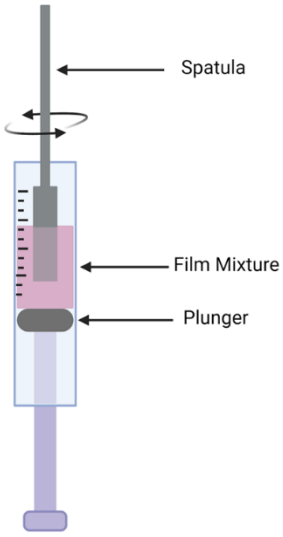

Figure 60: Illustration showing the syringe that the film mixture is paddle mixed in. Created with BioRender.

Film Mixture 1

Table 8: Ingredients and amounts of ingredients added to Film Mixture 1.

Ingredient	Amount (g)	Weight Percentage (%)
Pullulan	16.5	32.9
Trehalose	2.9	5.8
Dimethyl Sulfone	0.1	0.2
Glycerol	2.2	4.4
0.29 mg/mL Tween in DI Water	28.4	56.7
Total	50.1	100

Film Mixture 1 was prepared by adding the ingredients as described in Table 8 to a 200 mL beaker. The ingredients were paddle mixed at 60 RPM for 24 hours. The solution was then covered with parafilm and stored in the fridge until needed.

Film Mixture 2

Table 9: Ingredients and amounts of ingredients added to Film Mixture 2.

Ingredient	Amount (g)	Weight Percentage (%)
Pullulan	16.5	32.9
Trehalose	2.9	5.8
Dimethyl Sulfone	0.1	0.2
Glycerol	2.2	4.4
DI Water	28.4	56.7
Total	50.1	100

Film Mixture 2 was prepared by adding the ingredients as described in Table 9 to a 200 mL beaker. The ingredients were paddle mixed at 60 RPM for 24 hours. The solution was then covered with parafilm and stored in the fridge until needed.

Film Mixture 3

Table 10: Ingredients and amounts of ingredients added to Film Mixture 3.

Ingredient	Amount (g)	Weight Percentage (%)
Pullulan	16.5	32.9
Trehalose	2.9	5.8
Dimethyl Sulfone	0.1	0.2
Glycerol	2.2	4.4
Tris Buffer (0.1 M, pH 8) Prepared with Sterile Water	28.4	56.7
Total	50.1	100

Film Mixture 3 was prepared by adding the ingredients as described in Table 10 to a 200 mL beaker. The ingredients were paddle mixed at 60 RPM for 24 hours. The solution was then covered with parafilm and stored in the fridge until needed.

Film Mixture 4

Table 11:Ingredients and amounts of ingredients added to Film Mixture 4.

Ingredient	Amount (g)	Weight Percentage (%)
Pullulan	0.64	32.3
Trehalose	0.116	5.9
Glycerol	0.086	4.4
1X TE Buffer (pH=7) Prepared with Sterile Water	1.134	57.4
Total	1.976	100

Film Mixture 4 was prepared by adding the ingredients as described in Table 11 to a 5 mL syringe. The ingredients were paddle mixed at 60 RPM for 1 hour. The solution was then covered with parafilm and stored in the fridge until needed.

Preparation of FITC-LNP-OTF

FITC-LNPs were diluted 1:10, 1:100, and 1:1000, using DI water. To a 3 mL syringe, 1 gram of Film Mixture 1, 150 µL of dilute FITC-LNPs, and 350 µL of DI water was added. The film mixture was paddle mixed at 20 RPM for 15 minutes and immediately cast at 50˚C for 30 minutes. A FITC-LNP-OTF was prepared for each of the three dilutions. To image the films, the FITC-LNP-OTFs were taped onto a plasma cleaned glass coverslip. The sample was submerged in methanol during imaging.

Acuitas-LNP-OTF Imaged Using Epifluorescence and Super Resolution Microscopy

Acuitas-LNP were diluted 1:10, 1:100, 1:1000, and 1:10 000 in water. To a 3 mL, 0.5 grams of Film Mixture 1, and 0.25 mL of dilute Acuitas-LNP was added. The Mixture was paddle mixed at 60 RPM for 20 minutes. The film was cast directly onto a plasma cleaned glass coverslip at 35˚C. A hole was punctured into the mylar, allowing for the vacuum to hold the coverslip in place while

the doctor blade moved the film mixture over the glass coverslip. Acuitas-LNP-OTFs were prepared with all 4 different Acuitas-LNP dilution factors.

Quant-iT RiboGreen Assay Calibration Curve

1X TE working solution was prepared by diluting 20X concentrated TE buffer, 20-fold using sterile-filtered water, suitable for cell culture. 200-fold diluted Quant-iT RiboGreen reagent was prepared by diluting the concentrated DMSO stock solution, 200-fold in TE buffer. A 2 µg/mL RNA solution was prepared by diluting the 100 µg/mL RNA stock solution. A high-range standard curve was prepared by adding the values of TE buffer and 2 µg/mL RNA solution as described in Table 12, to a microplate. The microplate was incubated at 37˚C for 10 minutes in the microplate reader. The 200-fold diluted Quant-iT RiboGreen reagent was then added to the samples as described in Table 12. The sample was shaken for 10 seconds in the microplate reader, the fluorescence of the sample was immediately measured at an excitation wavelength of 485 nm and an emission wavelength of 535 nm.

Table 12: Volumes of 1X TE buffer, 2 µg/mL RNA standard solution, 200-fold diluted Quant-iT RiboGreen reagent, used to prepare the calibration curve for the RiboGreen assay.

Volume of 1X TE Buffer (µL)	Volume of 2 µg/mL RNA Solution (µL)	Volume of 200-Fold Diluted Quant-iT RiboGreen Reagent (µL)	Final RNA Concentration in Quant-iT RiboGreen Assay (µg/mL)
0	100	100	1
50	50	100	0.5
90	10	100	0.1
98	2	100	0.02
100	0	100	0

Quant-iT RiboGreen Assay on Samples

1X TE working solution was prepared by diluting 20X concentrated TE buffer, 20-fold using sterile-filtered water, suitable for cell culture. 200-fold diluted Quant-iT RiboGreen reagent was prepared by diluting the concentrated DMSO stock solution, 200-fold in TE buffer. 100X Triton was dissolved with TE buffer to make a 2% Triton solution.

LNP samples were diluted to a concentration of 2-5 µg/mL RNA using 1X TE buffer. All Acuitas-LNP-FMs and Acuitas-LNP-OTFs prepared prior to Control 1 were dissolved by gentle swirling by hand. Acuitas-LNP-FMs and Acuitas-LNP-OTFs dissolved after Control 1 were dissolved with the aid of an orbital shaker, set to a speed of 2, for 30-60 minutes. 50µL of the dilute Acuitas-LNP sample was loaded into two sets of microplate wells. 50 µL of 1X TE buffer was added to an additional well in each set of wells, as a blank. To the first set of wells, 50 µL of 1X TE buffer was added. To the second set of wells, 50 µL of 2% Triton solution was added. The microplate was incubated at 37˚C for 10 minutes in the microplate reader. Following this, 100 µL of the 200-fold diluted Quant-iT RiboGreen reagent was added to each well. The sample was shaken for 10 seconds in the microplate reader, the fluorescence of the sample was immediately measured at an excitation wavelength of 485 nm and an emission wavelength of 535 nm.

Acuitas-LNP-OTF-1

To a 5 mL syringe, 1 gram of Film Mixture 1, 50 µL of Acuitas-LNPs, and 450 µL of DI-water was added. The mixture was paddle mixed at 60 RPM for 20 minutes. The film was cast at 35˚C for 30 minutes.

Isolation of Acuitas-LNPs from Acutias-LNP-OTF-1 Using Pullulanase

Acuitas-LNP-OTF-1 was dissolved in 12 mL of tris buffer (0.1 M, pH=8). 1 mL of pullulanase was added and the sample was magnetically stirred for 1 hour at 500 RPM. The solution was then filtered through an Amicon centrifugal filter unit (100kDa MWCO) via centrifugation at 6000 *g*. Once all of the buffer had been removed from the particles, the particles were washed with increments of 3 mL of DI water until all brown residue from pullulanase was washed away. The Acuitas-LNPs were re-dispersed in TE buffer to give a theoretical concentration of 5 µg/mL of RNA.

Centrifuging Acuitas-LNPs

20 µL of Acuitas-LNPs was dispersed in 2 mL DI water. The sample was loaded into an Amicon centrifugal filter unit (100 kDa MWCO) and centrifuged for 2 hours at 6000 *g*. The LNPs were then re-dispersed in TE buffer to a concentration of 5 µg/mL.

Pullulanase added to Acuitas-LNPs

10 µL of Acuitas-LNPs were added to 2 mL TE buffer. 1 drop of pullulanase was added to the solution and the sample was magnetically stirred for 1 hour at 500 RPM.

Isolation of Acuitas-LNPs from Acutias-LNP-OTF-1 Using Filtration

Acuitas-LNP-OTF-1 was dissolved in 15 mL of DI water. The solution was then filtered through an Amicon centrifugal filter unit (100 kDa MWCO) via centrifugation at 6000 *g*. Additional 3 mL increments of DI water were added to the centrifuge tube to dissolve as much film mixture as possible. The sample was centrifuged for a total of 5 hours until approximately

250 µL of Acuitas-LNP-OTF-1 remained in the filter unit. The mixture was diluted to a theoretical concentration of 5 µL/mL of RNA.

Blank-OTF

To a 5 mL syringe, 1 gram of Film Mixture 1, and 500 µL of DI-water was added. The mixture was paddle mixed at 60 RPM for 20 minutes, and cast at 35˚C for 30 minutes.

RNA-FM

To a 5 mL syringe, 0.5 grams of Film Mixture 3, 100 µL 100 µg/mL RNA stock solution (from the Quant-iT RiboGreen RNA assay kit), and 150 µL of nuclease free tris buffer (0.1 M, pH = 8). The mixture was paddle mixed at 20 RPM for 30 minutes.

RNA-OTF

To a 5 mL syringe, 0.5 gram of Film Mixture 3, 100 µL 100 µg/mL RNA stock solution (from the Quant-iT RiboGreen RNA assay kit), and 150 µL of nuclease free tris buffer (0.1 M, pH = 8). The mixture was paddle mixed at 20 RPM for 30 minutes and was cast at 35˚C for 60 minutes.

Acutias-LNP-FM-1

To a 5 mL syringe, 1 gram of Film Mixture 1, 50 µL of Acuitas-LNPs, and 450 µL of DI-water was added. The mixture was paddle mixed at 60 RPM for 20 minutes.

Acuitas-LNP-FM-2

To a 5 mL syringe, 1 gram of Film Mixture 2, 50 µL of Acuitas-LNPs, and 450 µL of DI-water was added. The mixture was paddle mixed at 60 RPM for 20 minutes.

Acuitas-LNP-FM-3

To a 5 mL syringe, 1 gram of Film Mixture 2, 50 µL of Acuitas-LNPs, and 450 µL of tris buffer (0.1 M, pH=8) was added. The mixture was paddle mixed at 20 RPM for 30 minutes.

Acutias-LNP-OTF-2

To a 5 mL syringe, 1 gram of Film Mixture 2, 50 µL of Acuitas-LNPs, and 450 µL of tris buffer (0.1 M, pH=8) was added. The mixture was paddle mixed at 20 RPM for 30 minutes and was cast at 35˚C for 60 minutes.

Acuitas-LNP-FM-4

To a 5 mL syringe, 1 gram of Film Mixture 3, 50 µL of Acuitas-LNPs, and 450 µL of tris buffer (0.1 M, pH=8) was added. The mixture was paddle mixed at 20 RPM for 30 minutes.

Trehalose-Acuitas-LNP Sample

To a 5 mL syringe, 0.05 g of trehalose, 0.567 g of DI water, 20 µL of Acuitas-LNPs, and 0.480 g of tris buffer (0.1 M, pH=8) were added. The sample was paddle mixed at 20 RPM for 30 minutes.

Glycerol-Acuitas-LNP Sample

To a 5 mL syringe, 0.004 g of glycerol, 0.567 g of DI water, 20 µL of Acuitas-LNPs, and 0.480 g of tris buffer (0.1 M, pH=8) were added. The sample was paddle mixed at 20 RPM for 30 minutes.

Dimethyl-Sulfone-Acuitas-LNP Sample

To a 5 mL syringe, 0.003 g of dimethyl sulfone, 0.567 g of DI water, 20 µL of Acuitas-LNPs, and 0.480 g of tris buffer (0.1 M, pH=8) were added. The sample was paddle mixed at 20 RPM for 30 minutes.

33 wt.% Pullulan-Acuitas-LNP Sample (First Trial)

To a 5 mL syringe 0.32 g of pullulan was added to 0.567 g of DI water. The sample was paddle mixed at 20 RPM for 60 minutes. 20 µL of Acuitas-LNPs, and 0.480 g of tris buffer (0.1 M, pH=8) was added to the syringe. The sample was paddle mixed at 20 RPM for 60 minutes.

33 wt.% Pullulan-Acuitas-LNP Sample (Second Trial)

To a 5 mL syringe 0.33 g of pullulan was added to 0.567 g of tris buffer (0.1 M, pH=8). The sample was paddle mixed at 60 RPM for 30 minutes. 20 µL of Acuitas-LNPs, and 0.480 g of tris buffer (0.1 M, pH=8) was added to the syringe. The sample was paddle mixed at 20 RPM for 30 minutes.

12 wt.% Pullulan-Acuitas-LNP Sample

To a 5 mL syringe 0.1 g of pullulan was added to 0.567 g of tris buffer (0.1 M, pH=8). The sample was paddle mixed at 60 RPM for 30 minutes. 20 µL of Acuitas-LNPs, and 0.480 g of tris buffer (0.1 M, pH=8) was added to the syringe. The sample was paddle mixed at 20 RPM for 30 minutes.

42 wt.% Pullulan-Acuitas-LNP Sample

To a 5 mL syringe 0.495 g of pullulan was added to 0.567 g of tris buffer (0.1 M, pH=8). The sample was paddle mixed at 60 RPM for 30 minutes. 20 µL of Acuitas-LNPs, and 0.480 g of

tris buffer (0.1 M, pH=8) was added to the syringe. The sample was paddle mixed at 20 RPM for 30 minutes.

Drying then Re-Dispersing Acuitas-LNPs

To a glass vial, 20 µL of Acuitas-LNPs were added. The sample was allowed to dry. The Acuitas-LNPs were re-dispersed in 2 mL of TE buffer.

1% Agarose Gel Electrophoresis

0.4 grams of agarose was added to 40 mL of 1x TBE Buffer. The solution was microwaved for 1 minute until the solution began to boil. 4 µL of SYBR Safe DNA Gel Stain was mixed into the solution and poured into the casting tray. The well combs were added and the gel was allowed to set. 4 µL of Thermo Scientific RiboRuler High Range RNA Ladder was added to 4 µL of 2X loading dye. Gel electrophoresis was performed on Acuitas-LNPs, Acuitas-LNP-FM-5, and Acuitas-LNP-OTF-3. Acuitas-LNP samples were dissolved in TE buffer to an RNA concentration of 0.2 µg/µL. 10 µL of the 0.2 µg/µL samples were then added to 10 µL of 2X loading dye (xylene cyanol FF, bromophenol blue, ethidium bromide). Samples were heated at 70˚C for 10 minutes and then placed in ice for 3 minutes. The 8 µL of ladder solution and the 20 µL of the LNP-samples were added to the wells. The gel was run at 60V for 40 minutes. The gel was then visualized under UV-light.

Acuitas-LNP-FM-5

To a 3 mL syringe, 0.25 gram of Film Mixture 4, 100 µL of Acuitas-LNPs, and 25 µL of nuclease free TE buffer (pH=7) was added. The mixture was paddle mixed at 20 RPM for 30 minutes.

Acutias-LNP-OTF-3

To a 3 mL syringe, 0.25 gram of Film Mixture 4, 100 µL of Acuitas-LNPs, and 25 µL of nuclease free TE buffer (pH=7) was added. The mixture was paddle mixed at 20 RPM for 30 minutes and was cast at 35˚C for 40 minutes.

Control 1

To a 5 mL syringe, 20 µL of Acuitas-LNPs, and 4 mL nuclease free TE buffer (pH=7) were added. The sample was paddle mixed at 20 RPM for 30 minutes, added to a vial and stored in the fridge overnight.

Control 2

To a 5 mL syringe, 20 µL of Acuitas-LNPs, and 4 mL nuclease free TE buffer (pH=7) were added. The sample was paddle mixed at 20 RPM for 30 minutes, added to a vial and stored at room temperature overnight.

Control 3

To a 5 mL syringe, 20 µL of Acuitas-LNPs, and 4 mL nuclease free TE buffer (pH=7) were added. The sample was paddle mixed at 20 RPM for 30 minutes, added to a vial and stored in the fridge overnight. The sample was then vigorously shaken by hand for 20 minutes.

Control 4

To a 20 mL vial, 20 µL of Acuitas-LNPs, and 4 mL nuclease free TE buffer (pH=7) were added. The sample was magnetically stirred at 100 RPM for 30 minutes. The sample was then stored in the fridge overnight.

Control 5

To a 20 mL vial, 20 µL of Acuitas-LNPs, and 4 mL nuclease free TE buffer (pH=7) were added. The sample was mixed on the orbital mixer at a speed of 5 for 30 minutes. The sample was then stored in the fridge overnight.

Control 6

To a 20 mL vial, 20 µL of Acuitas-LNPs, and 4 mL nuclease free TE buffer (pH=7) were added. The sample was magnetically stirred at 100 RPM at 35˚C for 30 minutes. The sample was then stored in the fridge overnight.

Control 7

To a 5 mL syringe, 1 gram of Film Mixture 3, 20 µL of Acuitas-LNPs, and 480 µL of tris buffer (0.1 M, pH=8) was added. The mixture was paddle mixed at 20 RPM for 30 minutes.

Control 8

To a 5 mL syringe, 1 gram of Film Mixture 3, 20 µL of Acuitas-LNPs, and 480 µL of tris buffer (0.1 M, pH=8) was added. The mixture was paddle mixed at 20 RPM for 45 minutes.

Control 9

To a 5 mL syringe, 1 gram of Film Mixture 3, 20 µL of Acuitas-LNPs, and 480 µL of tris buffer (0.1 M, pH=8) was added. The mixture was paddle mixed at 20 RPM for 60 minutes.

Control 10

To a 5 mL syringe, 1 gram of Film Mixture 3, 20 µL of Acuitas-LNPs, and 480 µL of tris buffer (0.1 M, pH=8) was added. The mixture was paddle mixed at 35 RPM for 30 minutes.

Control 11

To a 5 mL syringe, 1 gram of Film Mixture 3, 20 µL of Acuitas-LNPs, and 480 µL of tris buffer (0.1 M, pH=8) was added. The mixture was paddle mixed at 50 RPM for 30 minutes.

Control 12

To a 5 mL syringe, 1 gram of Film Mixture 3, 20 µL of Acuitas-LNPs, and 480 µL of tris buffer (0.1 M, pH=8) was added. The mixture was paddle mixed at 20 RPM for 30 minutes and then cast at 35˚C for 60 minutes.

Control 13

To a 5 mL syringe, 1 gram of Film Mixture 3, 20 µL of Acuitas-LNPs, and 480 µL of tris buffer (0.1 M, pH=8) was added. The mixture was paddle mixed at 20 RPM for 30 minutes and then cast at 45˚C for 50 minutes.

Control 14

To a 5 mL syringe, 1 gram of Film Mixture 3, 20 µL of Acuitas-LNPs, and 480 µL of tris buffer (0.1 M, pH=8) was added. The mixture was paddle mixed at 20 RPM for 30 minutes and then cast at 55˚C for 30 minutes.

Sample Preparation for Confocal Microscopy

Acuitas-LNP samples were diluted to 2.5 µg/mL RNA and added to a plastic petri dish for imaging. When samples were imaged with RiboGreen dye, 2 mL of the solution were removed from the stock solution. 100 µL of 200-fold diluted RiboGreen dye was added to the 2 mL of stock solution. The sample was then added to a plastic petri dish for imaging.

Film Mixture 5

Table 13: Ingredients and amounts of ingredients added to Film Mixture 5.

Ingredient	Amount (g)	Weight Percentage (%)
Pullulan	1.74	32.3
Trehalose	0.58	10.8
Dimethyl Sulfone	0.01	0.1
Glycerol	0.22	4.1
Tris Buffer (0.1 M, pH 8) Prepared with Sterile Water	2.84	52.7
Total	5.39	100

Acuitas-LNP-FM-6

To a 5 mL syringe, 1 gram of Film Mixture 5, 20 µL of Acuitas-LNPs, and 480 µL of tris buffer (0.1 M, pH=8) was added. The mixture was paddle mixed at 20 RPM for 30 minutes.

Acutias-LNP-OTF-4

To a 5 mL syringe, 1 gram of Film Mixture 5, 20 µL of Acuitas-LNPs, and 480 µL of tris buffer (0.1 M, pH=8) was added. The mixture was paddle mixed at 20 RPM for 30 minutes and then cast at 35˚C for 60 minutes.

Acuitas-LNP-DOPE-PEG-OTF-1

A 10 mg/mL solution of DOPE-PEG dissolved in nuclease free tris buffer (0.1 M, pH=8) was prepared. To a 5 mL syringe, 1 gram of Film Mixture 3, 480 µL of the 10 mg/mL DOPE-PEG solution, and 20 µL of Acuitas-LNPs were added. The sample was paddle mixed at 20 RPM for 30 minutes. The sample was cast at 35˚C for 60 minutes.

Table 14: Summary of ingredients and amounts of ingredient in the wet film mixture of Acuitas-LNP-DOPE-PEG-OTF-1.

	Ingredient	**Amount (g)**	**Weight Percentage (%)**
1 gram of Film Mixture 3	Pullulan	0.32	21.7
	Trehalose	0.058	3.9
	Dimethyl Sulfone	0.002	0.1
	Glycerol	0.043	2.9
	Tris Buffer (0.1 M, pH 8) Prepared with Sterile Water	0.570	38.6
480 µL of the 10 mg/mL DOPE-PEG Solution	DOPE-PEG	0.0048	0.3
	Tris Buffer (0.1 M, pH 8) Prepared with Sterile Water	0.480	32.5
	Total	1.4778	100

Acuitas-LNP-DOPE-PEG-OTF-2

A 10 mg/mL solution of DOPE-PEG dissolved in nuclease free tris buffer (0.1 M, pH=8) was prepared. To a 5 mL syringe, 0.32 g of pullulan, 0.058 g of trehalose, 0.002 g of dimethyl sulfone, 0.043 g of glycerol, and 570 µL of the 10 mg/mL DOPE-PEG solution was added. The mixture was paddle mixed at a speed of 60 RPM for 60 minutes. 20 µL of Acuitas-LNPs and an additional 480 µL of the 10 mg/mL DOPE-PEG solution were added. The solution was paddle mixed at 20 RPM for 30 minutes. The film was cast at 35˚C for 45 minutes.

Table 15: Summary of ingredients and amounts of ingredient in the wet film mixture of Acuitas-LNP-DOPE-PEG-OTF-2.

	Ingredient	**Amount (g)**	**Weight Percentage (%)**
1 gram of Film Mixture	Pullulan	0.32	21.6
	Trehalose	0.058	3.9
	Dimethyl Sulfone	0.002	0.1
	Glycerol	0.043	2.9
	Tris Buffer (0.1 M, pH 8) Prepared with Sterile Water	0.570	38.4
	DOPE-PEG	0.0057	0.7
480 µL of the 10 mg/mL DOPE-PEG Solution	DOPE-PEG	0.0048	
	Tris Buffer (0.1 M, pH 8) Prepared with Sterile Water	0.480	32.4
	Total	1.4835	100

Acuitas-LNP-DOPE-PEG-OTF-3

A 20 mg/mL solution of DOPE-PEG dissolved in nuclease free tris buffer (0.1 M, pH=8) was prepared. To a 5 mL syringe, 0.32 g of pullulan, 0.058 g of trehalose, 0.002 g of dimethyl sulfone, 0.043 g of glycerol, and 570 µL of the 20 mg/mL DOPE-PEG solution was added. The mixture was paddle mixed at a speed of 60 RPM for 60 minutes. 20 µL of Acuitas-LNPs and an additional 480 µL of the 20 mg/mL DOPE-PEG solution were added. The solution was paddle mixed at 20 RPM for 30 minutes. The film was cast at 35˚C for 45 minutes.

Table 16:Summary of ingredients and amounts of ingredient in the wet film mixture of Acuitas-LNP-DOPE-PEG-OTF-3.

	Ingredient	**Amount (g)**	**Weight Percentage (%)**
1 gram of Film Mixture	Pullulan	0.32	21.4
	Trehalose	0.058	3.9
	Dimethyl Sulfone	0.002	0.1
	Glycerol	0.043	2.9
	Tris Buffer (0.1 M, pH 8) Prepared with Sterile Water	0.570	38.1
	DOPE-PEG	0.0114	1.4
480 µL of the 20 mg/mL DOPE-PEG Solution	DOPE-PEG	0.0098	
	Tris Buffer (0.1 M, pH 8) Prepared with Sterile Water	0.480	32.1
	Total	1.4942	100

Acuitas-LNP-DOPE-PEG-OTF-4

100 mg of DOPE-PEG was dissolved in 1.05 mL nuclease free tris buffer (0.1 M, pH=8) to give a concentration of 95 mg/mL. To a 5 mL syringe, 0.32 g of pullulan, 0.058 g of trehalose, 0.002 g of dimethyl sulfone, 0.043 g of glycerol, and 570 µL of the 95 mg/mL DOPE-PEG solution was added. The mixture was paddle mixed at a speed of 60 RPM for 60 minutes. 20 µL of Acuitas-LNPs and an additional 480 µL of the 95 mg/mL DOPE-PEG solution were added. The solution was paddle mixed at 20 RPM for 30 minutes. The film was cast at 35˚C for 60 minutes.

Table 17: Summary of ingredients and amounts of ingredient in the wet film mixture of Acuitas-LNP-DOPE-PEG-OTF-4.

	Ingredient	**Amount (g)**	**Weight Percentage (%)**
1 gram of Film Mixture	Pullulan	0.32	20.3
	Trehalose	0.058	3.7
	Dimethyl Sulfone	0.002	0.1
	Glycerol	0.043	2.7
	Tris Buffer (0.1 M, pH 8) Prepared with Sterile Water	0.570	36.2
	DOPE-PEG	0.0542	6.3
480 µL of the 95 mg/mL DOPE-PEG Solution	DOPE-PEG	0.0456	
	Tris Buffer (0.1 M, pH 8) Prepared with Sterile Water	0.480	30.5
	Total	1.5728	100

Acuitas-LNP-lecithin-OTF-1

A 10 mg/mL solution of lecithin dissolved in nuclease free tris buffer (0.1 M, pH=8) was prepared. To a 5 mL syringe, 1 gram of Film Mixture 3, 480 µL of the 10 mg/mL lecithin solution, and 20 µL of Acuitas-LNPs were added. The sample was paddle mixed at 20 RPM for 30 minutes. The sample was cast at 35˚C for 60 minutes.

Table 18: Summary of ingredients and amounts of ingredient in the wet film mixture of Acuitas-LNP-lecithin-OTF-1.

	Ingredient	**Amount (g)**	**Weight Percentage (%)**
1 gram of Film Mixture 3	Pullulan	0.32	21.7
	Trehalose	0.058	3.9
	Dimethyl Sulfone	0.002	0.1
	Glycerol	0.043	2.9
	Tris Buffer (0.1 M, pH 8) Prepared with Sterile Water	0.570	38.6
480 µL of the 10 mg/mL Lecithin Solution	Lecithin	0.0048	0.3
	Tris Buffer (0.1 M, pH 8) Prepared with Sterile Water	0.480	32.5
	Total	1.4778	100

Acuitas-LNP-lecithin-OTF-2

A 10 mg/mL solution of lecithin dissolved in nuclease free tris buffer (0.1 M, pH=8) was prepared. To a 5 mL syringe, 0.32 g of pullulan, 0.058 g of trehalose, 0.002 g of dimethyl sulfone, 0.043 g of glycerol, and 570 µL of the 10 mg/mL lecithin solution was added. The mixture was paddle mixed at a speed of 60 RPM for 60 minutes. 20 µL of Acuitas-LNP and an additional 480 µL of the 10 mg/mL lecithin solution were added. The sample was paddle mixed at 20 RPM for 30 minutes. The sample was cast at 35˚C for 60 minutes.

Table 19:Summary of ingredients and amounts of ingredient in the wet film mixture of Acuitas-LNP-lecithin-OTF-2.

	Ingredient	**Amount (g)**	**Weight Percentage (%)**
1 gram of Film Mixture	Pullulan	0.32	21.6
	Trehalose	0.058	3.9
	Dimethyl Sulfone	0.002	0.1
	Glycerol	0.043	2.9
	Tris Buffer (0.1 M, pH 8) Prepared with Sterile Water	0.570	38.4
	Lecithin	0.0057	0.7
480 µL of the 10 mg/mL Lecithin Solution	Lecithin	0.0048	
	Tris Buffer (0.1 M, pH 8) Prepared with Sterile Water	0.480	32.4
	Total	1.4835	100

Acuitas-LNP-lecithin-OTF-3

A 20 mg/mL solution of lecithin dissolved in nuclease free tris buffer (0.1 M, pH=8) was prepared. To a 5 mL syringe, 0.32 g of pullulan, 0.058 g of trehalose, 0.002 g of dimethyl sulfone, 0.043 g of glycerol, and 570 µL of the 20 mg/mL lecithin solution was added. The mixture was paddle mixed at a speed of 60 RPM for 60 minutes. 20 µL of Acuitas-LNPs and an additional 480

µL of the 20 mg/mL lecithin solution were added. The sample was paddle mixed at 20 RPM for 30 minutes. The sample was cast at 35˚C for 60 minutes.

Table 20: Summary of ingredients and amounts of ingredient in the wet film mixture of Acuitas-LNP-lecithin-OTF-2.

	Ingredient	**Amount (g)**	**Weight Percentage (%)**
1 gram of Film Mixture	Pullulan	0.32	21.6
	Trehalose	0.058	3.9
	Dimethyl Sulfone	0.002	0.1
	Glycerol	0.043	2.9
	Tris Buffer (0.1 M, pH 8) Prepared with Sterile Water	0.570	38.4
	Lecithin	0.0114	1.4
480 µL of the 20 mg/mL Lecithin Solution	Lecithin	0.0096	
	Tris Buffer (0.1 M, pH 8) Prepared with Sterile Water	0.480	32.4
	Total	1.4942	100

Acuitas-LNP-PEG-OTF-1

A 20 mg/mL solution of PEG-10 000 dissolved in nuclease free tris buffer (0.1 M, pH=8) was prepared. To a 5 mL syringe, 0.32 g of pullulan, 0.058 g of trehalose, 0.002 g of dimethyl sulfone, 0.043 g of glycerol, and 570 µL of the 20 mg/mL PEG solution was added. The mixture was paddle mixed at a speed of 60 RPM for 60 minutes. 20 µL of Acuitas-LNPs and an additional 480 µL of the 20 mg/mL PEG solution were added. The sample was paddle mixed at 20 RPM for 30 minutes. The sample was cast at 35˚C for 60 minutes.

Table 21: Summary of ingredients and amounts of ingredient in the wet film mixture of Acuitas-LNP-PEG-OTF-1.

	Ingredient	**Amount (g)**	**Weight Percentage (%)**
1 gram of Film Mixture	Pullulan	0.32	21.6
	Trehalose	0.058	3.9
	Dimethyl Sulfone	0.002	0.1
	Glycerol	0.043	2.9
	Tris Buffer (0.1 M, pH 8) Prepared with Sterile Water	0.570	38.4
	PEG-10 000	0.0114	1.4
480 µL of the 20 mg/mL PEG-10000 Solution	PEG-10 000	0.0096	
	Tris Buffer (0.1 M, pH 8) Prepared with Sterile Water	0.480	32.4
	Total	1.4942	100

Acuitas-LNP-PEG-OTF-2

A 20 mg/mL solution of PEG-2000 dissolved in nuclease free tris buffer (0.1 M, pH=8) was prepared. To a 5 mL syringe, 0.32 g of pullulan, 0.058 g of trehalose, 0.002 g of dimethyl sulfone, 0.043 g of glycerol, and 570 µL of the 20 mg/mL PEG-2000 solution was added. The mixture was paddle mixed at a speed of 60 RPM for 60 minutes. 20 µL of Acuitas-LNPs and an additional 480 µL of the 20 mg/mL PEG-2000 solution were added. The sample was paddle mixed at 20 RPM for 30 minutes. The sample was cast at 35˚C for 60 minutes.

Table 22: Summary of ingredients and amounts of ingredient in the wet film mixture of Acuitas-LNP-PEG-OTF-2.

	Ingredient	**Amount (g)**	**Weight Percentage (%)**
1 gram of Film Mixture	Pullulan	0.32	21.6
	Trehalose	0.058	3.9
	Dimethyl Sulfone	0.002	0.1
	Glycerol	0.043	2.9
	Tris Buffer (0.1 M, pH 8) Prepared with Sterile Water	0.570	38.4
	PEG-2000	0.0114	1.4
480 µL of the 20 mg/mL PEG-2000 Solution	PEG-2000	0.0096	
	Tris Buffer (0.1 M, pH 8) Prepared with Sterile Water	0.480	32.4
	Total	1.4942	100

Acuitas-LNP-PEG-OTF-3

A 20 mg/mL solution of PEG-3350 dissolved in nuclease free tris buffer (0.1 M, pH=8) was prepared. To a 5 mL syringe, 0.32 g of pullulan, 0.058 g of trehalose, 0.002 g of dimethyl sulfone, 0.043 g of glycerol, and 570 µL of the 20 mg/mL PEG solution was added. The mixture was paddle mixed at a speed of 60 RPM for 60 minutes. 20 µL of Acuitas-LNPs and an additional 480 µL of the 20 mg/mL PEG-3350 solution were added. The sample was paddle mixed at 20 RPM for 30 minutes. The sample was cast at 35˚C for 60 minutes.

Table 23: Summary of ingredients and amounts of ingredient in the wet film mixture of Acuitas-LNP-PEG-OTF-3.

	Ingredient	Amount (g)	Weight Percentage (%)
1 gram of Film Mixture	Pullulan	0.32	21.6
	Trehalose	0.058	3.9
	Dimethyl Sulfone	0.002	0.1
	Glycerol	0.043	2.9
	Tris Buffer (0.1 M, pH 8) Prepared with Sterile Water	0.570	38.4
	PEG-3350	0.0114	1.4
480 µL of the 20 mg/mL PEG-3350 Solution	PEG-3350	0.0096	
	Tris Buffer (0.1 M, pH 8) Prepared with Sterile Water	0.480	32.4
	Total	1.4942	100

Chapter 4: Conclusions and Future Work

4.1 Conclusions

Having the capability to administer vaccines via OTFs would be valuable for many reasons. OTFs offer pain-free administration, they do not produce biohazardous waste, they can be self-administered, and they do not require cold-chain storage. All these factors contribute to reducing the associated costs of vaccine distribution.

This thesis focused on incorporating LNPs, comparable to those found in the Pfizer-BioNTech COVID-19 vaccine, into OTFs. The film formulation was based on that of the QuickStrip, developed by Rapid Dose Therapeutics. There were three main requirements once the Acuitas-LNPs were embedded into the OTF. It was essential to ensure that the LNPs remained intact after the film casting process, that the RNA remained encapsulated within the LNPs after the film casting process, and that the RNA was undamaged after the film casting process.

Chapter 2 discussed the synthesis and characterization of different LNPs. Lipid-polymer hybrid nanoparticles (h-LNP) were prepared using a probe sonication technique. The sonication amplitude and temperature were related to the size of the h-LNPs. The size of the h-LNPs was determined by DLS and AFM. There was no trend observed between particle size and increasing sonication amplitude. After determining the sonication power that corresponded to the three different amplitudes chosen, it was concluded that the difference of sonication power was not large enough to visualize a trend. The sonication power only ranged from 20-35 W. It was found however, that at a constant sonication amplitude but with increasing temperature, resulted in an increase in particle size.

Next, ibuprofen was loaded into h-LNPs using a nanoprecipitation technique. Using UV-Vis spectroscopy, the amount of ibuprofen loaded into the particles was determined. The loading efficiency of ibuprofen into the h-LNPs was calculated to be 48%.

Fluorescein isothiocyanate was then loaded into the h-LNPs using the probe sonication technique. These particles were imaged using AFM and super resolution optical microscopy. The FITC-LNPs were used as a model to determine if it was possible to image individual LNPs. It was determined that FITC was a poor choice of fluorescent dye due to its poor photostability and photo blinking properties.

Commercially produced LNPs were obtained from Acuitas Therapeutics, a company that supplies Pfizer-BioNTech with LNPs and specializes in the production of LNPs. The LNPs were fluorescently labelled with the DiI and contained model mRNA. DiI was chosen as a fluorescent dye as it has excellent photostability and photo blinking properties. The Acuitas-LNPs underwent a DLS temperature program, in which the size distribution of the particles was measured as the particles were heated from 25-90˚C. The DLS temperature program revealed that the Acuitas-

LNPs are stable at temperatures up to 65˚C, after which the particles began to aggregate. The Acuitas-LNPs were also imaged on a glass coverslip using super resolution optical microscopy.

In Chapter 3 the LNPs previously characterized in Chapter 2 were incorporated into OTFs and the stability of the LNPs was studied. The FITC-LNPs and Acuitas-LNPs were first incorporated into an OTF and imaged using super resolution optical microscopy. The super resolution images of the FITC-LNP-OTF and the Acuitas-LNP-OTF showed that the particles were within the expected size range and circular in shape. Indicating that the LNPs were not damaged during the film casting process.

Next, the Quant-iT RiboGreen RNA assay was used to determine RNA encapsulation. RiboGreen is a fluorescent dye that fluoresces when bound to nucleic acids, allowing for the quantification of RNA in a sample. LNP samples in which the RNA remained encapsulated showed little to no fluorescence, whereas samples where the RNA had been expelled from the LNPs showed high amounts of fluorescence. Triton could then be added to the LNP sample to break open the LNPs and quantify how much RNA was present in the sample. The first Acuitas-LNP-OTF showed that there was nearly no RNA that remained encapsulated in the LNPs. This resulted in several studies in which different variables regarding the film formulation and film preparation were adjusted. It was determined that an additional ingredient had to be added to the film formulation to aid in the stability of the LNPs. Trehalose, PEG, lecithin, and DOPE-PEG were all added to the film formulation to try and stabilize the LNPs. DOPE-PEG was found to be very efficient at stabilizing the LNPs. By adjusting the film formulation to have a 6.3 wt.% of DOPE-PEG, the Acuitas-LNPs were effectively stabilized.

To determine if the mRNA present within the Acuitas-LNPs remained intact after the film casting process, agarose gel electrophoresis was performed on Acuitas-LNPs, an Acuitas-LNP-

FM-5, and an Acuitas-LNP-OTF-3. The RNA band present in the Acuitas-LNP sample corresponded perfectly with the band present in Acuitas-LNP-FM-5 and in Acuitas-LNP-OTF-3. These results indicated that the RNA was not degraded during the film casting process.

4.2 Recommendations of Future Work

The most significant finding of this work was that the DOPE-PEG was able to stabilize the Acuitas-LNPs in the OTFs. As such, it is important to understand the mechanism by which the DOPE-PEG is protecting the LNPs. First, confocal microscopy should be performed on a dissolved Acuitas-LNP-DOPE-PEG-OTF in which RiboGreen dye has been added. This would be the same type of experiment as discussed in Chapter 3.3.10 and would confirm the absence of large aggregates previously seen with unstable LNP samples. Secondly, DOPE-PEG could be labelled with a fluorescent dye other than DiI prior to being incorporated into the Acuitas-LNP-DOPE-PEG-OTF. Using confocal microscopy, would allow for the visualization of how the DOPE-PEG interacts with the Acuitas-LNPs when in an OTF compared to after the OTF has been dissolved.

As previously mentioned, incorporating the DOPE-PEG into OTFs resulted in the film mixture having a high viscosity. Additional buffer could be added to the film mixture to help with uniform paddle mixing. Additional buffer might also allow for less bubbles within the film mixture and OTFs. Next, the mechanical properties of the Acuitas-LNP-DOPE-PEG-OTFs should be studied. The dissolution time, disintegration time, fold endurance, and tensile strength are all factors that should be investigated.

Finally, DOPE-PEG is only one of many available lipid-PEG molecules. Other, more cost effective, lipid-PEG molecules should be added to the film mixture to see if they are able to stabilize the LNPs.

References

(1) Alaei, S.; Omidian, H. Mucoadhesion and Mechanical Assessment of Oral Films. *Eur. J. Pharm. Sci.* **2021**, *159*, 105727. https://doi.org/10.1016/j.ejps.2021.105727.

(2) Kraan, H.; Vrieling, H.; Czerkinsky, C.; Jiskoot, W.; Kersten, G.; Amorij, J. Buccal and Sublingual Vaccine Delivery. *J. Control. Release* **2014**, *190*, 580–592. https://doi.org/10.1016/j.jconrel.2014.05.060.

(3) Fonseca-santos, B.; Chorilli, M. An Overview of Polymeric Dosage Forms in Buccal Drug Delivery : State of Art , Design of Formulations and Their in Vivo Performance Evaluation. *Mater. Sci. Eng. C* **2018**, *86*, 129–143. https://doi.org/10.1016/j.msec.2017.12.022.

(4) Rathbone, Michael J., E.; Pather, Indiran, E.; Şenel, Sevada, E. *Oral Mucosal Drug Delivery and Therapy*; Springer, 2015. https://doi.org/10.1007/978-1-4899-7558-4.

(5) Bajrovic, I.; Schafer, S. C.; Romanovicz, D. K.; Croyle, M. A. Novel Technology for Storage and Distribution of Live Vaccines and Other Biological Medicines at Ambient Temperature. *Sci. Adv.* **2020**, *6*. https://doi.org/10.1126/sciadv.aau4819.

(6) Coffey, J. W.; Gaiha, G. Das; Traverso, G. Oral Biologic Delivery: Advances Toward Oral Subunit, DNA, and MRNA Vaccines and the Potential for Mass Vaccination during Pandemics. *Annu. Rev. Pharmacol. Toxicol.* **2021**, *61*, 517–540. https://doi.org/10.1146/annurev-pharmtox-030320-092348.

(7) Morales, J. O.; Mcconville, J. T. Manufacture and Characterization of Mucoadhesive Buccal Films. *Eur. J. Pharm. Biopharm.* **2011**, *77* (2), 187–199.

https://doi.org/10.1016/j.ejpb.2010.11.023.

(8) Shirvan, A. R.; Bashari, A.; Hemmatinejad, N. New Insight into the Fabrication of Smart Mucoadhesive Buccal Patches as a Novel Controlled-Drug Delivery System. *Eur. Polym. J.* **2019**, *119*, 541–550. https://doi.org/10.1016/j.eurpolymj.2019.07.010.

(9) Laffleur, F. Mucoadhesive Polymers for Buccal Drug Delivery. *Drug Dev. Ind. Pharm.* **2014**, *45* (5), 591–598. https://doi.org/10.3109/03639045.2014.892959.

(10) Bhagurkar, A. M.; Darji, M.; Lakhani, P.; Thipsay, P.; Bandari, S.; Repka, M. A. Effects of Formulation Composition on the Characteristics of Mucoadhesive Films Prepared by Hot-Melt Extrusion Technology. *J. Phamacy Phamacology* **2019**, *71*, 293–305. https://doi.org/10.1111/jphp.13046.

(11) Bala, R.; Pawar, P.; Khanna, S.; Arora, S. Orally Dissolving Strips : A New Approach to Oral Drug Delivery System. *Int. J. Pharm. Investig.* **2013**, *3* (2), 67–76. https://doi.org/10.4103/2230-973X.114897.

(12) Eleftheriadis, G. K.; Ritzoulis, C.; Bouropoulos, N.; Tzetzis, D. European Journal of Pharmaceutics and Biopharmaceutics Unidirectional Drug Release from 3D Printed Mucoadhesive Buccal Fi Lms Using FDM Technology : In Vitro and Ex Vivo Evaluation. *Eur. J. Pharm. Biopharm.* **2019**, *144* (September), 180–192. https://doi.org/10.1016/j.ejpb.2019.09.018.

(13) Montenegro-nicolini, M.; Reyes, P. E.; Jara, M. O.; Vuddanda, P. R.; Neira-carrillo, A.; Butto, N.; Velaga, S.; Morales, J. O. The Effect of Inkjet Printing over Polymeric Films as Potential Buccal Biologics Delivery Systems. *AAPS PharmSciTech* **2018**, *19* (8), 3376–3387. https://doi.org/10.1208/s12249-018-1105-1.

(14) Sofi, H. S.; Abdal-hay, A.; Ivanovski, S.; Shrike, Y.; Sheikh, F. A. Materials Science & Engineering C Electrospun Nanofibers for the Delivery of Active Drugs through Nasal , Oral and Vaginal Mucosa : Current Status and Future Perspectives. *Mater. Sci. Eng. C* **2020**, *111* (July), 110756. https://doi.org/10.1016/j.msec.2020.110756.

(15) Giordani, B.; Abruzzo, A.; Musazzi, U. M.; Cilurzo, F.; Nicoletta, F. P.; Dalena, F.; Parolin, C.; Vitali, B.; Cerchiara, T.; Luppi, B.; Bigucci, F. Freeze-Dried Matrices Based on Polyanion Polymers for Chlorhexidine Local Release in the Buccal and Vaginal Cavities. *J. Pharm. Sci.* **2019**, *108* (7), 2447–2457. https://doi.org/10.1016/j.xphs.2019.02.026.

(16) Abo-shady, A. Z.; Elkammar, H.; Elwazzan, V. S.; Nasr, M. Journal of Drug Delivery Science and Technology Formulation and Clinical Evaluation of Mucoadhesive Buccal Fi Lms Containing Hyaluronic Acid for Treatment of Aphthous Ulcer. *J. Drug Deliv. Sci. Technol.* **2020**, *55* (December 2019), 101442. https://doi.org/10.1016/j.jddst.2019.101442.

(17) Tian, Y.; Visser, J. C.; Klever, J. S.; Woerdenbag, H. J.; Frijlink, H. W.; Hinrichs, W. L. J. Orodispersible Films Based on Blends of Trehalose and Pullulan for Protein Delivery. *Eur. J. Pharm. Biopharm.* **2018**, *133*, 104–111. https://doi.org/10.1016/j.ejpb.2018.09.016.

(18) Prasanth, V. V; Puratchikody, A.; Mathew, S. T.; Ashok, K. B. Effect of Permeation Enhancers in the Mucoadhesive Buccal Patches of Salbutamol Sulphate for Unidirectional Buccal Drug Delivery. *Res. Phamaceutical Sci.* **2014**, *9* (4), 259–268.

(19) Spence Leung, S.-H.; Leone, R. S.; Kumar, L. D. United States Patent - Fast Dissolving Orally Consumable Films. US 6,596,298 B2, 2003.

(20) Administration, U. F. and D. Onsolis (fentanyl buccal soluble film) Information https://www.fda.gov/drugs/postmarket-drug-safety-information-patients-and-providers/onsolis-fentanyl-buccal-soluble-film-information.

(21) Informaltion about Medicated-Assisted Treatment (MAT) Opioid Treatment Program Directory https://www.fda.gov/drugs/information-drug-class/information-about-medication-assisted-treatment-mat.

(22) FDA approves first generic versions of Suboxone sublingual film, which may increase access to treatment for opioid dependence https://www.fda.gov/news-events/press-announcements/fda-approves-first-generic-versions-suboxone-sublingual-film-which-may-increase-access-treatment.

(23) Tuma, R. S. FDA Approval for Zuplenz Ondansetron Oral Soluble Film for Prevention of Chemotherapy-Induced, Radiotherapy-Induced, and Postoperative Nausea and Vomiting. *Oncol. Times* **2010**, *32* (14).

(24) Ondansetron (marketed as Zofran) Information https://www.fda.gov/drugs/postmarket-drug-safety-information-patients-and-providers/ondansetron-marketed-zofran-information.

(25) Belbuca (buprenorphine buccal film) https://www.belbuca.com/.

(26) Sympazan (clobazam) oral film https://www.sympazan.com/.

(27) Exservan (riluzole) oral film https://www.exservan.com/.

(28) Fallon, K. Sunovion Announces U . S . FDA Approval of KYNMOBI ™ (apomorphine hydrochloride) Sublingual Film for the Treatment of Parkinson ’ s Disease OFF Episodes

https://news.sunovion.com/press-releases/press-releases-details/2020/Sunovion-Announces-US-FDA-Approval-of-KYNMOBI-apomorphine-hydrochloride-Sublingual-Film-for-the-Treatment-of-Parkinsons-Disease-OFF-Episodes/default.aspx.

(29) Robinson, K. Rapid Dose Therapeutics-Branded Cannabis Products in Retail Locations Across Canada Via Master Distribution Agreement with Namaste Technologies Subsidy Cann Mart https://www.rapid-dose.com/rapid-dose-therapeutics-branded-cannabis-products-in-retail-locations-across-canada-via-master-distribution-agreement-with-namaste-technologies-subsidiary-cannmart/.

(30) World Health Organization. Vaccines and Immunization https://www.who.int/health-topics/vaccines-and-immunization#tab=tab_1.

(31) Pollard, A. J.; Bijker, E. M. A Guide to Vaccinology: From Basic Principles to New Developments. *Nat. Rev. Immunol.* **2021**, *21* (February). https://doi.org/10.1038/s41577-020-00479-7.

(32) Jain, S.; Venkataraman, A.; Wechsler, M. E.; Peppas, N. A. Messenger RNA-Based Vaccines : Past , Present , and Future Directions in the Context of the COVID-19 Pandemic. *Adv. Drug Deliv. Rev.* **2021**, *179*. https://doi.org/10.1016/j.addr.2021.114000.

(33) Cucinotta, D.; Vanelli, M. WHO Declares COVID-19 a Pandemic. *Acta Biomed.* **2020**, *91* (6), 157–160. https://doi.org/10.23750/abm.v91i1.9397.

(34) Buschmann, M. D.; Carrasco, M. J.; Alishetty, S.; Paige, M.; Alameh, M. G.; Weissman, D. Nanomaterial Delivery Systems for MRNA Vaccines. *Vaccines* **2021**, *9* (65). https://doi.org/10.3390/vaccines9010065.

(35) Kowalzik, F.; Schreiner, D.; Jensen, C.; Teschner, D.; Gehring, S.; Zepp, F. MRNA-Based Vaccines. *Vaccines* **2021**, *9* (390).

(36) Semple, S. C.; Leone, R.; Barbosa, C. J.; Tam, Y. K.; Lin, P. J. C. Lipid Nanoparticle Delivery Systems to Enable MRNA-Based Therapeutics. *Pharmaceutics* **2022**, *14* (398). https://doi.org/10.3390/pharmaceutics 14020398.

(37) Han, X.; Zhang, H.; Butowska, K.; Swingle, K. L.; Alameh, M.; Weissman, D.; Mitchell, M. J. An Ionizable Lipid Toolbox for RNA Delivery. *Nat. Commun.* **2021**, *12* (7233). https://doi.org/10.1038/s41467-021-27493-0.

(38) Magini, D.; Giovani, C.; Mangiavacchi, S.; Maccari, S. Self-Amplifying MRNA Vaccines Expressing Multiple Conserved Influenza Antigens Confer Protection against Homologous and Heterosubtypic Viral Challenge. *PLoS One* **2016**. https://doi.org/10.1371/journal.pone.0161193.

(39) Hekele, A.; Bertholet, S.; Archer, J.; Gibson, D. G.; Palladino, G.; Brito, L. A.; Otten, G. R.; Brazzoli, M.; Buccato, S.; Bonci, A.; Casini, D.; Maione, D.; Qi, Z.; Gill, J. E.; Caiazza, N. C.; Urano, J.; Hubby, B.; Gao, G. F.; Shu, Y.; De, E.; Mandl, C. W.; Mason, P. W.; Settembre, E. C.; Ulmer, J. B.; Venter, J. C.; Dormitzer, P. R.; Rappuoli, R.; Geall, A. J. Rapidly Produced SAM H Vaccine against H7N9 Influenza Is Immunogenic in Mice. *Emerg. Micobes Infect.* **2013**, *2*. https://doi.org/10.1038/emi.2013.54.

(40) Mallory, K. L.; Taylor, J. A.; Zou, X.; Waghela, I. N.; Schneider, C. G.; Sibilo, M. Q.; Punde, N. M.; Perazzo, L. C.; Savransky, T.; Sedegah, M.; Dutta, S.; Janse, C. J.; Pardi, N.; Lin, P. J. C.; Tam, Y. K.; Weissman, D.; Angov, E. Messenger RNA Expressing PfCSP Induces Functional , Protective Immune Responses against Malaria in Mice. *npj*

Vaccines **2021**, *6* (84), 1–12. https://doi.org/10.1038/s41541-021-00345-0.

(41) Raj, D. K.; Mohapatra, A. D.; Jnawali, A.; Zuromski, J.; Jha, A.; Cham-kpu, G.; Sherman, B.; Rudlaff, R. M.; Nixon, C. E.; Oleinikov, A. V; Chesnokov, O.; Merritt, J.; Pond-tor, S.; Burns, L.; Jolly, G.; Mamoun, C. Ben; Kabyemela, E.; Lambert, L.; Orr-gonzalez, S.; Gnädig, N. F.; David, A.; Park, S.; Dvorin, J. D.; Pardi, N.; Weissman, D.; Mui, B. L.; Tam, Y. K.; Friedman, J. F.; Fried, M.; Duffy, P. E.; Kurtis, J. D. Anti-PfGARP Kills Parasites by Inducing PCD and Attenuates Severe Malaria. *Nature* **2020**, *582* (7810), 104–108. https://doi.org/10.1038/s41586-020-2220-1.

(42) BioNTech. BioNTech Provides Update on Plans to Develop Sustainable Solutions to Address Infectious Diseases on the African Continent. 2021.

(43) Blakney, A. K.; Mckay, P. F.; Shattock, R. J. Inside out : Optimization of Lipid Nanoparticle Formulations for Exterior Complexation and in Vivo Delivery of SaRNA. *Gene Ther.* **2019**, *26*, 363–372. https://doi.org/10.1038/s41434-019-0095-2.

(44) Saunders, K. O.; Pardi, N.; Parks, R.; Santra, S.; Mu, Z.; Sutherland, L.; Scearce, R.; Barr, M.; Eaton, A.; Hernandez, G.; Goodman, D.; Hogan, M. J.; Tombacz, I.; Gordon, D. N.; Rountree, R. W.; Wang, Y.; Lewis, M. G.; Pierson, T. C.; Barbosa, C.; Tam, Y.; Matyas, G. R.; Rao, M.; Beck, Z.; Shen, X.; Ferrari, G.; Tomaras, G. D.; Monte, D. C. Lipid Nanoparticle Encapsulated Nucleoside-Modi Fi Ed MRNA Vaccines Elicit Polyfunctional HIV-1 Antibodies Comparable to Proteins in Nonhuman Primates. *Nat. Partn. J. Vaccines* **2021**, *50*, 1–14. https://doi.org/10.1038/s41541-021-00307-6.

(45) Egan, K. P.; Id, L. M. H.; Naughton, A.; Pardi, N.; Id, S. A.; Cohen, G. H.; Weissman, D.; Id, H. M. F. An HSV-2 Nucleoside-Modified MRNA Genital Herpes Vaccine Containing

Glycoproteins GC , GD , and GE Protects Mice against HSV-1 Genital Lesions and Latent Infection. *PLOS Pathog.* **2020**, *16*. https://doi.org/10.1371/journal.ppat.1008795.

(46) Latourette, P. C.; Awasthi, S.; Desmond, A.; Pardi, N.; Cohen, G. H.; Weissman, D.; Friedman, H. M. Protection against Herpes Simplex Virus Type 2 Infection in a Neonatal Murine Model Using a Trivalent Nucleoside-Modified MRNA in Lipid Nanoparticle Vaccine. *Vaccine* **2020**, *38*. https://doi.org/10.1016/j.vaccine.2020.09.079.

(47) Awasthi, S.; Hook, L. M.; Pardi, N.; Wang, F.; Myles, A.; Michael, P.; Cohen, G. H.; Weissman, D.; Friedman, H. M. Nucleoside-Modified MRNA Encoding HSV-2 Glycoproteins C, D, E Prevents Clinical and Subclinical Genital Herpes Sita. *Sci Immunol* **2019**, *4* (39). https://doi.org/10.1126/sciimmunol.aaw7083.

(48) Fang, R. H.; Aryal, S.; Hu, C. M. J.; Zhang, L. Quick Synthesis of Lipid-Polymer Hybrid Nanoparticles with Low Polydispersity Using a Single-Step Sonication Method. *Langmuir* **2010**, *26* (22), 16958–16962. https://doi.org/10.1021/la103576a.

(49) Zhang, L.; Chan, J. M.; Gu, F. X.; Rhee, J. W.; Wang, A. Z.; Radovic-Moreno, A. F.; Alexis, F.; Langer, R.; Farokhzad, O. C. Self-Assembled Lipid-Polymer Hybrid Nanoparticles: A Robust Drug Delivery Platform. *ACS Nano* **2008**, *2* (8), 1696–1702. https://doi.org/10.1021/nn800275r.

(50) Keum, C. G.; Noh, Y. W.; Baek, J. S.; Lim, J. H.; Hwang, C. J.; Na, Y. G.; Shin, S. C.; Cho, C. W. Practical Preparation Procedures for Docetaxel-Loaded Nanoparticles Using Polylactic Acid-Co-Glycolic Acid. *Int. J. Nanomedicine* **2011**, *6*, 2225–2234. https://doi.org/10.2147/ijn.s24547.

(51) Yang, F.; Cabe, M. H.; Ogle, S. D.; Sanchez, V.; Langert, K. A. Optimization of Critical

Parameters for Coating of Polymeric Nanoparticles with Plasma Membrane Vesicles by Sonication. *Sci. Rep.* **2021**, *11* (1), 1–13. https://doi.org/10.1038/s41598-021-03422-5.

(52) Shim, S.; Xia, C.; Zhong, G.; Babcock, H. P.; Vaughan, J. C.; Huang, B. Super-Resolution Fluorescence Imaging of Organelles in Live Cells with Photoswitchable Membrane Probes. *Proc. Natl. Acad. Aciences* **2012**, *109* (35). https://doi.org/10.1073/pnas.1201882109.

(53) Farrell, E.; Brousseau, J. *Guide for DLS Sample Preparation - Technical Note*.

(54) Ohshima, H.; Miyagishima, A.; Kurita, T.; Makino, Y.; Iwao, Y.; Sonobe, T.; Itai, S. Freeze-Dried Nifedipine-Lipid Nanoparticles with Long-Term Nano-Dispersion Stability after Reconstitution. *Int. J. Pharm.* **2009**, *377* (1–2), 180–184. https://doi.org/10.1016/j.ijpharm.2009.05.004.

(55) Teekamp, N.; Tian, Y.; Visser, J. C.; Olinga, P.; Frijlink, H. W.; Woerdenbag, H. J.; Hinrichs, W. L. J. Addition of Pullulan to Trehalose Glasses Improves the Stability of β-Galactosidase at High Moisture Conditions. *Carbohydr. Polym.* **2017**, *176* (August), 374–380. https://doi.org/10.1016/j.carbpol.2017.08.084.